DEFINING THE MECHANISMS OF MICROBIAL SENSING AMONG MEMBERS OF THE TOLL-LIKE RECEPTOR 2 SUB-FAMILY

BY

DIANA ROSE E. RANOA

DISSERTATION

Submitted in partial fulfillment of the requirements
for the degree of Doctor of Philosophy in Microbiology
in the Graduate College of the
University of Illinois at Urbana-Champaign, 2014

Urbana, Illinois

Doctoral Committee

Associate Professor Dr. Richard I. Tapping, Chair
Professor Dr. James M. Slauch
Professor Dr. David M. Kranz
Assistant Professor Dr. Patrick H. Degnan

ABSTRACT

As pattern recognition receptors of the innate immune system, Toll-like receptors (TLRs) sense microbial components and mediate cell activation leading to protective inflammatory responses. TLRs are type-1 transmembrane receptors that are activated by forming dimers; an event driven by the coordinate binding of a cognate microbial ligand. Bacterial lipoproteins are the most potent microbial agonists for the TLR2 subfamily and this pattern recognition event induces cellular activation leading to host immune responses. TLR2 mediates cellular responses to triacylated and diacylated bacterial lipoproteins by forming heterodimers with either TLR1 or TLR6, respectively. Crystal structure analysis revealed that triacylated bacterial lipoproteins coordinately bind TLR1 and TLR2 resulting in a stable ternary complex that drives intracellular signaling. However, the order of complex formation upon recognition of microbial components is poorly understood. The primary objectives of this dissertation are to define the sequence of events by which lipoproteins from bacteria are delivered to TLR1 and TLR2 leading to the formation of a stable TLR1/TLR2/lipoprotein ternary complex as well as to identify important amino acid residues in the TLR1 extracellular domain that are necessary for ligand recognition and/or formation of the dimer interface with TLR2.

Chapter One of this thesis provides an overview of the field of innate immunity and a review of the latest developments in Toll-like receptor studies, with an emphasis on the members of the Toll-like receptor 2 subfamily. We describe in detail the extracellular domain of TLRs and their importance in ligand recognition.

Chapter Two assesses the role of two lipid-binding serum molecules, lipopolysaccharide binding proten (LBP) and cluster of differentiation 14 (CD14), in the

delivery of microbial components to TLRs 1 and 2. The sensitivity of TLR-expressing cells to lipoproteins is greatly enhanced by LBP and soluble CD14 (sCD14). However, the physical mechanism which underlies this increased sensitivity is not known. To address this, we have measured the ability of LBP and sCD14 to drive ternary complex formation between soluble extracellular domains of TLR1 and TLR2 and the synthetic triacylated lipopeptide agonist Pam_3CSK_4. Importantly, addition of sub-stoichiometric amounts of either LBP or sCD14 significantly enhances formation of a TLR1/TLR2/Pam_3CSK_4 ternary complex as measured by size exclusion chromatography. However, neither LBP nor sCD14 is physically associated with the final ternary complex. Similar results were obtained using OspA, a naturally-occurring triacylated lipoprotein agonist from *Borrelia burgdorferi*. Activation studies reveal that either LBP or sCD14 sensitize TLR-expressing cells to nanogram levels of either Pam_3CSK_4 lipopeptide or OspA lipoprotein agonist. Together, our results show that either LBP or sCD14 can drive ternary complex formation and TLR activation by acting as mobile carriers of triacylated lipopeptides or lipoproteins.

Chapter Three describes the measurement of interactions between TLRs and lipopeptides to assess the possible competition between TLR1 and TLR10 for lipopeptides and the TLR2 co-receptor. Using microtiter plate assays, we have demonstrated that Pam_3CSK_4 induces the formation of the TLR1/TLR2 and TLR2/TLR10 heterodimeric complexes, and have further shown that ternary complex formation is ligand-specific and can be blocked by monoclonal antibodies against the TLRs. TLR2 was shown to prefer TLR1 as co-receptor compared to TLR10 for assembly of a final ternary complex with Pam_3CSK_4. To quantitatively measure the

kinetics of the interaction, surface plasmon resonance experiments based on a two-component system were initially performed. However, two major problems encountered in this system were the aggregation of the small 1.5 kDa Pam_3CSK_4 ligand in solution, as well as the non-uniformity of binding conditions after each regeneration step. To address these issues, we purified a larger 12kDa lipoprotein (Lip12) expressed in *E. coli* and used the Octet system to obtain uniform and repeatable results. The calculated dissociation constant (K_D) of Lip12 binding to Fc-tagged TLRs 1, 2, and 10 immobilized on protein A sensors were $7.45x10^{-7}$ M (chi^2: 0.0193), $1.58x10^{-6}$ M (chi^2: 0.02892), and $3.34x10^{-7}$ M (chi^2: 0.07317), respectively, based on a 1:1 Langmuir binding model. Moreover, TLR4 did not show any binding to Lip12, and neutralizing mAbs against TLR2 and TLR1 prevented interaction with Lip12, suggesting that the binding events are real and specific. TLR1 showed the highest affinity for the agonist, followed by TLR10, and finally by TLR2. This, together with the reported CD14-Pam_3CSK_4 interaction ($K_D = 5.7x10^{-6}$M) suggest that CD14 preferentially delivers the lipopeptide to TLR1 first followed by the binding of TLR1-lipopeptide to TLR2. In cells that express both TLR1 and TLR10, a competition for the agonist could take place, and the receptor that has a higher expression level on the cell surface would most likely win. Measuring the K_D in a three-component system, while a critical step, is outside the scope of current work until the issues of protein aggregation, handling lipoproteins in solution, and steric hindrance brought about by non-specific dimerization of Fc-tagged TLRs can be resolved. Addition of LBP and/or sCD14 to this system did not resolve the aggregation problem.

Chapter Four addresses the important regions in the TLR1 extracellular domain (ECD) that are required for activation of TLR1/TLR2 in response to a variety of natural

agonists. We have previously shown that the central leucine-rich repeat motifs (LRRs 9 through 12) of TLR1 and TLR 6 are critical for lipoprotein discrimination. TLR1/TLR2 and TLR2/TLR6 heterodimers also mediate responses to a wide variety of other acylated microbial ligands and we show here that similar to lipopeptides, LRRs 9-12 of TLR1 and TLR6 are also required for this sensing function. To further delineate the residues important for this function, random mutagenesis was used to create a library of TLR1 clones with various single amino acid substitutions within LRRs 9-12. Using this library, the epitope of GD2.F4, an inhibitory anti-TLR1 mAb, was mapped to amino acid residues located in the flexible loop of LRR11. Additionally, the amino acids F314, P315, Q316 and V339, within LRRs 11 and 12, were each found to be necessary for the sensing of triacylated lipopeptides by TLR1. More importantly, mutation of these same critical residues greatly inhibited cellular responses to other TLR1/TLR2 microbial agonists. These results demonstrate that regardless of the molecular structure of the agonist, the same critical residues of TLR1 are required for ternary complex formation with TLR2 to initiate cellular activation. These residues lie at the interface between TLR1 and TLR2 in the TLR1/TLR2/lipopeptide complex suggesting that the overall structure of the ternary complex is the same regardless of the activating microbial agonist.

Chapter Five summarizes the important findings from this dissertation, highlighting the contributions and implications of this work to the TLR field. We also describe future experiments that are predicted to provide further insights on the structure and function relationship between TLRs and their agonists. A better understanding of TLR sensing of bacterial cell wall components may lead to improved therapeutic strategies for treating inflammatory diseases.

ACKNOWLEDGEMENTS

"*If everyone whose experiments failed stopped doing science, there wouldn't be any science*." – Dr. Allan Charles Wilson (UC Berkeley)

"*No matter what accomplishments you make, somebody helps you*."

- Wilma Rudolph

The road towards the completion of this dissertation has not been a very easy path, and having reached this point marks a very important milestone in my life. This body of work would not have been possible without the assistance of several people in so many ways. I am mostly and forever grateful to my thesis advisor, Dr. Richard I. Tapping, for your guidance throughout this project and for the countless words of encouragement especially during challenging and difficult times. To me, you have always been the epitome of a "glass half-full" person, gently and patiently pushing everyone in the lab towards the right direction, and always reminding us that every result in every experiment, be it a negative data, is trying to tell us something. Thank you for being a great mentor, always patiently showing us how to interpret results, how to be critical of scientific reports, how to go about in designing and troubleshooting experiments, how to express and convey scientific results in both written and oral form, and how to do good science in general. Thank you for giving me the freedom to "own" my project and for letting me test some of my ideas. Thank you for being very understanding. Even with all the road blocks and bumps that I've encountered in this project, you always believed that I can get through it. So many times, I've thought about giving up, but your helping hand was always there to put me right back on track.

I am very grateful to everyone who has been a part of my thesis committee, both as permanent and temporary members: Dr. David Kranz, Dr. James Slauch, Dr. Peter Orlean, Dr. Patrick Degnan, Dr. Brenda Wilson, and Dr. Joanna Shisler. Each of them made significant contributions towards my scientific career growth and the development of my thesis. Before I started this thesis, I have almost zero background in the protein field. Their helpful comments collectively made it easier for me develop the skills needed to perform biochemical and biophysical work that are essential for this project. Special thanks to Dr. Kranz for providing the Fc-tagged pDisplay vector construct that initiated this whole project and allowed me to generate soluble TLR extracellular domains. He also made several insightful comments on how to go about characterizing my purified proteins, as well as how to set-up reliable BIAcore experiments. I am grateful to Dr. Slauch for giving several constructive criticisms with regards to my experimental approaches and data analyses. I also thank Dr. Peter Orlean for doing a great job on following up on my research progress year after year. I am grateful to Dr. Patrick Degnan, for agreeing to take over Dr. Orlean's place in my committee during my final defense. He asked several questions prior to my thesis defense, and also gave a thorough review of this dissertation during the final stages of writing. All of his questions and comments significantly improved the contents of this dissertation. I thank Dr. Brenda Wilson and Dr. Joanna Shisler for being a part of my temporary committee prior to passing my preliminary exams. Both of them asked very good questions that in a way contributed to the improvement of my thesis proposal.

I would like to acknowledge all of my colleagues from the Tapping Lab, both past and present members. I am grateful to Dr. Katherine Omueti for patiently guiding me

through my early years in the lab. She made me feel very welcome in the lab, and her sunny disposition made it easier for me adapt to life in the United States. She unselfishly shared her data and research findings, which formed the foundation of my thesis project. I am also very grateful to my good friend Dr. Yue Guan, for providing both intellectual and emotional support in the lab. Like Katherine, Yue welcomed me to the lab with open arms. She made my lab rotation days really fun by allowing me to shadow her in her TLR10 work. She also unselfishly let me collaborate with her on some TLR10 work. Both Katherine and Yue were very instrumental in training me how to do animal cell culture and the TLR reconstitution assay. I thank Dr. Stacy Kelley for sharing some of her purified CD14 protein, which allowed me to study the mode of lipopeptide delivery to the TLRs. She also shared her expertise on protein work, which helped me optimize my purification protocol. I thank Dr. Xinyan Li for providing expertise in several areas such as mice work, flow cytometry, and statistical analysis. It was a pleasure getting to know you, and I had fun sharing most of my lunch hours with you. I thank Dr. Bryan Hart, Dr. Chris Johnson, Dr. Joshua Turner, Vitaly Stepensky, Song Jiang, Mike Tencati, Nicholas Hess for sharing their expertise and for making life in the lab more fun. I also would like to thank the numerous undergraduate students and rotation students who performed research in the lab, and provided assistance in several research experiments.

I am grateful to several collaborators who shared reagents as well as expertise on different aspects of this study. Special thanks to Dr. Jerrold P. Weiss and Dr. Theresa Gioaninni from the University of Iowa Department of Internal Medicine for generously providing their precious recombinant LBP protein. I thank Dr. Taras V. Pogorelov from the UIUC School of Chemical Sciences for his assistance in the basic use of the VMD

software. I also would like to thank Dr. Liping Wang, the former supervisor of the UIUC Immunological Resource Center, for providing helpful guidelines on the use of the BIAcore equipment. She also shared her expertise on protein purification and generation of monoclonal antibodies. I am extremely grateful to Dr. Steve Huber and Dr. Xia Wu of the UIUC Department of Plant Biology for generously sharing their Octet equipment and their expertise on the technology, which allowed me to perform reliable biophysical work on TLRs and lipopeptides.

I would like to thank the UIUC Department of Microbiology, especially Deb LeBaugh and Diane Tsevelekos. Both of them have been very good in taking care of the administrative portion of my PhD program, and they made sure that I did not miss any requirements by the department. Their reminders about departmental deadlines have been very helpful, and they do a really great job of preparing all the necessary paperwork for my program and RA appointments.

I am grateful to my MCB 150 family, especially Brad Mehrtens and Melissa Reedy, for making my TA days really fun and enjoyable. Thank you for your patience and understanding.

Last but definitely not the least, I would like to thank my family in the Philippines, my immediate relatives in the United States, and my numerous multi-cultural friends whom I met in my almost eight years of living in Champaign-Urbana. I am very grateful to my parents (Dino and Rose) and brothers (Van and Ranel) for always believing in me, for giving me unconditional love and support, and for being patient about my career choice. Even though my parents didn't initially like the idea of me living

all by myself in the United States, they still were very supportive and understanding of my career decisions. I know deep down in their hearts they wanted me to become a medical doctor, but they respected my decision of becoming a research scientist instead. I thank both of my parents for being very good role models for integrity, humility, hard-work and perseverance. It is with deep sorrow to say that my dad did not live to see me finish my PhD program, but I know that he is very happy looking down at me from heaven. I am also very grateful to my aunt Alena and uncle Tom in San Diego CA, who made my life here in the US so much easier. They are like parents to me, providing me assistance and support in every step of the way. Finally, I would like to thank all my friends both in the US and in the Philippines, especially my Filipino friends in Champaign-Urbana, for providing a very welcoming, fun, and intellectual environment. This whole PhD program has been a very long and crazy ride, and I am very fortunate to have all these people around me to help keep me sane and more importantly, to help keep me going.

This work is dedicated to my wonderful parents

Capt. Segundino C. Ranoa[§] and Mrs. Rosario E. Ranoa

[§]To my dad, forever in my heart you'll stay, until we meet again someday.

TABLE OF CONTENTS

LIST OF ABBREVIATIONS

Ac_2CSK_4, S-[2,3-bis(acetyloxy)-(2RS)-propyl]-[R]-cysteinyl-[S]-seryl-[S]-lysyl-[S]-lysyl-[S]-lysyl-[S]-lysine x 3 CF_3COOH

ArALAM, non-mannose capped lipoarabinomannan

BCAP, B cell adaptor for PI3K

CD14, cluster of differentiation 14

sCD14, soluble cluster of differentiation 14

DAMPs, damage-associated molecular patterns

ECD, extracellular domain

Fc, constant fragment of immunoglobulin G

FRET, fluorescence resonance energy transfer

HKLM, heat-killed *Listeria monocytogenes*

HKSA, heat-killed *Staphylococcus aureus*

HMGB1, high-mobility group box 1

HSA, human serum albumin

IFN, interferon

IκB, inhibitor of NFκB

IL-1, interleukin-1

IL-1R1, interleukin-1 receptor 1

IRAKs, IL-1R-associated kinases

IRFs, interferon regulatory factors

JNK, c-Jun N-terminal kinase

K_D, dissociation constant

LBP, lipopolysaccharide-binding protein

Lip12, 12kDa lipoprotein from *E. coli*

LPS, lipopolysaccharide

LRR, leucine-rich repeat

LTA, lipoteichoic acid

MAL, MyD88 adaptor-like

MALP-2, Macrophage-activating Lipopeptide-2; S-[2,3-*bis* (Palmitoyloxy)-(2R)-propyl-cysteinyl-GNNDESNISFKEK]

MAMPs, microbe-associated molecular patterns

MAPKs, mitogen-activated protein kinases

MD-2, myeloid differentiation factor 2

Mtb mem, Mycobacterial membrane fraction

Mya, million years ago

MyD88, myeloid differentiation antigen protein 88

NFκB, nuclear factor kappa B

OspA, outer surface protein A

Pam_2AcCSK_4, S-[2,3-Bis(palmitoyloxy)-(2-RS)-propyl]-N-acetyloxy- (R)-Cys-(S)-Ser-(S)-Lys_4- x 3 CF_3COOH

Pam_3CSK_4, (S)-[2,3-Bis(palmitoyloxy)-(2-RS)-propyl]-N-palmitoyl-(R)-Cys-(S)-Ser-(S)-Lys_4-OH•3HCl]

PAMP, pathogen-associated molecular pattern

PgLPS, *P. gingivalis* lipopolysaccharide

PI3K, phosphoinositide-3 kinase

PRR, pattern recognition receptor

SARM1, sterile-α- and armadillo-motif-containing protein 1

TIR, Toll/interleukin-1 receptor

TIRAP, TIR-domain containing adaptor protein

TLR, Toll-like receptor

sTLR, soluble TLR

TNF, tumor necrosis factor

TRAF-6, TNF receptor associated factor 6

TRAM, TRIF-related adaptor molecule

TRIF, TIR-related adaptor protein inducing interferon

CHAPTER ONE

INTRODUCTION

The innate immune system and its link to adaptive immunity

Innate immunity is the first-line of host defense that protects vertebrate and invertebrate animals from infectious microorganisms and viruses. The innate immune response happens instantaneously after infection with a wide variety of infectious agents, and systemically in mammals, is characterized by fever, increased white blood cell counts, and elevated acute phase proteins. Innate immune responses are driven by a limited diversity of invariant, germline-encoded receptors. Since cells of the innate immune system do not have memory, they generate the same response upon subsequent exposure to an infectious agent. Adaptive immune responses on the other hand, are highly-specific and directed to the infectious agent that initiated it. However, adaptive immune responses are not immediate, and usually take several days (4-7 days) to develop. The lymphocytes, B cells and T cells, which facilitate the adaptive immune response, have extensive diversity due to a wide range of randomly generated B-cell receptors and T-cell receptors. Moreover, memory cells confer amplified responses upon subsequent exposure to the same infectious agent. Only vertebrate animals possess adaptive immune systems (Janeway Jr. et al., 2001).

Invertebrates do not possess an adaptive immune system, yet, they are able to mount immune responses against natural pathogens, suggesting that they have a system for recognizing foreign components. In 1883, Elie Metchnikoff (1845-1916), a Russian scientist considered to be the father of the field of innate immunity, observed that starfish larvae are able to engulf particles. He used a wide range of experimental model

organisms, some of them transparent, to test the susceptibility of an organism to infection. He described that white blood cells of the human body have the ability to engulf or phagocytose foreign bodies and microbes, and believed that these cells played a central role in natural immunity to microbial infection. He also identified microphages (polymorphonuclear leukocytes) and macrophages as important components of the innate immune system involved in phagocytosis and production of lytic agents, resulting in the killing and inactivation of infectious microorganisms (Gordon, 2008).

Louis Pasteur (1822-1895) was the first to show that microbes cause infectious diseases and are responsible for the decomposition of organic matter. Robert Koch (1843-1910) then showed that an infectious living microorganism that has entered a host species is able to multiply within and eventually cause disease together with all its symptoms. Ludwig Brieger (1849-1919) further advanced the field by discovering that microbes secrete poisonous substances, which he called "toxins". Emil von Behring (1854-1917) and Shibasaburo Kitasato (1856-1931) discovered an anti-toxin for diphtheria and used it for therapeutic applications. Richard Pfeiffer (1858-1945) discovered that the toxicity of *Vibrio cholerae* was not dependent on a viable microbial cell, since heat-killed *Vibrio cholerae* retained their poisonous activity. He then referred to this heat-stable substance "endotoxin", and also identified the presence of this substance in other Gram-negative microorganisms such as *Salmonella typhi* and *Haemophilus influenzae*. Today, we know that endotoxin is an important structural component of the outer membrane of Gram-negative bacteria called lipopolysaccharide (LPS), that is sensed by leukocytes resulting in the production of endogenous pyrotoxins which cause fever in an individual [Reviewed in (Beutler & Rietschel, 2003)].

For a long time, it was a mystery as to how the innate immune system recognizes microbes and ultimately distinguishes between self and non-self. Furthermore, it was not understood how foreign antigen alone was insufficient to elicit an adaptive immune response. It was known that foreign components (antigens) had to be mixed with crude extracts or adjuvants like mineral oil, mycobacteria, and aluminum hydroxide in order to get T and B cells activated. In 1989, Charlie Janeway Jr. (1943-2003) was the first to hypothesize that there exists a group of receptors, which he termed "pattern recognition receptors (PRRs)", that recognize "pathogen-associated molecular patterns (PAMPs)" (Janeway Jr., 1989). Pattern recognition receptors (PRRs) act as a barrier in the host cell and serve as the first line of innate immune defense against infectious microorganisms. He hypothesized that innate immune cells recognize microorganisms through PRRs, and ultimately provided evidence that this interaction transmits a "second signal" required for lymphocyte activation.

The path to the discovery of the Toll-like receptors

In 1940, Interleukin-1 (IL-1) was the first pro-inflammatory cytokine discovered by researchers. IL-1 is secreted by macrophages in response to LPS from Gram-negative bacteria [Reviewed in (Bowie & O'Neill, 2000)]. It is a cytokine known to be involved in T-cell activation, pyrogenicity, and the acute phase response (Dinarello, 1991). Around 1988, the gene for the IL-1 receptor 1 (IL-1R1) was cloned, but its signaling mechanism remained unknown, because its cytoplasmic domain had no recognizable motif (Sims et al., 1988).

In 1985, the German word "Toll", which means "fantastic" or "super", was used by C. Nüsslein-Volhard to describe a new mutant of abnormal embryonic development in

the fruit fly *Drosophila melanogaster* (Anderson et al., 1985). The *Toll* gene was found to be involved in the development of the dorso-ventral axis of the embryo as a loss-of-function mutation led to dorsalization, while a gain-of-function mutation resulted to ventralization (Anderson et al., 1985). In 1991, the cytoplasmic domain of *Drosophila* Toll and human IL-1R were found to be homologous, suggesting that their signaling pathway may have similar mechanisms [Reviewed in (Gay & Keith, 1991)]. Shortly thereafter, the *Drosophila* toll and the IL-1 receptor were both demonstrated to signal through the NF-kB pathway (Baeuerle & Henkel, 1994; Belvin & Anderson, 1996; Wasserman, 1993). In 1994, the N-protein (encoded by the virus-resistance gene in tobacco plants) was shown to be homologous to the Toll protein with both a leucine-rich repeat (LRR) extracellular domain and a Toll/IL-1R signaling domain (Whitham et al., 1994). In 1995, adult fruit flies with a mutation in their *Toll* gene were observed to be more susceptible to fungal infection, reflecting the role of the Toll receptor in the induction of anti-fungal peptide production as part of their innate immune response. (Lemaitre et al., 1996).

Toll is a transmembrane protein with an extracellular domain (ECD) and a cytoplasmic domain. The ECD is characterized by its LRRs, while the cytoplasmic domain is related to the human interleukin-1 receptor (IL-1R). The stimulation of human cells with IL-1 leads to the phosphorylation of IkB, which in turn leads to the dissociation of the IkB-NFkB complex, thus enabling NF-kB to migrate to the nucleus (Wasserman, 1993). NF-kB is a transcription factor that activates a number of genes known to be involved in immunity and inflammation (Sen & Baltimore, 1986). Dorsal is a transcription factor in *Drosophila* that is homologous to NF-kB, while Cactus is a

cytoplasmic protein whose role in *Drosophila* is analogous to that of the IkB (Belvin & Anderson, 1996). Analogously, activation of Toll on the membrane is correlated with the accumulation of Dorsal in the nucleus.

In 1997, the first human homologue of *Drosophila* Toll was cloned and characterized by Charlie Janeway Jr.'s group (Medzhitov et al., 1997). Without knowing the ligand for the human receptor, they performed an elegant experiment to generate a constitutively active receptor. They engineered a recombinant human Toll (hToll) by fusing the mouse CD4 ectodomain, a receptor that naturally forms dimers, to the transmembrane and cytoplasmic domains of human Toll gene homologue. They then transfected human cell lines such as Jurkat cells and the human monocytic cell line THP-1 cells with their recombinant constructs and measured NF-kB activation using the NF-kB reporter assay. They also detected the expression of NF-kB-controlled genes for proinflammatory cytokines (IL-1, IL-6, and IL-8) along with the co-stimulatory molecule B7.1 (Medzhitov et al., 1997). B7 molecules are expressed by B cells, macrophages, and dendritic cells, collectively known as antigen presenting cells of the immune system, and are required for activation of naïve T cells. This provided preliminary evidence that the human homologue of *Drosophila* Toll has a functional link to adaptive immunity (Janeway Jr., 1989). Other homologues of Toll were later identified and named Toll-like receptors.

In the early 1960s, a strain of inbred mice (C3H/HeJ) at The Jackson Laboratory was found to be resistant to LPS. Genetic studies led to a single LPS resistance locus that was named *Lps* and mapped to mouse chromosome 4. Using inbred strains of mice, Bruce Beutler's group demonstrated that the C3H/HeJ defect reflects a proline to

histidine mutation at amino acid position 712 in the cytoplasmic domain of Toll-like receptor 4 (TLR4). This mutation was demonstrated to create a dominant negative form of the TLR4 receptor and the LPS hyporesponsive phenotype (Poltorak et al., 1998). Additionally, another LPS-hyporesponsive mouse strain, C57BL/10ScCn, was found to be missing an exon in TLR4 (Poltorak et al., 1998). In 1999, Shizuo Akira and colleagues generated TLR4 knock-out mice and showed that they were unresponsive to LPS, affirming that TLR4 is the pattern recognition receptor for LPS (Hoshino et al., 1999). This led to the search for ligands recognized by other TLRs.

Even though TLR4 was the first TLR whose ligand was identified, other TLRs were quickly mapped in the human chromosome using expressed sequence tags (Taguchi et al., 1996). The identification, molecular characterization, and cloning of TLRs 1 through 5 were first published in 1998 (Rock et al., 1998). However, their function remained obscure as their ligands were still unknown. Gene targeting studies performed by Akira and colleagues led to the generation and phenotypic characterization of knockout mutant mice for TLRs 2, 6, and 9 (Hemmi et al., 2000; Takeuchi et al., 1999; Takeuchi et al., 2001). They demonstrated that these TLRs can mediate induction of NF-kB in mammalian cells in response to different sets of microbial molecules. This set the stage for an in-depth analysis of TLRs in microbial sensing (Takeuchi et al., 1999).

The discovery of the *Drosophila* Toll, the identification of human TLRs, and the demonstration of LPS/endotoxin as ligand of human TLR4 were landmark discoveries in the field of immunology research, and led to a rapid increase in research studies focused on TLRs. Jules Hoffmann and Bruce Beutler, the principal investigators who respectively pioneered research on *Drosophila* Toll and TLR4 as the LPS receptor, were recently

awarded with the 2011 Nobel Prize in Physiology or Medicine together with Ralph Steinman, for his discovery of dendritic cells.

Toll-like receptors

Through sensing of microbial components, Toll-like receptors (TLRs) act as immediate triggers of the innate immune system in response to infection. TLRs are type 1 transmembrane proteins that recognize pathogen-associated molecular patterns (PAMPs) in both the extracellular and intracellular compartments of the mammalian cell. Their extracellular domains contain 19-25 leucine-rich repeat (LRR) motifs involved in ligand recognition, while their intracellular domains, referred to as Toll/Il-1 receptor (TIR) domains, are involved in signaling. This intracellular signaling activates the transcription factor nuclear factor kappa B (NFκB), leading to the expression of proinflammatory cytokines such as TNF-α, IL-1β, IL-6, IL-8, and IL-12 [Reviewed in (Takeda & Akira, 2005).

There are currently ten TLRs identified and characterized in humans. They can be grouped primarily based on their subcellular location. TLRs 1,2,4,5,6, and 10 have direct access to the external environment as they are found on the surface of the cell membrane, while TLRs 3,7,8, and 9 are expressed within endosomal compartments inside the cell (Figure 1.1). All TLRs are directly involved in the recognition of conserved structural components of bacteria, viruses, and fungi. For example, TLRs 4, 5, and 9 recognize bacterial lipopolysaccharides, flagellin, and unmethylated cytosine-phosphate-guanine (CpG) DNA, respectively. On the other hand, TLRs 3, 7 and 8 discriminate viral double stranded and single stranded RNA [Reviewed in (Takeda & Akira, 2005).

The TLR signaling pathways

Toll-like receptors and IL-1 receptors are two classes of membrane receptors that belong to a superfamily of proteins that have a Toll-IL-1 receptor (TIR) cytoplasmic domain in their structure (O'Neill, 2006). Following TLR recognition of specific microbial molecular patterns, it is now known that TLRs form either homodimers (in the case of TLR3, TLR4, TLR5) or heterodimers (in the case of TLR1/TLR2 and TLR2/TLR6) in order to initiate signaling (Figure 1.1). The dimerization of two TLRs upon recognition of ligand leads to the assembly of a TIR-TIR platform at the cytoplasmic domain of the receptors. This sets the stage for various cytoplasmic adaptor molecules to dock and initiate a signaling cascade, culminating in the expression of pro-inflammatory cytokines, chemokines, and co-stimulatory molecules. The first signaling adaptor molecule to be characterized was MyD88. It has a domain that associates with the TIR domain of all human TLR dimers except for TLR3 (O'Neill, 2006). At present, there are three other adaptors aside from MyD88 that are involved in TLR signaling: the TIR-domain containing adaptor protein (TIRAP) also known as MyD88 adaptor-like (MAL), the TIR-related adaptor protein inducing interferon (TRIF), and the TRIF-related adaptor molecule (TRAM) (O'Neill et al., 2013). All of these adaptor proteins have TIR domains and are differentially recruited by TLRs through TIR-TIR interactions. Adaptor recruitment induces assembly and the activation of kinases in a series of downstream signaling events. The preferential association of TLRs with any of these four adaptor proteins provides differential responses and gene expression profiles (O'Neill et al., 2013).

The MyD88-dependent pathway drives the synthesis of TNF-α, IL-1, and IL-6 (Akira & Takeda, 2004). Upon binding to the TIR domain of TLRs, MyD88 recruits IRAK-4 through its "death" domain. The activation of IRAK-4 leads to the phosphorylation of IRAK-1, followed by the activation of the TNF receptor associated factor 6 (TRAF-6). A series of ubiquitinylation and phosphorylation steps eventually leads to the degradation of the inhibitor of NF-κB kinase, thus allowing NF-κB translocation to the nucleus where transcription of proinflammatory genes takes place (O'Neill, 2006). In addition to NF-κB, p38 MAPK and an N-terminal kinase (JNK) are also activated downstream of TRAF-6 (Figure 1.1). For TLRs that are activated in endosomal compartments via a MyD88-dependent pathway (TLRs 7, 8, and 9), the transcriptional regulator that gets activated downstream of IRAK-4 is the interferon regulatory factor 7 (IRF-7), which has a role in the induction of the type I interferon (IFN) gene expression (Honda et al., 2005). MyD88 knockout mice are resistant to LPS, peptidoglycan, and lipopeptides. MyD88-deficient mice are also defective in T-cell proliferation (Takeda et al., 2003).The adaptor TIRAP/Mal is a bridging adaptor involved in the MyD88-dependent pathway of TLR4 and, to a lesser extent, TLR2, as TIRAP/Mal-deficient mice had impaired responses to TLR2 and TLR4 ligands (Yamamoto et al., 2002).

TRIF is a third TIR adaptor molecule involved in the MyD88-independent signaling pathway observed in TLR3 and TLR4, and leads to the activation of interferon genes through the transcription factor interferon regulatory factor-3 (IRF-3) (Yamamoto et al., 2003). The fourth TIR adaptor protein TRAM is required for optimal recruitment of TRIF to TLR4 (Yamamoto et al., 2003).

In addition to the four known TIR adaptor proteins, two other adaptors were discovered recently. The sterile-α- and armadillo-motif-containing protein 1 (SARM1) inhibits gene induction downstream of TRIF, but not of MyD88 (Carty et al., 2006). The sixth adaptor molecule is called B cell adaptor for PI3K (BCAP) (Ni et al., 2012; Troutman et al., 2012). BCAP is a cytoplasmic protein expressed in B cells, and were originally shown to mediate B-cell signaling through the B cell receptor and the co-stimulatory molecule CD19 via activation of phosphoinositide 3-kinase (PI3K) (Okada et al., 2000). The phosphorylation of PI3K leads to Akt activation, which is critical for survival and proliferation of B cells (Inabe & Kurosaki, 2002). BCAP is also expressed in myeloid cells (such as macrophages, monocytes, and dendritic cells) and connects TLRs to PI3K/Akt pathway via a cryptic TIR domain (Troutman et al., 2012). Macrophages deficient for BCAP produce higher amounts of pro-inflammatory cytokines compared to wild-type controls upon stimulation of TLR agonists (Ni et al., 2012; Troutman et al., 2012). Moreover, BCAP-deficient mice are more susceptible to LPS toxicity as well as a model of inflammatory colitis as a result of reduced PI3K activation, suggesting that BCAP acts as a negative regulator of inflammation through TLRs (Troutman et al., 2012).

The TLR2 sub-family

TLR2 is phylogenetically related to TLRs 1, 6, and 10. The latter three receptors are the most highly related and are believed to have arisen from successive gene duplication as they share a common locus on chromosome 4 (Roach et al., 2005). The gene for TLR2 is also found on chromosome 4 (http://www.ncbi.nlm.nih.gov). Evolutionary studies show that the first of these gene duplication events took place 300

Mya leading to the establishment of TLR10 in the mammalian lineage. This was followed by the emergence of TLR1 and TLR6 in placental mammals 130 Mya (Temperley et al., 2008). This presumably increases the diversity of agonists that the host is able to recognize. The extracellular domains of TLRs were also found to have a higher functional divergence compared to the cytoplasmic TIR domain, suggesting that the ECD is important for ligand recognition (Zhou, et al., 2007).

Studies on chicken TLRs have revealed that they possess two TLR1 genes that share ancestral origins with the TLR1-6-10 cluster in mammals and two additional TLR isoforms that share origins with TLR2 (Temperley et al., 2008). The chicken TLRs are thought to predate the mammalian duplication events of the TLR1-6-10 cluster. Co-expression of chTLR1 with chTLR2 resulted in lipopeptide-mediated NF-kB activation, suggesting that the ligand recognition function predates the mammalian divergence of the TLR1-6-10 cluster (Keestra et al., 2007; Temperley et al., 2008). As a result, human TLR10 has been speculated to be a potential partner for TLR2. In addition, the independent maintenance of TLR10 and its associated TIR domain suggest a distinct biological role for this receptor (Roach et al., 2005). Another unusual aspect about TLR10 is that there is no homologue in mice due to the interruption of the mouse TLR10 gene by deletions and retroviral gene insertion (Hasan et al., 2005). However, TLR10 is conserved in rat, pig, cow, dog, macaque, platypus, and opossum among other mammals (Temperley et al., 2008).

TLRs 1, 2, 6, and 10 are differentially expressed in various cell types, as measured by mRNA transcript levels. TLR1 is highly or ubiquitously expressed in most cell types (Muzio et al., 2000). TLR2 is widely expressed in myeloid-derived cells

(including monocytes, macrophages and dendritic cells), non-myeloid cells (such as endothelial and epithelial cells), and B cells. TLR expression pattern also depends on maturity of cells. In immature dendritic cells, for example, TLR1 and TLR2 are expressed at high levels, but gradually decrease as the DCs mature. Expression of TLRs is also upregulated in the presence of their specific agonists [Reviewed in (Akira & Hemmi, 2003)]. Unlike the wide expression pattern of TLR1 and TLR6, TLR10 expression appears to be more tissue- and cell type- specific, indicative of the functional divergence of TLR10 from the other two receptors. TLR10 mRNA is highly expressed in lymphoid tissues such as the spleen, lymph nodes, thymus, tonsils, and lung (Chuang & Ulevitch, 2001). The analysis in isolated cell types has shown a high level of TLR10 expression in the B cell lineage and weak expression in plasmacytoid dendritic cells (pDC), a cell type known to produce large amounts of IFNs upon recognition of viral components by TLRs (Bourke et al., 2003; Hasan et al., 2005).

TLR2 recognizes a wide variety of molecules such as bacterial lipoproteins, atypical lipopolysaccharide (LPS) from non-enteric bacteria, peptidoglycan and lipoteichoic acid (LTA) from Gram-positive bacteria, lipomannans and lipoarabinomannans from mycobacteria, zymosan yeast particles, and microbial components from spirochetes [Reviewed in (Takeda & Akira, 2005)]. The extracellular domain of TLR2 has been confirmed to interact directly with peptidoglycan from *S. aureus* (Iwaki et al., 2002) and the yeast cell wall particle zymosan (Sato et al., 2003). Studies in TLR2 knockout mice have demonstrated that TLR2 is absolutely required for cellular response to *Staphylococcus aureus* peptidoglycan and mycoplasmal lipopeptide (Takeuchi et al., 1999). Using TLR1- and TLR6-deficient mice, it has been shown that

TLR2 cooperates with TLR1 and TLR6 for the recognition of triacylated and diacylated lipopeptides, respectively (Ozinsky et al., 2000; Sandor et al., 2003; Takeuchi et al., 2001; Takeuchi et al., 2002; Wyllie et al., 2000). It has also been shown that human TLR10 interacts with TLR2 by co-immunoprecipitation experiments, suggesting that TLR10 acts as another TLR2 co-receptor (Guan et al., 2010; Hasan et al., 2005). Recently, several studies have shown that TLR2 also serves as the receptor for endogenous ligands such as β-defensins (Funderburg et al., 2007; Gariboldi et al., 2008; Lee et al., 2008), eosinophil-derived neurotoxins (Yang et al., 2008), acute-phase serum amyloid A proteins, and high-mobility group box 1 (HMGB1) (Park et al., 2004; van Zoelen et al., 2009).

TLR2 knockout mice serve as an excellent model for assessing the importance of the inflammatory response induced by TLR2 ligands in protecting the host from diseases. Studies using TLR1- and TLR2-deficient mice have shown that TLR1 and TLR2 are necessary for signaling induced by the triacylated outer surface lipoprotein (OspA) from *Borrelia burgdorferi* (Alexopoulou et al., 2002), the causative agent of Lyme disease. TLR2 knockout mice infected with *B. burgdorferi* have a higher bacterial load and develop greater ankle swelling due to Lyme arthritis several days post infection compared to their wild-type littermates (Wooten et al., 2002). Macrophages from TLR2-deficient mice are unresponsive to lipoproteins and are characterized by the lack of IL-6 production (Wooten et al., 2002).

TLR2 deficient mice have also served to establish TLR2 function in response to *Streptococcus pneumoniae* and *Listeria monocytogenes* infection. Serum IL-6 levels and bacterial load in the blood and peripheral organs were similar for both wild-type and

TLR2-deficient mice. However, it was observed that there is a higher bacterial load in the brain of TLR2 knockout mice compared to wild-type mice. As a result, TNF-α levels in the central nervous system are also greater in the TLR2-deficient mice. This increase correlated with an earlier time of death in untreated knockout mice due to pneumococcal meningitis (Echchannaoui et al., 2002).

The role of TLRs in disease

TLRs are important components in the regulation of both innate and adaptive immunity. Activation of TLRs in response to microbial infection leads to the production of a variety of proinflammatory cytokines, chemokines, and costimulatory molecules, an excess of which could lead to profound deleterious effects, including septic shock and death. A number of reports have implicated TLRs in the pathogenesis of chronic inflammatory and infectious diseases. TLR2, for example, has been linked to candidiasis (Netea et al., 2004), diabetes (Kolek et al., 2004), and cardiomyopathy (Eriksson et al., 2003). It is quite logical to assume that there must be a mechanism that tightly regulates TLR-mediated activation of these proinflammatory molecules. Several mechanisms of negative regulation of TLR-mediated immune response exist [Reviewed in (Liew et al., 2005)], some of which include production of extracellular decoy receptors, transcriptional regulation of TLRs, and prevention of intracellular signaling.

Iwami et al. reported the existence of naturally-occurring soluble forms of TLR4 in mice (Iwami et al., 2000). This soluble mouse TLR4 inhibited LPS-mediated TNF-α production as well as NF-kB activation in mouse macrophage cell lines (Iwami et al., 2000). Naturally occurring soluble forms of TLR2 (varying in molecular weight) have been detected in human plasma, breast milk, and saliva (Kuroishi et al., 2007; LeBouder

et al., 2003). Stimulation of monocytes with Pam_3Cys in the presence of soluble TLR2 inhibits IL-8 production (LeBouder et al., 2003). Moreover, immunodepletion of soluble TLR2 from serum increases sensitivity of peripheral blood monocytes to Pam_3Cys, as evidenced by increased IL-8 production (LeBouder et al., 2003). Ongoing studies in the lab (Johnson and Tapping, unpublished results) have shown that upon stimulation of monocytes with synthetic ligands for TLR2, there is an upregulation of TLR2 transcription and a down-regulation of both TLR1 and TLR6 required for TLR2 signaling, suggesting a regulatory response. How upregulation of TLR2 transcription correlates with the production of soluble TLR2 remains to be elucidated.

Mutations in TLRs have profound effects on the development of inflammatory diseases. In humans, numerous polymorphisms have been associated with inflammatory diseases. For example, polymorphisms in the TLR4 gene have been linked to the development of septic shock from Gram-negative bacterial infections. The single nucleotide polymorphism D299G has been identified in human patients that exhibit poor response to LPS upon inhalation, thus making them susceptible to systemic inflammatory syndrome and an increased risk of septic shock (Agnese et al., 2002). As expected, since patients with the D299G polymorphism exhibit diminished response to Gram-negative pathogens, they have a decreased risk of atherosclerosis (Kiechl et al., 2002). In TLR2, patients that were heterozygous for the R753Q polymorphism were protected from late stage Lyme disease due to their impaired pro-inflammatory cytokine responses to lipoproteins from *Borrelia* (Schröder et al., 2005).

MyD88 is a key adaptor molecule that functions downstream of all TLRs (with the exception of TLR3) and MyD88-deficient mice are susceptible to numerous

pathogens. A genetic study performed on nine children with a history of recurring pyogenic bacterial disease revealed deleterious mutations in the *MyD88* gene. Fibroblast cell lines isolated from these *MyD88*-deficient patients stimulated with IL-1β exhibit no phosphorylation of the mitogen-activated protein kinases (MAPKs) p38 and c-Jun N-terminal kinase (JNK), and no production of IL-6, IL-8, interferon-β (IFN-β), and IFN-λ. Interestingly, recurring severe infections are no longer clinically observed in patients beyond 6 years of age, suggesting either there are other redundant innate immune mechanisms independent of the MyD88 signaling pathway that compensate for the clearance of pathogens, or the development of the adaptive immune system at later age compensates for the MyD88 mutation (von Bernuth et al., 2008). In an earlier study, children suffering from recurring infections and poor inflammatory response were found to have a deficiency in IRAK-4, thus affecting the TIR-IRAK signaling pathway. Blood cells and fibroblast cells from these patients did not respond to agonists for TLRs 1 through 6 and TLR9, based on the absence of NF-kB and p38-MAPK activation (Picard et al., 2003).

Accessory molecules that assist in TLR recognition of agonists

Some TLRs possess accessory molecules that increase their sensitivity towards minute amounts of agonists. Accessory molecules of TLRs also direct specific downstream signaling events, as in the case of TLR4, which uses MAL to activate the MyD88 pathway and TRAM to engage the TRIF pathway (Figure 1.1). As previously mentioned, TLR4 is the receptor for LPS molecules from Gram-negative bacteria. TLR4 recognition of LPS requires the assistance of three different accessory molecules, namely the LPS-binding protein (LBP), CD14, and MD-2. LBP is a serum protein that binds to

LPS (Tobias et al., 1986) and catalytically delivers it to CD14, rendering cells more sensitive to LPS by at least 1,000-fold (Wright et al., 1990). CD14 is a GPI membrane-anchored glycoprotein in myeloid cells (Antal-Szalmas et al., 1997; Haziot et al., 1988; Setoguchi et al., 1989), but a soluble form of the protein is also found in the serum (Funda et al., 2001; Haziot et al., 1993). Both membrane-bound and soluble forms of CD14 are able to mediate LPS responses (Frey et al., 1992; Lee et al., 1993). Several biophysical studies have demonstrated that CD14 delivers the monomeric form of LPS to MD-2 (Gioannini et al., 2005; Nagai et al., 2002). Myeloid differentiation factor 2 (MD-2) is a small protein that physically associates with TLR4 and confers LPS responsiveness to TLR4 (Hoshino et al., 1999; Schromm et al., 2001). Taken together, LBP delivers monomeric LPS to CD14, which then presents the agonist to either soluble MD-2 or to MD-2 bound to TLR4.

Accessory molecules also directly assist in TLR2 stimulation [Reviewed in (Botos et al., 2011; Kang & Lee, 2011). LBP has been shown to physically bind various TLR2 agonists, and enhance TLR2 sensing of microbial agonists in cell-based assays (Schröder et al., 2004; Schröder & Schumann, 2005). However, very little information is available about how LBP interacts with TLR2. Additionally, it is not well understood how CD14 mediates lipopeptide recognition and how it delivers the agonist to the TLR1/2 complex. There have been conflicting reports on the affinity of CD14 for lipidated agonists. Also, conflicting reports have been made with regards to how CD14 enhances Pam_3CSK_4 recognition of the TLR1/2 complex. Using fluorescence resonance energy transfer (FRET), confocal microscopy, and flow cytometry to demonstrate protein interactions, Manukyan *et al.* (Manukyan et al., 2005) proposed that CD14 facilitates binding to

lipoprotein, followed by formation of a stable receptor complex composed of lipoprotein, CD14, TLR2, and TLR1. Similarly, using both coimmunoprecipitation experiments as well as surface plasmon resonance analysis, Nakata et al. (2006) demonstrated that CD14 enhances recognition of the synthetic triacylated lipopeptide Pam_3CSK_4 by the TLR1/TLR2 complex and that it directly binds Pam_3CSK_4. However, in contrast to the results generated by Manukyan et al. (2005), they showed that CD14 does not coimmunoprecipitate with the TLR1/TLR2 receptor complex, suggesting that it does not stably bind to the complex. Despite all these data, the sequence of events following ligand recognition by TLR2, in cooperation with TLR1 remains ill-defined and therefore requires further studies.

The role of the extracellular domain of TLRs in ligand recognition

Even though TLR1 and TLR6 are highly homologous, the greatest amount of variation occurs in the ECD, which is the region responsible for ligand recognition (Takeuchi et al., 1999). The TLR ECD forms an evolutionarily conserved structure comprised of the leucine rich repeat (LRR) motifs. Each LRR is typically made up of 22-29 amino acid residues starting with a consensus sequence of LxxLxLxxN (Bell et al., 2003; Botos et al., 2011; Kang & Lee, 2011). TLR1, TLR2, and TLR6 each have 20 LRRs with N-terminal LRR-NT and C-terminal LRR-CT capping modules (Jin et al., 2007; Kang et al., 2009). Upon protein folding, the LRRs stack upon one another to form a solenoid structure with each LRR forming a complete turn of the solenoid. The entire solenoid is bent with a concave and convex side. The hydrophobic residues of each LRR form short β-strands that collectively form parallel β sheets lining the concave side (Bella

et al., 2008). The convex side is made up of loops and α-helices formed by the variable regions of each LRR (Bella et al., 2008).

To date, the crystal structures of seven TLRs in complex with their respective agonists have been solved: TLR1/TLR2/Pam_3CSK_4 (Jin et al., 2007), TLR2/TLR6/Pam_2CSK_4 (Kang et al., 2009), TLR4/MD2/LPS (B. S. Park et al., 2009), TLR3/double-stranded RNA (Liu et al., 2008), TLR5/FliC flagellin (Yoon et al., 2012), and TLR8/single-stranded RNA (Tanji et al., 2013). The TLR4/MD-2/LPS complex reveals that five of the six lipid chains of LPS are buried inside the hydrophobic pocket of MD-2, which is in turn anchored to the concave surface of the TLR4 ECD. The sixth lipid chain of LPS interacts with hydrophobic phenylalanine residues on the surface of the neighboring TLR4 that is also bound to another MD-2 and LPS molecule (Park et al., 2009). In the TLR3-dsRNA crystal structure, a double stranded RNA that is at least 45bp in length is sandwiched between the glycan-free surface of two TLR3 ECDs, with the dsRNA interacting at two sites in each of the TLR3 ECD – one near the N-terminus and the other near the C-terminus (Leonard et al., 2008; Liu et al., 2008). In the TLR5 complex, one TLR5 ECD binds one molecule of FliC flagellin, and together, this TLR5-FliC heterodimer binds to another TLR5-FliC to form a functional quaternary complex that is stabilized by a couple of interaction sites between FliC and the convex surface of the neighboring TLR5 molecule. TLR8 has been demonstrated to exist as a pre-formed homodimer that undergoes conformational changes upon binding to two molecules of a small/short single-stranded RNA ligand (Tanji et al., 2013). The unifying theme taken from all these available TLR-ligand crystal structures is that upon ligand binding, the TLRs undergo conformational changes to form a stable “m-shaped” complex that allows

the TIR cytoplasmic signaling domains of the two interacting TLRs to come into close proximity with one another. This sets the stage for intracellular signaling (Figure 1.2).

Early mutational studies mapped the region of the TLR2 extracellular domain responsible for ligand recognition. Seven LRR motifs at the N-terminal region of the TLR2 extracellular domain are not required for recognition of di- or tri-palmitoylated peptides (Meng et al., 2003). Moreover, it has also been shown that the LRR regions 7-12 of TLR2 are critical for species-specific recognition of triacylated lipopeptides (Grabiec et al., 2004). Similarly, domain swapping experiments on the extracellular domain of TLR 1 and TLR 6, each containing 19 LRR motifs, have shown that LRRs 9-12 of both TLR1 and TLR6 are important for recognizing ligands specific to these receptors (Omueti et al., 2005). Interestingly, a naturally-occurring but rare variant of TLR1 with a single nucleotide polymorphism P315L located at the outer loop of LRR motif 11 exhibits attenuated responses towards synthetic lipopeptide as well as a variety of other microbial agonists (Omueti et al., 2007). These early mutational studies performed on the TLR1 and TLR2 ECD provided solid support for the crystal structure of TLR1/TLR2/Pam_3CSK_4 later solved by Jie-Oh Lee and colleagues (Jin et al., 2007).

TLR2 is unique because instead of forming homodimers, it heterodimerizes with either TLR1 or TLR6 to recognize triacylated and diacylated lipoproteins, respectively. Lipoproteins are potent agonists of TLR2 and its co-receptors, which bind to the extracellular domain of the TLRs tightly and induce dimer formation by orienting the receptors in their proper signaling conformation. The triacylated synthetic agonist Pam_3CSK_4 coordinately binds TLR1 and TLR2. Two ester-bound palmitoyl chains are bound with a hydrophobic binding pocket of TLR2, while the single amide-bound

palmitoyl chain is accommodated within a narrow hydrophobic channel of TLR1 (Jin et al., 2007) (Figure 1.3). In TLR6, two phenylalanine residues (F343 and F365) block the entrance to its lipid-binding channel thus leading to the selectivity of the TLR2/TLR6 pair for diacylated lipopeptides (Kang et al., 2009).

Thesis outline

Despite the availability of the TLR1/TLR2/Pam_3CSK_4 crystal structure, it remains unclear as to how TLR2 and its co-receptors recognize naturally-occuring ligands to form the ternary complex and how accessory proteins play a role in the delivery of monomeric forms of microbial agonists to the TLRs. It has been proposed that the large surface area of the TLR extracellular domain confers TLRs with the ability to bind a broad range of ligands (Bell et al., 2003), but there has been very little work showing the physical interaction of the TLR2 sub-family of receptors to their respective natural agonists. The studies described here aim to further our understanding of the molecular mechanisms by which TLR2, in cooperation with either TLR1 or TLR10, recognize a wide array of PAMPs and form a stable ternary complex.

This chapter provides an overview of Toll-like receptors (TLRs), focusing on the members of the TLR2 sub-family. Chapter 2 describes the biophysical studies we performed to elucidate the role of LBP and CD14 in TLR1/TLR2/Pam_3CSK_4 ternary complex formation. These studies utilized functional soluble forms of human LBP, CD14 and the extracellular domains of TLR1 and TLR2. LBP and CD14 are accessory molecules known to be required in TLR4/MD2 sensing of LPS. Even though several studies have shown that both LBP and CD14 can bind to known TLR2 agonists, it is not clear how the two proteins play a role in the delivery of agonists to TLR1/TLR2 system.

We performed size exclusion chromatography experiments to demonstrate that the addition of substoichiometric amounts of either LBP or soluble CD14 (sCD14) to a mixture of TLR1, TLR2, and Pam_3CSK_4 significantly enhances ternary complex formation. Western blot analyses of the eluted fractions from the size exclusion column show that neither LBP nor sCD14 are physically associated with the final TLR1-TLR2-Pam_3CSK_4 ternary complex. We also show that a naturally-occurring lipoprotein agonist from *B. burgdorferi*, outer surface protein A (OspA), can induce TLR1/TLR2 ternary complex formation. Furthermore, this complex formation can be enhanced by the addition of LBP and sCD14. Cell-based assays likewise reveal that the addition of either LBP or sCD14 to TLR1/TLR2-transfected HEK 293F cells grown in serum-free media can independently sensitize the cells to low amounts of either Pam_3CSK_4 (0.6nM) or OspA (0.036nM), with sCD14 requiring a longer time to bind to the agonist prior to delivery to the TLRs. The amount of agonists used is approximately 20-fold lower than the typical amount (~13nM for Pam_3CSK_4) used for stimulation assays. Our results show that either LBP or sCD14 can drive ternary complex formation by acting as a mobile carrier of the triacylated lipopeptide Pam_3CSK_4 or lipoprotein OspA. These findings define a critical role for LBP and CD14 in TLR2 signaling with implications for improved drugs designed to target this receptor system.

Chapter 3 describes our efforts to quantitatively measure TLR-ligand interactions in order to assess the competition between TLR1 and TLR10 for the lipopeptide agonist and the co-receptor TLR2. We performed microtiter plate assays to qualitatively measure receptor-agonist interactions and demonstrated specificity of TLR2 binding to either TLR1 or TLR10 in the presence of a triacylated lipopeptide agonist. TLR2-Pam_3CSK_4

was also found to prefer TLR1 over TLR10 in our plate assays. Using the Octet system and purified proteins, we were able to measure the strength of TLR binding to a 12kDa lipoprotein and found that TLR1 has the highest affinity to the lipoprotein followed by TLR10, and finally by TLR2. However, we failed to get kinetic measurements for ternary complex formation due to the nature of both the purified proteins and the amphipathic nature of the lipopeptide agonist. The challenges encountered with the biosensors are discussed in detail in this chapter.

Chapter 4 is a follow-up to the study initiated by Dr. Katherine Omueti, a previous graduate student in the laboratory. In her dissertation, she was able to generate TLR1 and TLR6 chimeric receptors via domain swapping experiments to demonstrate the extracellular regions required for recognition of the lipopeptides. Using the synthetic triacylated and diacylated agonists (Pam_3CSK_4 and Pam_2CSK_4, respectively), she was able to show that LRRs 9-12 of TLR1 and TLR6 are important for discrimination of the two ligands. Here we show that the same region (LRRs 9-12) of the TLR1 ECD is required for recognition of a variety of microbial cell wall components. To further delineate the residues important for TLR1 function, we screened a library of TLR1 clones with various single amino acid substitutions within LRRs 9 through 12 that were previously generated by random mutagenesis. We found that the amino acids F314, P315, and Q316 within LRR 11 and V339 within LRR12 of TLR1, are involved in mediating cellular responses to other microbial agonists for TLR1/TLR2. The results demonstrate that regardless of the molecular structure of the agonist, the same critical residues of TLR1 are required for formation of an “m-shaped” heterodimeric complex with TLR2 to initiate cellular activation. We attempted to demonstrate complex

formation of TLR1/TLR2 with either *P. gingivalis* LPS or mycobacterial lipomannan in solution using size exclusion chromatography. Unfortunately, we were never able to detect complex formation in solution, possibly due to a lower binding affinity of TLRs to non-lipoprotein agonists.

Finally, Chapter 5 is a summary chapter that integrates all the work done and the findings described in previous chapters. Here we highlight the contributions and implications of this work to the exponentially expanding field of TLR studies. Because of their role as a first line of host defense against certain microbial pathogens, TLR2 and its co-receptors may be a potential target for treating TLR-mediated inflammatory diseases. For example, understanding the role of accessory molecules LBP and CD14 could help treat lipoprotein-induced bacterial sepsis by blocking their ability to deliver lipoproteins to the TLRs. Knowing the order of ternary complex formation may be helpful in targeted gene therapy in which either inhibitory monoclonal antibodies against TLRs or soluble TLRs that compete with their membrane-bound counterparts may be used for treatment. Identifying the critical regions in the TLR1 extracellular domain important for ligand recognition and formation of a dimer interface with the co-receptor TLR2 can aid in the design of inhibitory compounds that can compete with the natural agonists in order to prevent the formation of a signaling ternary complex. Thus, understanding the molecular mechanism of how TLR2 signaling, in cooperation with either TLR1 or TLR10, is initiated would greatly facilitate the development of new therapeutic strategies for dampening microbial agonist-induced inflammation.

Figures

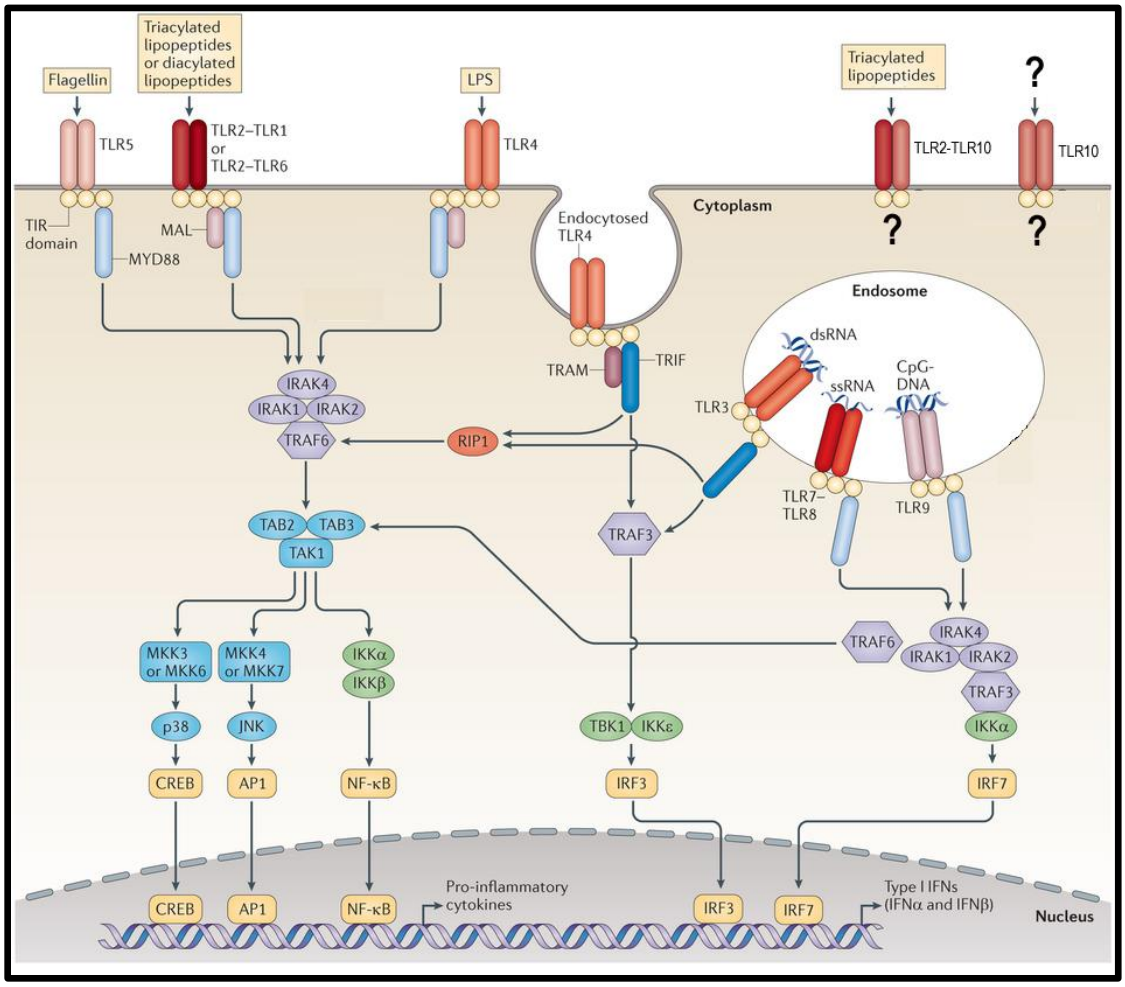

Figure 1.1. Mammalian TLR signaling pathways. To date, 10 TLRs have been identified in humans[1].

[1] Figure adapted from O'Neill, LAJ *et al.* 2013. Nat. Rev. Immunol 13:453-460.

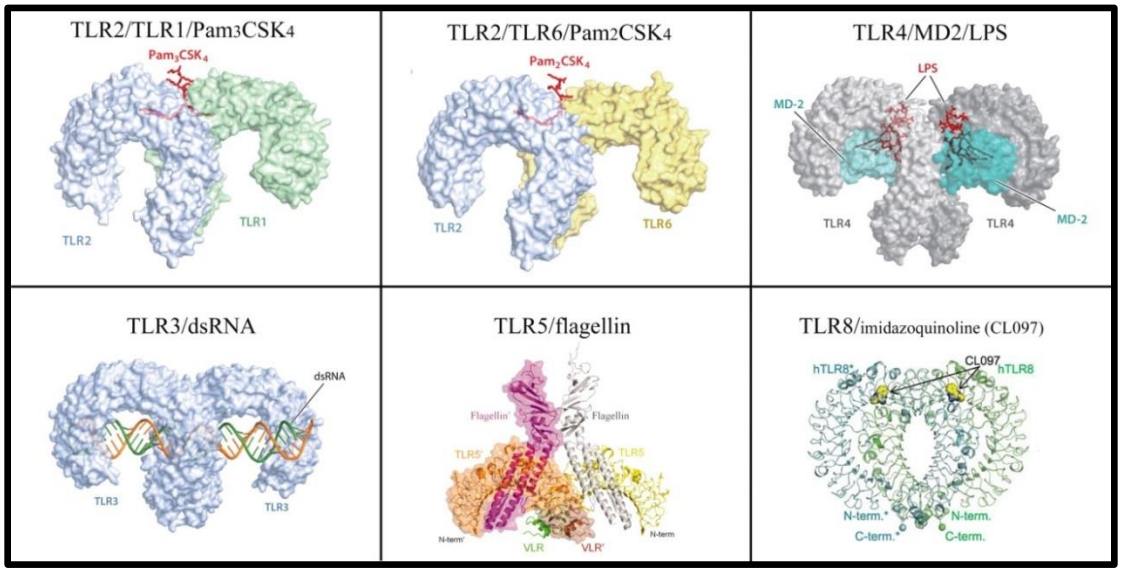

Figure 1.2. The overall shape of the TLR-ligand complexes is strikingly similar[2].

[2] Figure adapted from Kang, JY and Lee, J. 2011. Annu. Rev. Biochem. 80: 917-941; Yoon, S *et al*. 2012. Science 335: 859-864; and Tanji, H *et al*. 2013. Science 339: 1426-1429.

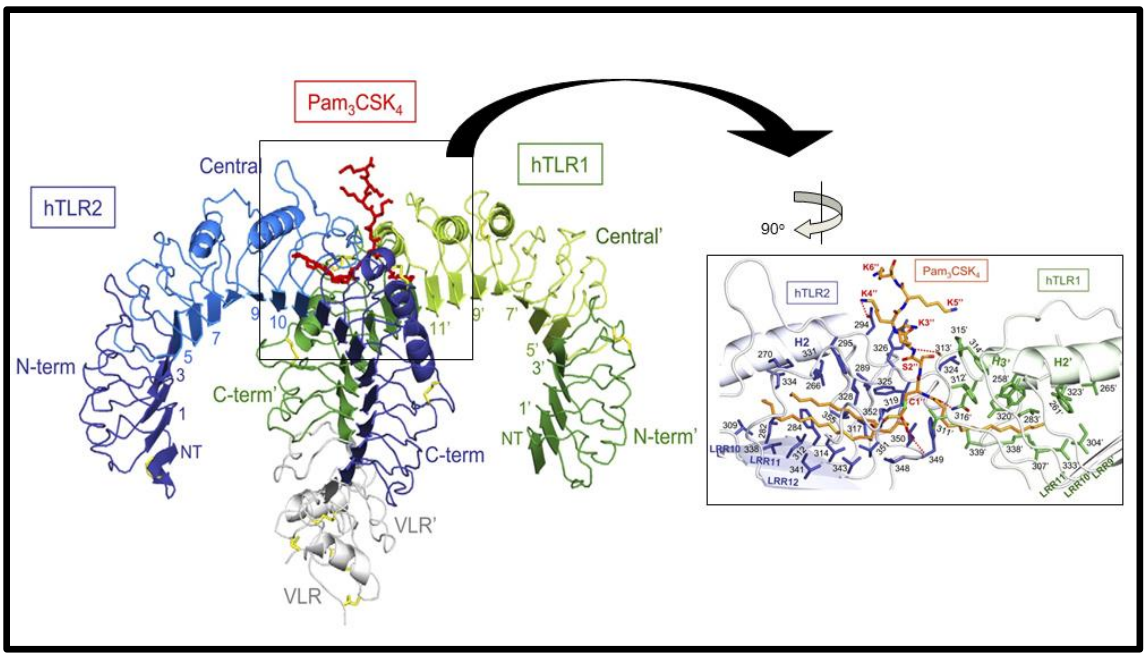

Figure 1.3. The crystal structure of TLR1/TLR2/Pam$_3$CSK$_4$ ternary complex[3].

[3] Figure adapted from Jin, MS *et al.* 2007. Cell 130: 1073-1075.

CHAPTER TWO

HUMAN LBP AND CD14 INDEPENDENTLY DELIVER TRIACYLATED LIPOPROTEINS TO TLR1 AND TLR2 AND ENHANCE FORMATION OF THE TERNARY SIGNALING COMPLEX[4]

Introduction

As central elements of the innate immune system Toll-like receptors provide a first line of immune defense against infectious agents. Through direct sensing of bacterial, fungal or viral components TLRs activate intracellular signaling events that drive the cellular expression and release of immune mediators (Akira et al., 2009). These activation events not only induce inflammatory processes, but also initiate and orchestrate the long lasting protective responses of the adaptive immune system (Iwasaki & Medzhitov, 2004). Humans possess 10 TLR family members, numbered 1 through 10, subsets of which are expressed in leukocytes and the epithelial cells of mucosal surfaces (Muzio et al., 2000; Zarember & Godowski, 2002). TLRs 1, 2, 4 and 6 are expressed on the plasma membrane, sense microbial and fungal cell wall components and stimulate the production of classic proinflammatory molecules. TLRs are type-1 transmembrane receptors comprised of an extracellular leucine rich repeat domain and an intracellular TIR (Toll-Interleukin-1Receptor homology) signaling domain. TLRs signal via ligand-induced receptor dimerization resulting in the juxtaposition of two TIR domains which act as a scaffold for the recruitment of proximal signaling adaptor molecules (Akira et al., 2006; O'Neill, 2008).

[4] Ranoa, D.R.E., Kelley, S.L., and Tapping, R.I. *Journal of Biological Chemistry*. 2013 April 5, 288(14): 9729-9741.

The potent proinflammatory activity of Gram-negative bacterial lipopolysaccharide (LPS; endotoxin) can be largely ascribed to activation of the cell surface TLR4 complex (Poltorak et al., 1998). MD-2, a small secreted protein associated with TLR4, is largely responsible for the direct binding of LPS; an event that results in TLR4 homodimerization and proinflammatory gene expression (Nagai et al., 2002; Shimazu et al., 1999). LPS is a highly amphipathic molecule that naturally exists in solution as large aggregates. LPS-binding protein (LBP) and CD14 are two proteins whose coordinate actions result in the disaggregation and delivery of LPS monomers to the TLR4-MD-2 complex. LBP is a 60kDa glycoprotein, and a member of the fatty-acid binding protein superfamily, which is expressed in the liver and released into the bloodstream (Schumann et al., 1990; Tobias et al., 1986). CD14 is a 55kDa GPI membrane-anchored glycoprotein on myeloid cells (Antal-Szalmas et al., 1997; Haziot et al., 1988; Setoguchi et al., 1989; Wright et al., 1990) and also exists as a soluble protein found in a variety of body fluids (Funda et al., 2001; Haziot et al., 1993). Numerous biophysical studies have revealed that CD14 delivers LPS monomers to MD-2 (da Silva Correia et al., 2005; Kim et al., 2007; Nagai et al., 2002; Park et al., 2009; Poltorak et al., 1998; Shimazu et al., 1999; Teghanemt et al., 2008). Since CD14 binds LPS aggregates poorly, the efficiency of TLR4-mediated cell activation is greatly enhanced by LBP which quickly disaggregates LPS and then catalytically delivers LPS monomers to CD14 (Schumann et al., 1990; Wright et al., 1990). In the presence of both LBP and CD14, the sensitivity of TLR4-expressing cells to LPS is enhanced more than 100-fold (Martin et al., 1992; Schumann et al., 1990; Ulevitch & Tobias, 1999).

TLR2 mediates inflammatory responses to a wide variety of lipidated microbial components including bacterial lipoproteins, atypical lipopolysaccharides, and lipomannans (Hirschfeld et al., 2001; Lien et al., 1999; Vignal et al., 2003). Among these microbial agonists, bacterial lipoproteins are by far the most potent (Hirschfeld et al., 1999; Lien et al., 1999; Ozinsky et al., 2000; Takeuchi et al., 1999). OspA, an outer surface protein of the lyme disease-causing bacterium *Borrelia burgdorferi*, is a widely studied bacterial lipoprotein with potent TLR2 stimulatory activity (Brandt et al., 1990; Erdile & Guy, 1997; Morrison et al., 1997). The immunogenic activity of OspA requires the N-terminal acyl chains of the lipoprotein (Erdile et al., 1993; Weis et al., 1994). Pam_3CSK_4 is a triacylated N-terminal analogue of OspA and is a widely used synthetic lipopeptide agonist for TLR2 (Hoffmann et al., 1988). TLR2-mediated cellular responses are the result of microbial agonist-induced TLR2 heterodimerization with either TLR1, TLR6 or TLR10 (Guan et al., 2010; Takeuchi et al., 2000; Takeuchi et al., 2001). The crystal structure of human TLR1 and TLR2 bound to Pam_3CSK_4 reveals that the lipopeptide coordinately binds to both receptors to form a stable TLR1-TLR2-Pam_3CSK_4 ternary signaling complex (Jin et al., 2007). In this coordinate binding, two acyl chains of Pam_3CSK_4 accommodate a hydrophobic pocket of TLR2 and the third acyl chain accommodates a narrow hydrophobic channel of TLR1 (Jin et al., 2007). These lipopeptide binding interactions drive TLR1 and TLR2 dimerization enabling the two intracellular TIR domains to form a scaffold which subsequently recruits adaptor molecules necessary for signaling (Jin & Lee, 2008).

Similar to LPS, LBP and CD14 have been shown to sensitize cells to lipopeptides and lipoproteins (Schröder et al., 2004; Sellati et al., 1998). Since LPS, lipopeptides and

lipoproteins are all amphipathic it has generally been assumed that similar to their interaction with LPS, LBP functions to disaggregate lipopeptide for delivery to CD14 which subsequently delivers monomeric lipopeptide agonist to the corresponding TLR. However, the mechanism that underlies LBP- and CD14-mediated lipoprotein sensitization has not been formally explored. In this study, we examined the role of LBP and CD14 in the physical generation of the ternary TLR1-TLR2-lipopeptide complex by performing biophysical measurements with functional soluble forms of the TLR1 and TLR2 extracellular domains. We found that either LBP or sCD14 was able to independently enhance ternary TLR1-TLR2-Pam_3CSK_4 complex formation even at sub-stoichiometric concentrations, and that neither protein is associated with the final ternary complex. We also found, in cell based assays, that the sensitivity of cells to minute amounts of agonist was enhanced by the addition of either LBP or sCD14.

Materials and Methods

Reagents

The synthetic bacterial lipopeptide (S)-[2,3-Bis(palmitoyloxy)-(2-RS)-propyl]-N-palmitoyl-(R)-Cys-(S)-Ser-(S)-Lys_4-OH•3HCl] (Pam_3CSK_4) was purchased from Enzo Life Sciences (formerly Alexis Biochemicals; Plymouth Meeting, PA). The non-acylated synthetic peptide S-[2,3-bis(acetyloxy)-(2RS)-propyl]-[R]-cysteinyl-[S]-seryl-[S]-lysyl-[S]-lysyl-[S]-lysyl-[S]-lysine x 3 CF_3COOH (Ac_2CSK_4) was purchased from EMC Microcollections (Tuebingen, Germany). The recombinant outer surface protein A (OspA) purified from *Borrelia burgdorferi* bacterial extract (Recombitek Lyme) was purchased from Merial Inc. (Athens, GA).

HRP-conjugated anti-FLAG (clone M2) monoclonal Ab was purchased from Sigma Aldrich (St. Louis, MO), while the HRP-conjugated anti-hemagglutinin (HA) monoclonal antibody was purchased from Miltenyi Biotec Inc. (Auburn, CA). Unconjugated polyclonal anti-human LBP and anti-human CD14 goat IgG antibodies were kind gifts from Dr. Peter Tobias (The Scripps Research Institute, La Jolla, CA). Anti-OspA rabbit IgG polyclonal antibody was purchased from Rockland Immunochemicals, Inc. (Gilbertsville, PA). The secondary antibodies, HRP-conjugated rabbit anti-goat IgG and HRP-conjugated goat anti-rabbit IgG were purchased from Jackson ImmunoResearch Laboratories (West Grove, PA). The unconjugated anti-human TLR1 mAb (clone GD2.F4, CD281) and anti-human TLR2 mAb (clone T2.5, CD282) were obtained from eBioscience (San Diego, CA).

Human LBP from Xoma Corp. (Berkeley, CA) was generously provided by Dr. Theresa L. Gioannini and Dr. Jerrold P. Weiss (University of Iowa, Iowa City, IA). Low endotoxin albumin from bovine serum was purchased from Sigma Aldrich (St. Louis, MO), and human serum albumin (25%) was obtained from Octopharma (Hoboken, NJ). Human soluble CD14 used in HEK 293F cell-based assays was purchased from Peprotech Inc. (Rocky Hill, NJ).

Construction and expression of soluble TLR-Fc fusion proteins

Soluble extracellular domains of FLAG-tagged TLR2, HA-tagged TLR1, and HA-tagged $TLR1_{P315L}$ were produced using the hybrid LRR technique described by Jin, MS *et al*. (Jin et al., 2007). The soluble TLR-Fc fusion expression vectors were constructed by overlap extension PCR using primers and methods described previously (Guan et al., 2010). Briefly, coding regions for the extracellular domains of TLR1 or

TLR2 (aa 22-476 and 17-508, respectively) were fused to the highly conserved LRR C-terminal capping module of a hagfish variable lymphocyte receptor (VLRB.61) by overlap extension PCR and subsequently cloned as *Bgl*II/*Nhe*I fragments into a modified pDisplay vector (kindly provided by Dr. David M. Kranz, Department of Biochemistry, University of Illinois at Urbana Champaign). This vector contains the Fc domain of human IgG1 downstream of the NheI site, and the sequence for either the FLAG or HA tag upstream of the *Bgl*II site. A thrombin cleavage site (LVPRGS) was added at the 3'-end of the TLRvlr hybrid to allow cleavage of the soluble TLR from the Fc fusion protein. Recombinant DNA plasmids were verified by DNA sequencing (UIUC Core Sequencing Facility).

Freestyle HEK 293F cells (Invitrogen Life Technologies) were adapted to grow in Freestyle serum-free expression medium (Invitrogen Life Technologies). Adherent cells were cultured at 37˚C in a humidified environment containing 5% CO_2. Stable HEK 293F cell lines expressing soluble TLR2, TLR1, and $TLR1_{P315L}$ were generated by transfection followed by G418 selection and limiting dilution as previously described (Guan et al., 2010). Stable cell lines were grown in Freestyle serum-free expression medium containing 0.25 mg/ml G418 and cultured in suspension at 37^{o}C with continuous shaking at 125 rpm in a humidified environment containing 8% CO_2.

Purification of soluble TLRs

Soluble TLR-Fc fusion proteins were purified from stable HEK 293F cell supernatant by affinity chromatography using Protein G sepharose for fast flow (GE Healthcare; Piscataway, NJ) on an AKTA prime purification system (GE Healthcare), as previously described (Guan et al., 2010). The Fc tag was removed after the first round of

purification by adding restriction grade thrombin protease (Novagen; Madison, WI) at a concentration of 1U thrombin per 0.25mg TLR-ECD-Fc protein. After 18 hours incubation at room temperature, the TLR extracellular domain was separated from the Fc fragments by another round of affinity chromatography in the AKTA prime system using a 1ml pre-packed protein A column (Pierce, Rockford, IL) and PBS pH 7.4 running buffer. The TLRs were concentrated from the flow-through using an Amicon Ultra-4 centrifugal device (Millipore) and centrifuged at 2500xg for 15-25 minutes at 4^{o}C, to a volume of 0.5ml. The concentrated protein was then loaded on a Superdex 200 10/300GL gel filtration column (GE Healthcare) in PBS pH 7.4 running buffer at a flow rate of 0.5 ml/min. The eluted fractions containing monomeric TLR extracellular domains were pooled and concentrated using size exclusion centrifugation (Amicon). Final protein concentration after three rounds of purification was measured using the Pierce BCA protein assay kit (Rockford, IL). The protein yield for recombinant soluble TLR1, $TLR1_{P315L}$, and TLR2 were 0.5mg, 0.3mg, and 0.25mg per liter of media, respectively. Protein purity was determined by mass spectrometry (Mass Spectrometry Laboratory, School of Chemical Sciences, University of Illinois at Urbana-Champaign) using MALDI as the ionization technique and sinapinic acid as a calibration matrix.

Soluble TLR ELISA assays

Briefly, 0.5 ug/mL of commercially available anti-TLR 1 (clone GD2F4) and anti TLR2 (clone T2.5) monoclonal antibodies were coated onto 96-well microtiter plates at 4^{o}C overnight. Non-specific binding was blocked by 5% BSA in PBS. Diluted samples of purified sTLR proteins (1.0 ug/mL) were added to the wells, and incubated at room temperature for 2 hours. Binding of soluble TLR1 and TLR2 to their respective

antibodies was detected using HRP-conjugated anti-HA antibody and HRP conjugated anti-FLAG antibody, respectively, followed by the addition of o-phenylenediamine (OPD) substrate. The colorimetric detection was quantified by measuring absorbance at 490 nm.

Soluble TLR competition assays

SW620 cells (a human colonic epithelial cell line, ATCC CCL-227) were seeded in 24-well plates overnight at a density of $1x10^5$ cells/ml in RPMI 1640 media supplemented with 10% (v/v) FBS and 2mM L-glutamine. Cells were co-transfected with full-length genes for membrane bound TLR2 and TLR1 together with a firefly luciferase gene driven by the IL-8 promoter and a Renilla luciferase gene driven by a basal promoter (pRL-null) as a transfection control (Promega; Madison, WI). Transfections were performed using a cationic lipid agent, Fugene-6 (Roche), at a 4:1 lipid:DNA ratio. Forty-eight hours post-transfection, the media was replaced with Gibco Opti-mem media (Invitrogen Life Technologies) and the cells were stimulated for 6 hours by the addition of the triacylated agonist Pam_3CSK_4 (10ng/ml) with or without sTLR2 or sTLR1 (1ug/ml). Following the manufacturer's protocol for the dual luciferase assay (Promega), cell lysates were collected 6 hours post-stimulation and analyzed for firefly and Renilla luciferase activity using a BioTek Synergy HT plate reader (BioTek; Winooski, VT). The transfection efficiency across different wells was normalized by dividing the firefly luciferase activity by the Renilla luciferase control.

Generation of bioactive soluble CD14

Human soluble CD14 protein was cloned, expressed, and purified as previously described (Kelley et al., 2012), with the following exceptions. Briefly, human CD14 (aa 1-337) was amplified from genomic DNA and cloned into a modified pDisplay vector (kind gift from Dr. David Kranz, University of Illinois, Urbana-Champaign), preceding a thrombin cleavage site (LVPRGS) and the Fc domain of human IgG1. The final construct was sequenced (UIUC Sequencing Center) following site directed mutagenesis (C306S) via primer extension to avoid unnatural disulfide bonding resulting from the truncated coding region of our construct. Following transfection and stable selection of human HEK 293F cells (Invitrogen), human soluble CD14 was purified from cell supernatant in three chromatographic steps, including protein G affinity chromatography, thrombin cleavage, protein A affinity chromatography, and size-exclusion chromatography. Finally, fractions containing CD14 were pooled and concentrated to 10 mg/mL using an Amicon Ultra-4 unit (Milipore) as measured by Pierce BCA assay (Rockford, IL). Human soluble CD14 (aa 1-337; C306S) was stored at 4^{o}C for up to 6 months and is bioactive as measured by LPS binding activity and ability to facilitate LPS-induced IL-8 production from human epithelial SW620 cells (Kelley et al., 2012).

Size exclusion chromatography assays

The TLR1-TLR2-lipopeptide ternary complex was formed by pre-incubating 0.25uM TLR2, 0.25uM TLR1, and 2.5uM Pam_3CSK_4 (with or without 0.05uM LBP and/or 0.25uM sCD14) in PBS pH 7.4 buffer to a final volume of 0.5ml. The mixture was incubated in a 37^{o}C water-bath for 2 hours and injected into a Superdex 200 10/300GL gel filtration column (GE Healthcare) at a flow rate of 0.5 ml/min in PBS pH 7.4 running

buffer. Twenty minutes after injection of the sample, 0.5ml fractions were collected covering one column bed volume (about 24ml, 48 min). The chromatogram was recorded using a manual UV recorder. The data was then re-plotted using the xyExtract v5.1 graph digitizer software (Wilton and Cleide Pereira da Silva; Campina Grande, Paraíba, Brazil).

Eluted fractions were separated on a 7.5% SDS-PAGE gel and transferred to an Immobilon-P membrane (Millipore). The membranes were blocked with 5% non-fat dry milk (NFDM) in TBS buffer containing 0.05% Tween-20. Western blotting was performed to detect TLR1 and TLR2 using HRP-conjugated anti-HA and anti-FLAG antibodies (both diluted at 1:1000 in 5% NFDM), respectively. LBP and/or CD14 was detected using either a polyclonal goat anti-LBP or goat anti-CD14 (diluted 1:500 in 5% NFDM), followed by a HRP-conjugated rabbit anti-goat IgG polyclonal antibody (diluted 1:5000 in 5% NFDM). Chemiluminescence was detected using the Pierce ECL Western blotting substrate (Rockford, IL). Membranes were then exposed to a HyBlot CL autoradiograpy film (Denville Scientific Inc.; Metuchen, NJ) and developed.

Cell activation assays

HEK 293F cells were seeded in a 48-well tissue culture plate overnight at a density of $1.6x10^5$ cells/ml (50,000 cells/well) in Freestyle serum-free expression medium (Invitrogen Life Technologies). Cells were co-transfected with 50ng each of TLR1 and TLR2 together with 75ng of a firefly luciferase reporter gene driven by an NF-kB promoter and 25ng of a Renilla luciferase (pRL-null) transfection control (Promega; Madison, WI). Transfections were performed using a cationic lipid agent, 293fectin (Invitrogen), at a 3:1 lipid:DNA ratio. Forty-eight hours post-transfection, LBP, sCD14 (Peprotech), or a combination of both, was added to the wells to a final concentration of

0.1ug/ml. Cells were then stimulated with 1 ng/ml agonist for 6 hours. Alternatively, LBP and/or sCD14 were pre-incubated with the agonists for 1 hour at 37^{o}C prior to addition to cells. Following the manufacturer's protocol for the dual luciferase assay (Promega), cell lysates were collected and analyzed for NF-kB-luciferase and renilla activity using a BioTek Synergy HT plate reader (BioTek; Winooski, VT). The transfection efficiency across different wells was normalized by dividing the IL-8 luciferase activity with the Renilla activity.

Results

Purified soluble TLRs are monomeric and biologically functional

To define the role of LBP and sCD14 in driving the formation of a TLR1-TLR2-lipoprotein ternary complex, recombinant soluble extracellular domains of TLR1 and TLR2 were isolated and purified from HEK 293F cells by affinity chromatography (See Materials and Methods). As expected, both proteins were isolated and verified as monomeric proteins by gel filtration chromatography (Figs. 2.1A and 2.1B). The size of the protein monomers were estimated using gel filtration standard markers that are composed of globular proteins. Based on these standard proteins, TLR1 and TLR2 were estimated to have a relative molecular weight of about 65 kDa and 83 kDa, respectively. This is slightly different from the molecular mass calculated by mass spectrometry (70.65 kDa for TLR1 and 71.85 kDa for TLR2) since TLRs are extended proteins and not globular in nature. TLR1 and TLR2 were recognized by their respective monoclonal antibodies and did not exhibit any cross reaction indicating that each protein is properly folded (Fig. 2.1C).

To assess the biological activity of the purified proteins, we performed TLR reconstitution experiments in human epithelial cells (SW620) and measured the relative expression of a luciferase reporter gene driven by the human IL-8 promoter. As expected, luciferase expression was induced in cells transfected with TLR1 and TLR2 upon stimulation with 10ng/ml Pam_3CSK_4. However, upon addition of either soluble TLR1 or soluble TLR2, SW620 cells showed diminished responses to Pam_3CSK_4, suggesting that each soluble receptor has bioactivity presumably by either actively competing for the agonist or by forming a signaling-deficient complex with the transmembrane TLR partner (Fig. 2.1D).

LBP and sCD14 enhance TLR1-TLR2-Pam_3CSK_4 formation but are not part of the stable ternary complex

To measure receptor complex formation, we performed size exclusion chromatography using a Superdex 200 column (GE Healthcare) to distinguish monomeric TLRs from larger TLR complexes. First, we pre-incubated equimolar amounts of soluble TLR1 and TLR2 in the absence of agonist for two hours at 37^{o}C, but did not observe the formation of larger TLR complexes by size exclusion chromatography (Fig. 2.2A). When soluble TLR1 and TLR2 were incubated for 2 hours at 37^{o}C with a 10-fold molar excess of Pam_3CSK_4 a novel peak eluted at an earlier time compared to the monomeric proteins, which correspond to the expected size of a ternary TLR1-TLR2-Pam_3CSK_4 complex. Western blot analysis revealed that both TLR1 and TLR2 were present in the fractions that constitute the small peak with a calculated relative molecular weight of approximately 183 kDa (Fig. 2.2B). The modest peak size indicates that only a small

amount of stable ternary complex is formed from the incubation of purified soluble TLR monomers with lipopeptide agonist.

Since LBP and CD14 are known to sensitize TLR1- and TLR2-mediated inflammatory responses to lipopeptides and lipoproteins, we assessed their ability to drive ternary complex formation. To this end, purified LBP and sCD14, along with TLR1, TLR2 and Pam_3CSK_4, were incubated for 2 hours at 37^{o}C followed by size exclusion chromatography. This incubation resulted in a more robust peak corresponding to the ternary complex compared to that observed in the absence of LBP and sCD14 (Fig. 2.2C). Western blot analysis revealed that LBP and sCD14 continued to elute in fractions expected of monomers suggesting that they are not part of the final ternary complex (Fig. 2.2C). Additionally, a 2 hour incubation of LBP and sCD14 with Pam_3CSK_4 alone did not induce any higher order protein complexes (Fig. 2.2D). Ternary complexes were not formed when protein mixtures were loaded directly onto the gel filtration column, suggesting that incubation at 37^{o}C is required to form stable complexes in solution (data not shown). Taken together, these results demonstrate that LBP and sCD14 can enhance TLR1-TLR2-Pam_3CSK_4 ternary complex formation without becoming part of the stable complex.

Lipopeptide induces TLR1 and TLR2 heterodimers, but not homodimers

To demonstrate that lipopeptides induce heterodimers, and not homodimers, of TLR1 and TLR2, we incubated LBP, sCD14, and Pam_3CSK_4 together with either TLR1 alone or TLR2 alone. Size exclusion chromatography revealed that neither TLR1 nor TLR2 form homodimers even in the presence of LBP, sCD14, and excess agonist (Figs. 2.3A and 2.3B). The two peaks observed in Fig. 2.3B correspond to the size discrepancy

between the soluble TLR2 monomer (relative molecular weight of ~87.3 kDa) and the sCD14 monomer (relative moleacular weight of ~48.3 kDa). Western blot analysis revealed that even though TLR1 and TLR2 did not form stable homodimers, sCD14 behaved differently in the two conditions (Figs. 2.3A and 2.3B, right panel). In the presence of TLR1 alone (Fig. 2.3A right panel), sCD14 eluted in earlier fractions, while in the presence of TLR2, sCD14 elute in later fractions as a monomeric protein (Fig. 2.3B right panel). This suggests that sCD14 and TLR1 interact in a Pam_3CSK_4-dependent fashion. Since sCD14 behaves as a monomeric protein in the presence of all 5 components, Fig. 2.3C suggests that the binding of TLR2 to the sCD14-TLR1-Pam_3CSK_4 complex displaces sCD14 leading to formation of the final ternary TLR1-TLR2-Pam_3CSK_4 ternary complex. To our knowledge, this is the first experiment to suggest a defined order of events for ternary complex formation.

P315L is a naturally-occurring TLR1 polymorphism that has previously been shown to greatly attenuate cellular responses to synthetic lipopeptides as well as a variety of other microbial TLR1 agonists (Omueti et al., 2007). Subsequent protein crystallography work has shown that P315 is physically located at the entrance of the hydrophobic channel of TLR1 and forms part of TLR1-TLR2 dimer interface in the ternary complex (Jin et al., 2007). We generated the soluble form of the TLR1 315L variant which, similar to wild type TLR1, purified as a monomeric protein with a relative molecular weight of 77.5 kDa calculated by size exclusion chromatography and a molecular mass of 70.84 kDa measured by mass spectrometry (Figs. 2.1A and 2.1B). We have previously demonstrated that the P315L mutation destroys the epitope of GD2F4, a monoclonal antibody against TLR1 that inhibits lipopeptide-induced cell activation

(Omueti et al., 2007). As expected, GD2F4 did not bind soluble TLR1 315L in our ELISA assay (Fig. 2.1C). To directly assess the effect of the P315L mutation on complex formation, we incubated TLR1 315L with TLR2, Pam_3CSK_4, LBP, and sCD14 for two hours at 37^{o}C and analyzed the reaction products by size exclusion chromatography. In contrast to wild type TLR1, TLR1 315L did not form a stable ternary complex with TLR2 and Pam_3CSK_4 (Fig. 2.3D). The fact that TLR1 P315 is critical for ternary complex formation explains the highly attenuated responses of this naturally occurring TLR1 variant to triacylated lipopeptides.

TLR1 and TLR2 form a ternary complex with the OspA lipoprotein of Borrelia burgdorferi

We next tested our system using a naturally occurring lipoprotein, the outer surface protein A (OspA) from *Borrelia burgdorferi*. OspA is a 30 kDa membrane-associated lipoprotein with a typical tripalmitoyl-S-glycerylcysteine (Pam_3Cys) moiety covalently attached to the amino terminus of the protein (Belisle et al., 1994; Brandt et al., 1990). Although OspA has been shown to activate cells through TLR1 and TLR2, to date there has been no direct physical evidence demonstrating that OspA induces formation of a stable ternary complex. On the gel filtration column, OspA did not elute as a single peak at 30kDa, perhaps reflecting the amphipathic nature of the molecule which may drive aggregation and/or nonspecific binding to the column matrix (Fig. 2.4B). However, when TLR1 and TLR2 were incubated with a 5-fold molar excess of OspA prior to column loading, a small peak was observed in the region consistent with formation of a ternary TLR1-TLR2-OspA complex (Fig. 2.4C). When LBP, sCD14, OspA, TLR1, and TLR2 were incubated altogether, we observed a more robust peak

corresponding to the ternary complex, suggesting that addition of LBP and sCD14 enhances TLR1-TLR2-OspA ternary complex formation (Fig. 2.4E). In the absence of OspA, TLR1 and TLR2 elute as monomers (Fig. 2.4A) as do LBP and sCD14 (Fig. 2.4D). Taken together, our data demonstrate that, similar to Pam_3CSK_4, the naturally-occurring OspA lipoprotein from *B. burgdorferi* induces ternary complex formation which is enhanced by the addition of LBP and sCD14.

Either LBP or sCD14 can independently enhance TLR1-TLR2-Pam_3CSK_4 ternary complex formation

In the TLR4 system, it is known that LPS is sequentially delivered in monomeric form first by LBP to CD14 and then by CD14 to either soluble MD2 or the MD2-TLR4 complex. To validate whether both LBP and sCD14 are required to enhance TLR recognition of lipopeptide, we assessed the ability of either protein to independently enhance TLR1-TLR2-Pam_3CSK_4 ternary complex formation. Surprisingly, we observed that addition of either LBP or sCD14 to the two hour incubation independently enhanced TLR1-TLR2-Pam_3CSK_4 ternary complex formation (Figs. 2.5B and 2.5C). Consistent with our earlier Western blot data, neither LBP nor sCD14 were part of the final stable complex (Figs. 2.5B and 2.5C). Bovine serum albumin (BSA), a well-established lipid carrier protein, did not enhance ternary complex formation (compare Fig. 2.5A with Fig. 2.2B). To our knowledge, this is the first report showing that LBP can independently and directly deliver a triacylated lipopeptide to TLR1 and TLR2.

To determine if enhanced ternary complex formation is mediated by sub-stoichiometric amounts of either LBP or sCD14, varying concentrations of these proteins were independently incubated with a constant amount of TLR1, TLR2 and Pam_3CSK_4 for

two hours at 37^{o}C followed by size exclusion chromatography analysis. Sub-stoichiometric amounts of either LBP or sCD14 enhanced TLR1-TLR2-Pam_3CSK_4 ternary complex formation even at 5nM, a concentration which is 50 times lower than that of each TLR, and 500 times lower than that of the Pam_3CSK_4 agonist in the reaction (Fig. 2.6A and 2.6B). This demonstrates that neither LBP nor sCD14 is consumed in the reaction and suggests that either protein can catalytically deliver lipopeptide agonist to the TLRs. Compared to CD14, ternary complex formation was far less dependent on the concentration of LBP suggesting that LBP is a more robust catalyst than sCD14 (Figs. 2.6A and 2.6B).

Cellular responses to microbial lipoproteins are enhanced by either LBP or sCD14

To assess the biological significance of our biophysical measurements, we measured the effects of LBP and sCD14 on cellular responses to synthetic lipopeptide and natural microbial lipoprotein agonists. To this end, HEK 293F cells were transfected with full-length TLR1 and TLR2, together with a luciferase reporter gene driven by NF-κB, and then stimulated with either Pam_3CSK_4 or OspA. To ensure that the cell activation assay completely lacked endogenous sources of either LBP or CD14, the HEK 293F cells were grown in serum-free media and maintained in this media throughout the assay. In the absence of LBP or sCD14, 1ng/ml of either Pam_3CSK_4 or OspA elicited a 20-fold induction of NF-κB-driven luciferase activity that was dependent on prior transfection of the HEK 293F cells with TLR1 and TLR2 (Fig. 2.7). Nanogram levels of LBP, but not sCD14 nor human serum albumin (HSA), enhanced the sensitivity of TLR1- and TLR2-expressing HEK 293F cells to either Pam_3CSK_4 or OspA when compared to cells stimulated with agonists in the absence of any lipid carrier. We modified the same

experiment by pre-incubating either LBP or sCD14 with agonist for one hour at 37^{o}C prior to addition to the HEK 293F cells. This pre-incubation had little effect on LBP-mediated cell stimulation, but enabled sCD14 to significantly enhance the stimulation of cellular NF-kB to either Pam_3CSK_4 or OspA (Fig. 2.7). Taken together, these results demonstrate that either LBP or sCD14 can enhance cellular responses to lipopeptide or lipoprotein. This finding is entirely consistent with our biophysical studies which show that TLR1-TLR2-lipopeptide ternary complex formation is enhanced by either protein. The fact that sCD14, but not LBP, requires pre-incubation with the agonist to increase cellular responses is consistent with our biophysical data suggesting that sCD14 is a poor catalyst, compared to LBP, in the delivery of agonist to TLR1 and TLR2 (Fig. 2.6). The addition of both LBP and sCD14 further enhanced cellular responses to Pam_3CSK_4 and OspA over that of either sCD14 or LBP alone, suggesting that LBP and sCD14 may act in a cooperative manner to efficiently deliver the agonists to the TLRs (Fig. 2.7).

Discussion

LBP and CD14 have previously been shown to directly bind diacylated and triacylated lipopeptides (Schröder et al., 2004), suggesting a role in delivery of these potent agonists to the TLR2 system. Despite the abundance of evidence demonstrating direct binding of lipopeptides to LBP and CD14, only a few studies have carefully examined the functional roles of these two proteins in the activation of TLR2. sCD14 has been shown to mediate the transfer of lipopeptides to TLR2 on the cell surface of HEK 293 cells, CHO cells, and primary monocytes in vitro (Manukyan et al., 2005; Nakata et al., 2006; Vasselon et al., 2004). Pull-down assays performed with HEK cells overexpressing TLR1 and TLR2 have shown that sCD14 does not stably bind to the

TLR1-TLR2-Pam_3CSK_4 complex (Nakata et al., 2006). Additionally, immobilized TLR2 incubated with preformed lipopeptide-sCD14 complexes has been shown to bind lipopeptide but not sCD14 (Vasselon et al., 2004). Our size exclusion chromatography experiments using entirely soluble components are consistent with the above findings in that LBP and sCD14 drive formation of TLR1-TLR2-Pam_3CSK_4 ternary complexes but are not themselves part of the final complex. Interestingly, in the absence of TLR2 we observed that both CD14 and TLR1 elute in earlier fractions (Fig. 2.3A). While not proven, this observation supports a model where, upon binding lipopeptide, CD14 stably interacts with TLR1 but is then displaced by TLR2 during formation of the final ternary complex.

To date we are unaware of any studies that have formally assessed whether LBP and sCD14 function in coordinated or sequential fashion, similar to that established for the TLR4 system. Cell-based *in vitro* studies, suggest that lipopeptides are sequentially delivered from LBP to CD14 and then to TLR1-TLR2 (Schröder et al., 2003; Schröder et al., 2004). In this paper, we provide physical evidence that either LBP or sCD14 can independently catalyze the formation of a TLR1-TLR2-Pam_3CSK_4 ternary complex. Thus, unlike their non-redundant and sequential role in the delivery of LPS to the TLR4 complex, our data suggests that LBP and sCD14 are functionally redundant in the direct presentation of lipopeptides to TLR1 and TLR2. To our knowledge, this is the first report demonstrating that LBP can deliver agonists directly to the TLRs in a CD14-independent manner.

In addition to existing as a soluble protein found in body fluids (Krüger et al., 1991), CD14 also exists as a glycophosphatidylinositol (GPI) anchored membrane

receptor (mCD14) predominantly expressed on the surface of myeloid cells (Haziot et al., 1988). Flow cytometry experiments have demonstrated that LBP transfers lipopeptides to mCD14 on peripheral blood monocytes (Schröder et al., 2004). Importantly, in two independent studies, anti-CD14 antibodies have been shown to block the responses of mCD14-expressing myeloid cells to lipopeptide suggesting that in membrane form, CD14 is absolutely required for delivery of lipopeptides to TLR2 (Schröder et al., 2004; Sellati et al., 1998). While this may seem to contradict the data presented in this paper which shows a redundant function for LBP and sCD14, the mechanism of agonist delivery to TLRs may be different for membrane anchored versus soluble forms of CD14. Indeed, confocal microscopy and fluorescence resonance energy transfer studies have shown that upon lipopeptide binding, mCD14 stably physically associates with TLR1 and TLR2 (Manukyan et al., 2005). This situation is quite different from that observed for sCD14 which does not form part of the ternary complex.

Pam_3CSK_4 is a 1.5kDa amphipathic molecule which forms aggregates or micelles in solution and exhibits non-specific hydrophobic interactions. The TLRs, on the other hand, recognize monomeric forms of this triacylated lipidated agonist (Jin et al., 2007). Thus, the aggregated state of Pam_3CSK_4 in PBS buffer may explain why the formation of ternary complex in solution is inefficient and could be enhanced by the disaggregating activities of LBP or sCD14. It is well established that human LBP and CD14 directly bind to a variety of TLR2 agonists which largely comprise acylated microbial components. The agonists include bacterial lipoproteins (Sellati et al., 1998; Sellati et al., 1999; Wooten et al., 1998), Gram-positive bacterial lipoteichoic acids (Fan et al., 1999; Schröder et al., 2003), mycobacterial lipomannans and lipoarabinomannans (Elass et al.,

2007), pneumococcal peptidoglycans (Weber et al., 2003), and *Treponema*-derived glycolipids (Opitz et al., 2001). Thus, LBP and CD14 may function to disaggregate and deliver a variety of acylated microbial agonists to the TLR2 system.

LBP-deficient mice are hyporesponsive to LPS as well as to Gram-negative bacteria as evidenced by lower levels of serum inflammatory cytokines and lower survival rates following infection with *Salmonella* or *E. coli* (Jack et al., 1997; Knapp et al., 2003; Wurfel et al., 1997). In contrast, the responses of LBP-deficient mice are indistinguishable from that of wild-type mice following infection with the Gram-positive organisms *Staphylococcus aureus* (Fierer et al., 2002) and *Streptococcus pneumoniae* (Branger et al., 2004). Additionally, LBP deficiency has no effect on murine responses to intranasal infection with mycobacterial pathogens (Branger et al., 2005). Similar to LBP knockouts, CD14 deficient mice are resistant to septicemic shock mediated by either LPS injection or by Gram-negative bacterial infection (Haziot et al., 1996). However, following exposure to either live or killed *Staphylococcus aureus*, CD14-deficient and control wild-type mice exhibit similar symptoms of shock and proinflammatory cytokine production (Haziot et al., 1999). Additionally, following intravenous infection with *Mycobacterium avium*, CD14-deficient mice and wild-type control mice have indistinguishable levels of serum TNF-α production, macrophage inducible nitric oxide synthase expression and bacterial loads (Ehlers et al., 2001). The phenotypes of both LBP and CD14 knock-out mice support the idea that LBP and CD14 have a non-redundant function in the delivery of Gram-negative bacterial LPS to the TLR4 complex but a redundant function in the delivery of Gram-positive bacterial or mycobacterial components to the TLR1-TLR2 system.

Taken altogether, we have demonstrated that recognition of lipoproteins by TLR1 and TLR2 involves multiple players that assist in the delivery of agonists to the final receptor complex. Understanding this fluid and dynamic process of TLR sensing of agonists mediated by LBP and CD14 has a profound impact on therapeutic strategies designed to treat chronic inflammatory conditions, sepsis, and infection. The use of neutralizing antibodies or inhibitory molecules against human CD14 has been suggested as a possible therapeutic approach against sepsis (Piazza et al., 2010; Schimke et al., 1998). While this approach may be effective for treating Gram-negative bacterial sepsis, it may not be as effective in the treatment of sepsis caused by other bacteria due to the redundancy of function between LBP and CD14 for the direct delivery of lipoproteins, or other bacterial agonists, to the TLR1-TLR2 system.

LBP is an acute phase protein and clinical studies have shown that serum concentrations increase about 10- to 50-fold in human patients with either Gram-negative or Gram-positive bacteremia (Froon et al., 1995). While it has been shown that high concentrations of LBP in acute phase serum may confer protection to the host by inhibiting LPS response in human monocytes (Zweigner et al., 2001), the opposite has been observed for lipoproteins. Human monocytes stimulated with either triacylated or diacylated lipopeptides exhibit an increase in tumor necrosis factor (TNF) expression that is proportional to the amount of added LBP (Schröder et al., 2004). This may lead to an overwhelming systemic inflammatory response and consequently a profound deleterious effect on the host. Thus, understanding the role of LBP in the TLR2 system may be essential for treating bacterial-induced septicemia.

Figures

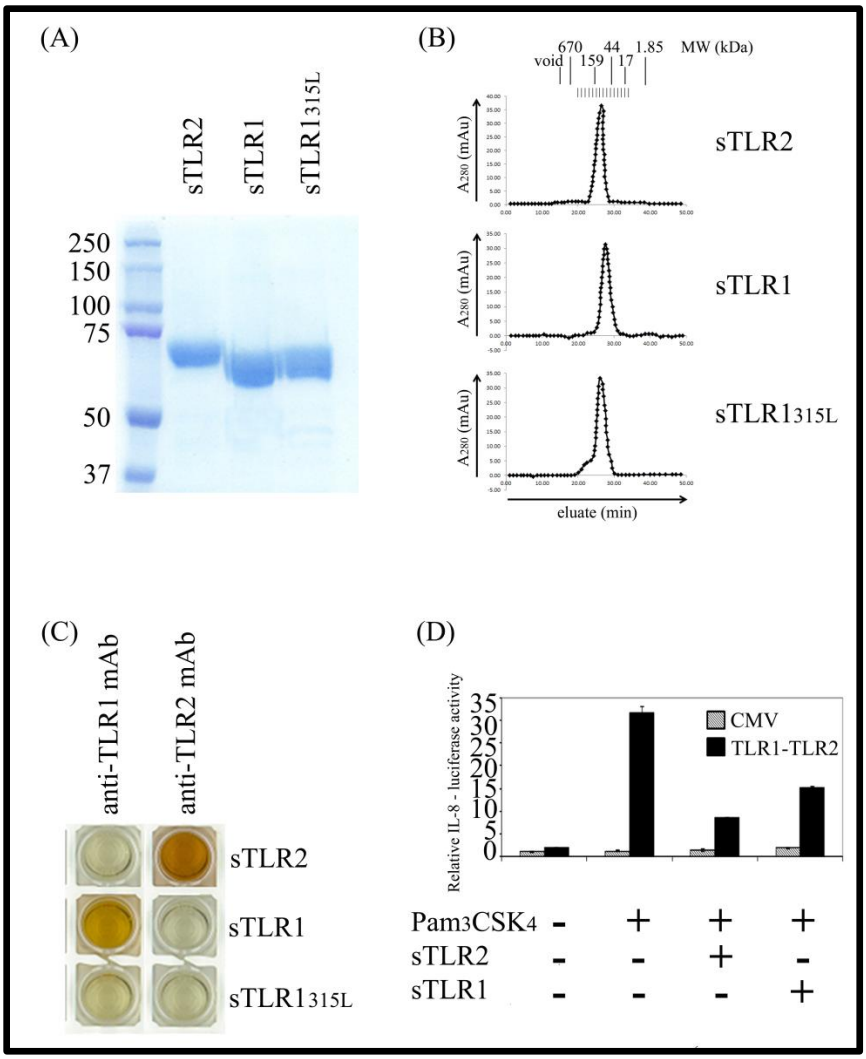

Figure 2.1. Recombinant soluble TLR (sTLR) proteins are monomeric, properly folded and biologically functional. (A) 100ug of each purified sTLR protein, as indicated, was loaded on a 7.5% SDS-PAGE gel and stained with Coomassie blue dye. (B) Each purified sTLR protein, as indicated, was analyzed by size exclusion chromatography using a Superdex 200 column. (C) Soluble TLRs were incubated in microtiter plate wells coated with either the anti-TLR1 mAb (clone GD2F4) or the anti-TLR2 mAb (T2.5), as indicated. Binding of soluble TLR1, $TLR1_{315L}$, or TLR2 was detected using either HRP-conjugated anti-HA and anti-FLAG mAbs. (D) SW620 cells were co-transfected with full length TLR1, TLR2, an IL-8 promoter-driven luciferase reporter gene and a Renilla luciferase transfection control. 48 hours post-transfection the cells were stimulated with 10ng/ml Pam_3CSK_4, with or without 1ug/ml of soluble TLR1 or TLR2, as indicated. Firefly luciferase activities were normalized to that of the Renilla luciferase control. These values were normalized to that of empty CMV vector whose value was taken as 1. Error bars represent the standard deviation of three independent events.

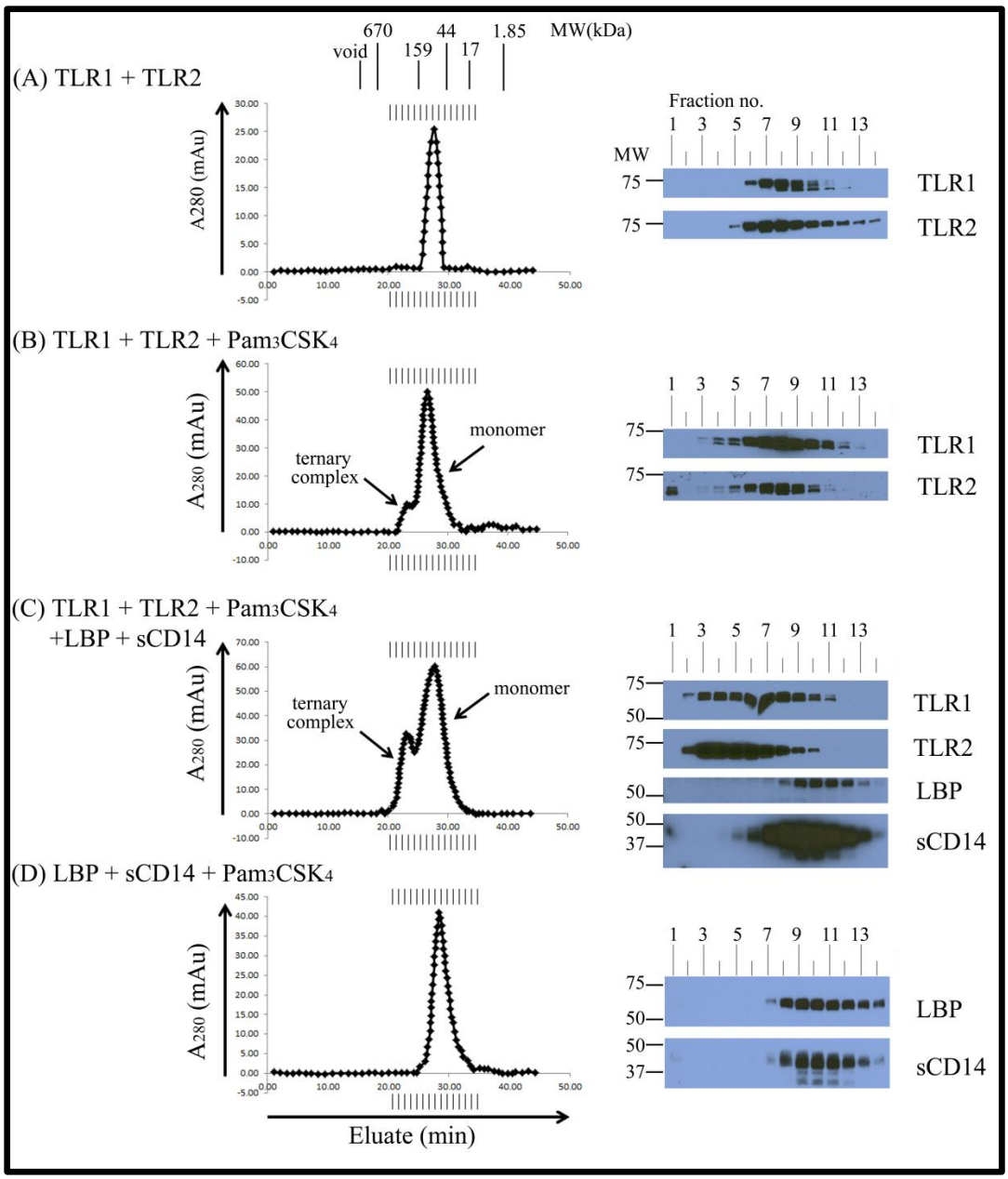

Figure 2.2. LBP and soluble CD14 enhance soluble TLR1-TLR2-Pam$_3$CSK$_4$ ternary complex formation but are not part of the final ternary complex. Various combinations of 0.25uM TLR1, 0.05uM TLR2, 2.5uM Pam$_3$CSK$_4$, 0.05uM LBP and/or 0.25uM sCD14 were incubated for two hours at 37^{o}C in a 500ul volume of PBS buffer pH 7.4, as indicated. Protein complexes were separated by size exclusion chromatography. The expected molecular weight of the TLR monomers and dimers was estimated by column calibration using known molecular weight standards. Proteins in eluted fractions were separated on a 7.5% SDS-PAGE gel, transferred by Western blotting and TLR1, TLR2, LBP or sCD14 were detected using suitable antibodies and HRP conjugates (see Materials and Methods). The results shown are representative of at least three independent experiments.

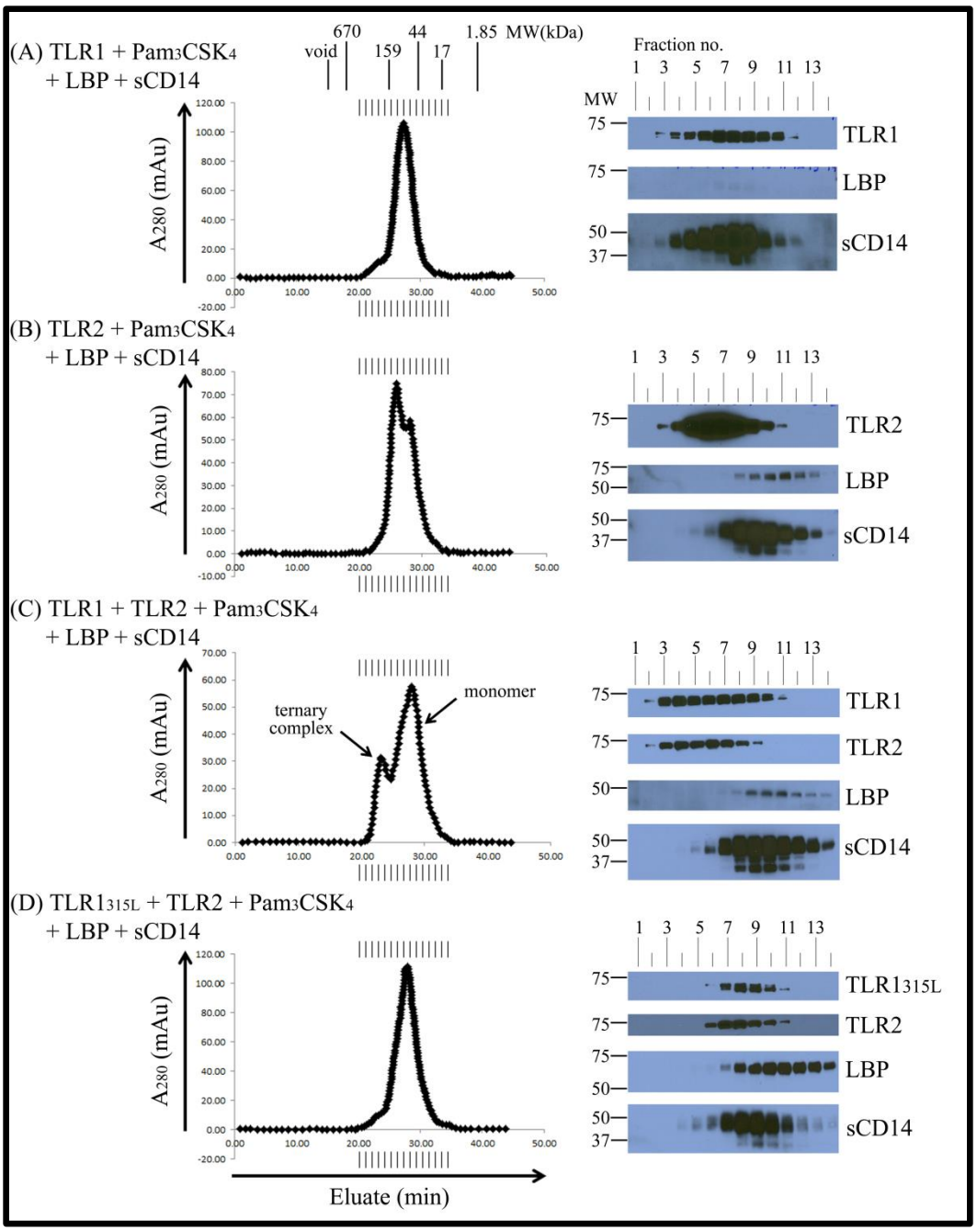

Figure 2.3. Soluble TLRs do not form homodimers when incubated with Pam_3CSK_4. 0.5uM TLR1 (A), or 0.5uM TLR2 (B), 0.25uM each of TLR1 and TLR2 (C), or 0.25uM each of $TLR1_{315L}$ and TLR2 (D) were pre-incubated with a 5 fold molar excess of Pam_3CSK_4 (2.5uM) together with 0.05uM LBP and 0.25uM sCD14 in PBS pH 7.4 buffer for two hours at 37°C in a 500ul reaction volume. Proteins and protein complexes were separated and analyzed as described in the legend of Fig. 2.2. The results shown are representative of at least three independent experiments.

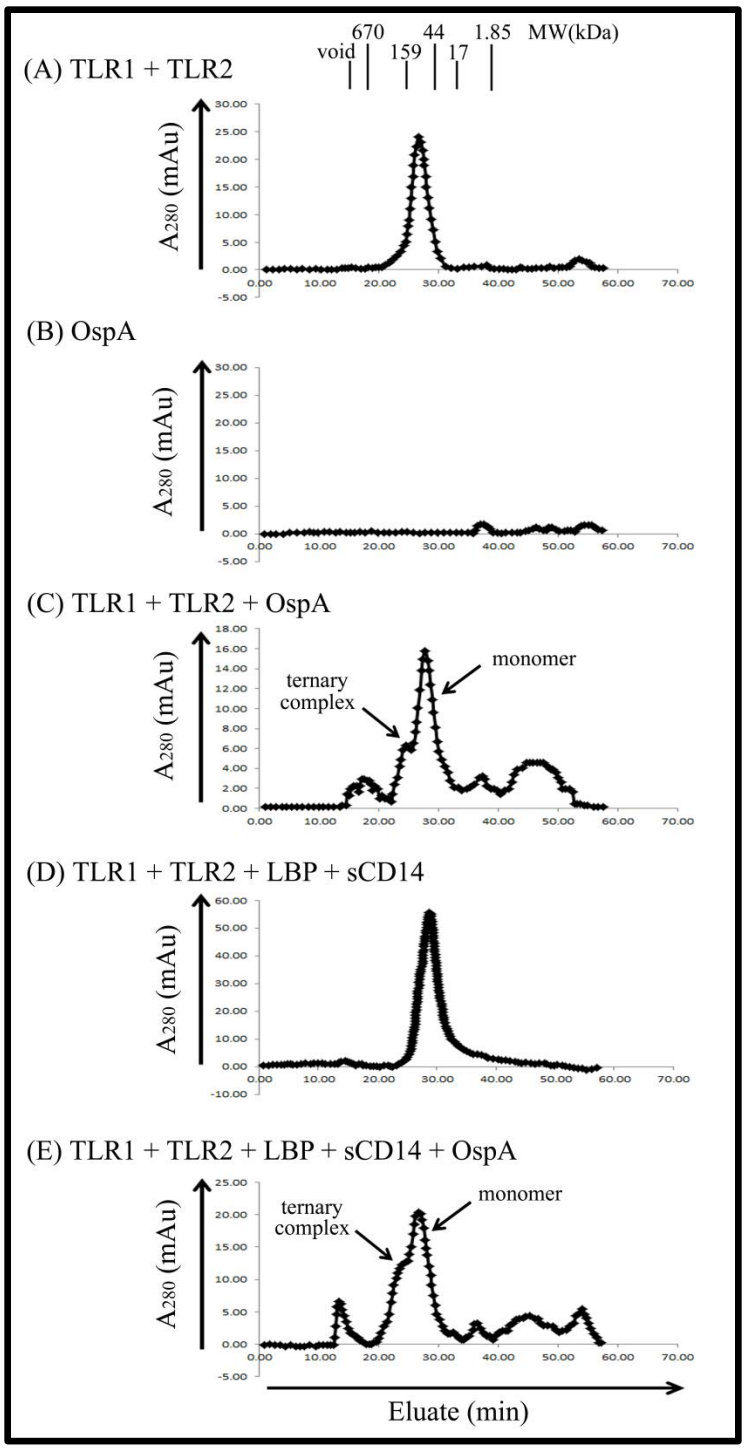

Figure 2.4. LBP and soluble CD14 enhance complex formation between TLR1, TLR2 and the OspA lipoprotein of B. burgdorferi. Various combinations of 0.25uM TLR1, 0.25uM TLR2, 1.25uM OspA, 0.05uM LBP and/or 0.25uM sCD14 were incubated for two hours at 37^{o}C in a 500ul volume of PBS buffer pH 7.4, as indicated. Proteins and protein complexes were separated and analyzed as described in the legend of Fig. 2.2. The results shown are representative of at least three independent experiments.

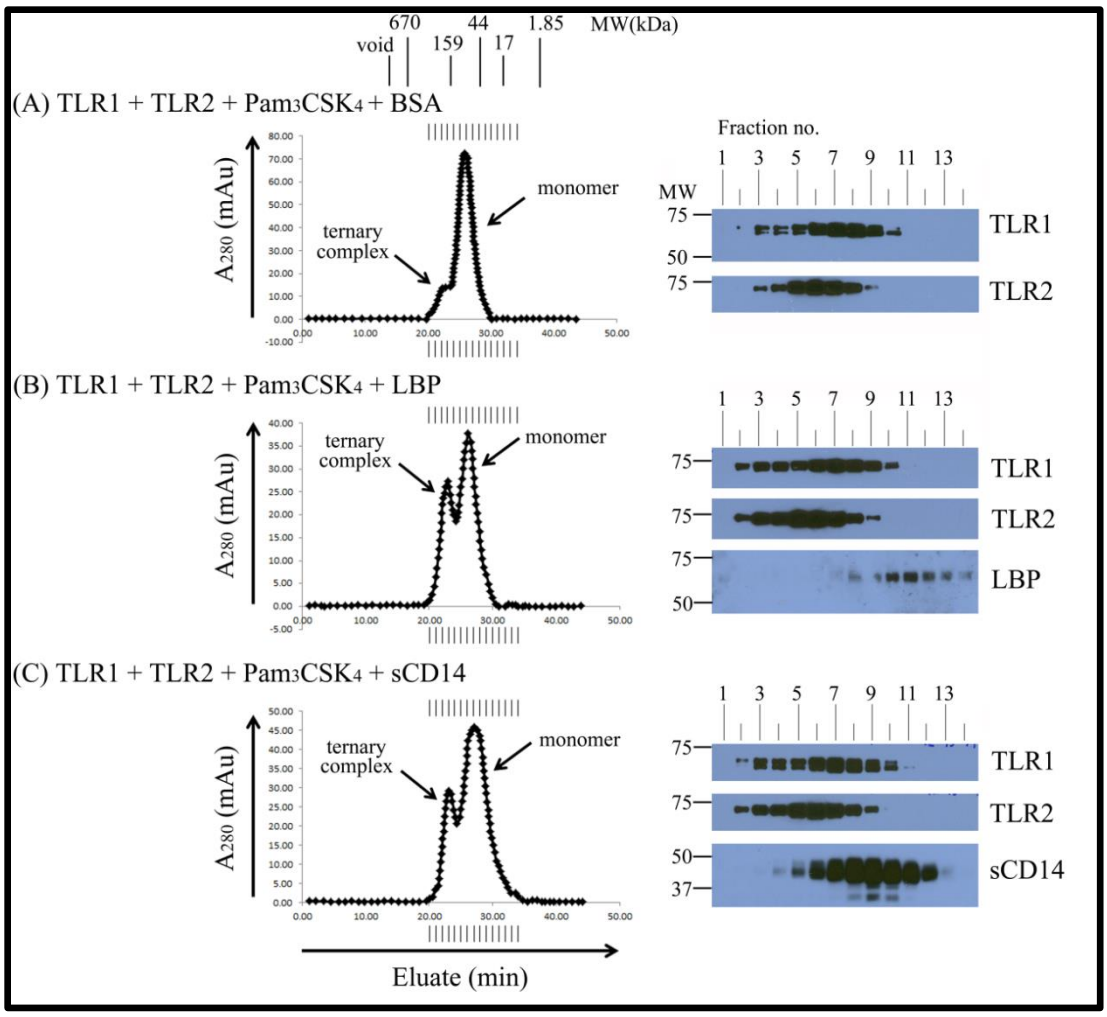

Figure 2.5. Either LBP or soluble CD14 can independently enhance TLR1-TLR2-Pam_3CSK_4 ternary complex formation. 0.25uM TLR1, 0.25uM TLR2 and 2.5uM Pam_3CSK_4 were incubated with (A) 0.25uM BSA, (B) 0.05uM LBP, and (C) 0.25uM sCD14 for two hours at 37^{o}C in a 500ul volume of PBS pH 7.4 buffer. Proteins and protein complexes were separated and analyzed as described in the legend of Fig. 2.2. The results shown are representative of at least three independent experiments.

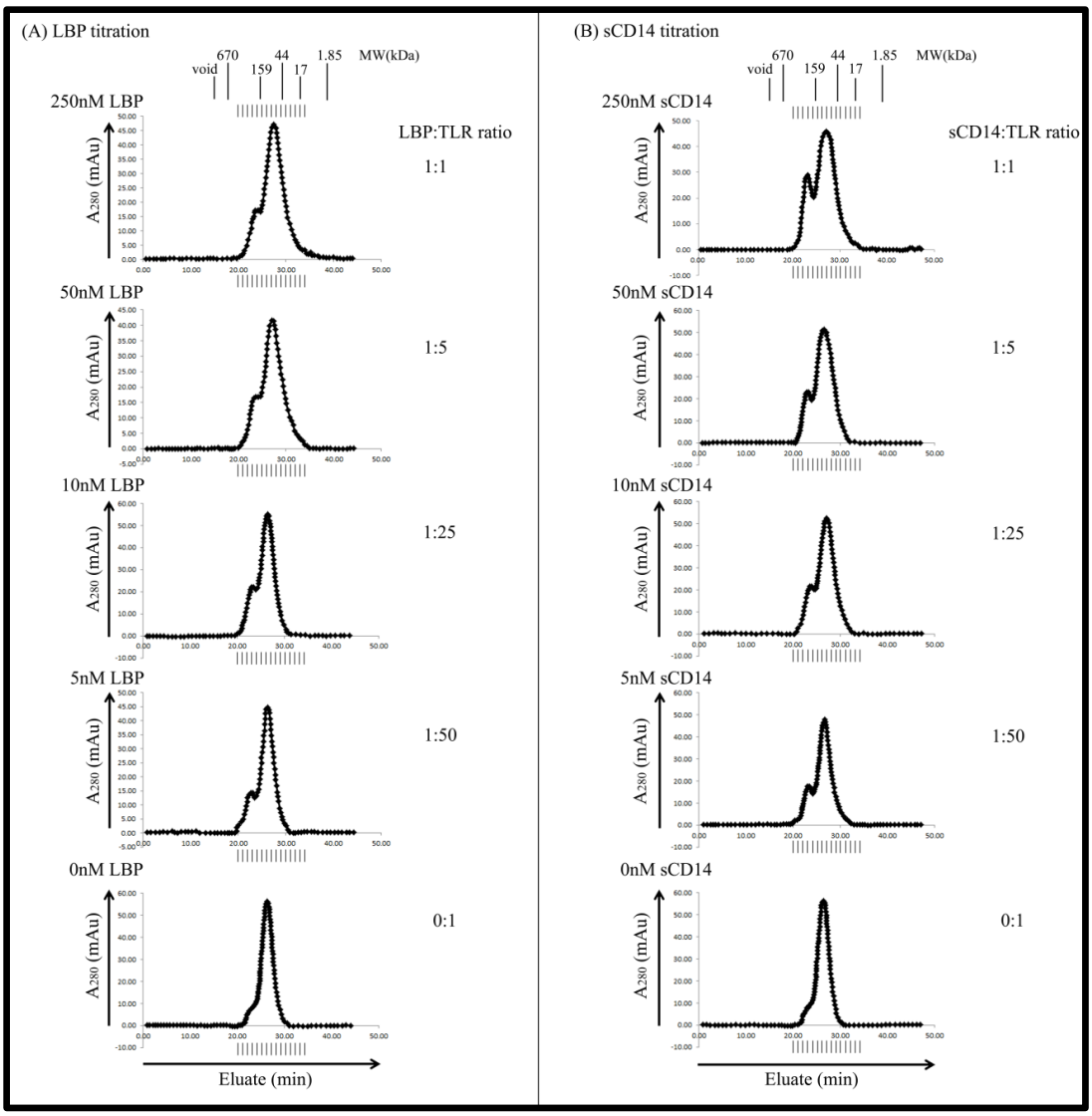

Figure 2.6. Sub-stoichiometric concentrations of either LBP or soluble CD14 are sufficient to enhance TLR1-TLR2-Pam$_3$CSK$_4$ ternary complex formation. 0.25uM TLR1, 0.25uM TLR2, and 2.5uM Pam$_3$CSK$_4$ were incubated with various concentrations (250nM, 50nM, 10nM, 5nM, and 0nM) of either LBP (left panel) or sCD14 (right panel) for two hours in a 500ul volume at 37^{o}C in PBS buffer pH 7.4. Proteins and protein complexes were separated and analyzed as described in the legend of Fig. 2.2. The results shown are representative of at least three independent experiments.

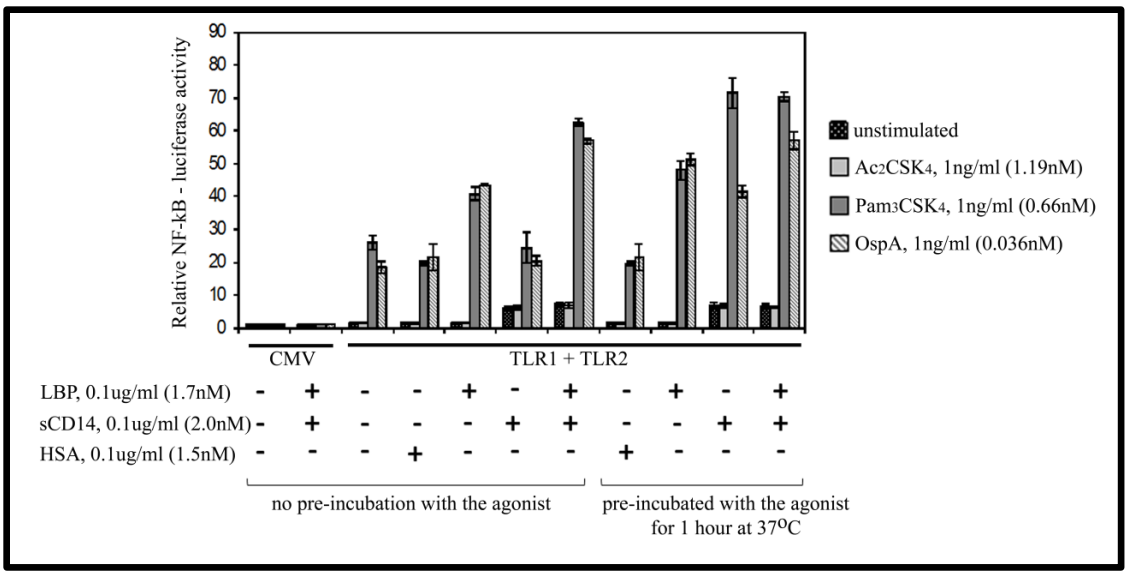

Figure 2.7. Either LBP or soluble CD14 enhance cellular responses to Pam_3CSK_4 and OspA. HEK 293F cells were co-transfected with vectors expressing full length TLR1 and TLR2, or empty CMV control vector as indicated, together with an NF-kB-promoter driven luciferase reporter gene and a Renilla luciferase reporter gene. About 48-hours post transfection cells were stimulated with 1ng/ml Pam_3CSK_4, OspA, or the non-acylated Ac_2CSK_4 control in the presence of 0.1ug/ml LBP, sCD14 or human serum albumin (HSA), as indicated (left side). In one set of experiments agonists were pre-incubated with proteins for one hour at 37°C prior to addition to transfected cells (right side). Cell Values on the Y-axis represent the level of constitutive reporter activation normalized to the empty CMV vector control (value of 1). Error bars represent the standard deviation of three independent values.

CHAPTER THREE

MEASUREMENT OF TLR-LIPOPEPTIDE INTERACTION TO ASSESS COMPETITION BETWEEN TLR1 AND TLR10 FOR MICROBIAL AGONISTS AND THE CO-RECEPTOR TLR2

Introduction

Human TLRs play an important role in the recognition of microbe-associated molecular patterns. The TLR2 subfamily, comprised of TLRs 2, 1, and 6 are differentially expressed on the surface of myeloid as well as some non-myeloid cells (Kawai & Akira, 2010). TLR2 mediates cellular responses to a wide variety of microbial cell wall components, most of which are acylated molecules. The most potent, and well characterized agonists recognized by TLR2 are lipopeptides and lipoproteins. It has been demonstrated that TLR2 requires either TLR1 or TLR6 in order to mediate cellular responses to triacylated or diacylated lipopeptides, respectively (Massari et al., 2006; Ozinsky et al., 2000; Sandor et al., 2003; Takeuchi et al., 2001; Takeuchi et al., 2002; Vasselon et al., 2004; Wyllie et al., 2000). Upon TLR2 engagement with its co-receptor and ligand, a core signaling pathway is initiated leading to the activation of NF-kB, AP-1, CREB, and other transcription factors that drive the expression of proinflammatory mediators such as cytokines, chemokines, and co-stimulatory molecules (O'Neill et al., 2013).

TLR10 is an orphan receptor that belongs to the TLR2 subfamily and is most closely related to TLR1 and TLR6. The genes encoding TLRs 1, 6 and 10 are tandemly arranged on chromosome 4 and phylogenetic analysis suggests that they arose from successive gene duplication of an ancestral gene (Roach et al., 2005). Notably, the gene

for TLR10 arose before TLR1 and TLR6, suggesting that it is independently maintained and may have a distinct function (Roach et al., 2005). This functional divergence is manifested in the unique expression profile of TLR10. Unlike the wide expression pattern of TLR1 and TLR6, TLR10 expression, as measured by mRNA levels, appears to be more tissue-specific. TLR10 mRNA is detected in lymphoid tissues such as the spleen, lymph nodes, thymus, tonsils, and lung (Chuang & Ulevitch, 2001). TLR10 is also highly expressed in B cells following stimulation with microbial agonists (Bourke et al., 2003). Despite extensive studies on TLRs, the ligand and function of TLR10 remain unknown.

Recently, it has been demonstrated that TLR2 directly interacts with TLR10 (Guan et al., 2010). Curiously, TLR2 and TLR10 recognize the same set of agonists recognized by the TLR1 and TLR2 pair (Guan et al., 2010). However, TLR2 and TLR10 fail to activate cells in response to cognate microbial agonists, suggesting that its signaling mechanism is different from its related family members (Guan et al., 2010). Whether there is a competition between TLR1 and TLR10 for its co-receptor TLR2 and/or agonist Pam_3CSK_4 is not known, but there are several cell populations that express TLR1, TLR2, and TLR10 on the surface. It is possible that TLR10 competes with TLR1 in recognition of TLR1/TLR2 agonists, and because it does not signal via the canonical TLR2-mediated signaling pathway, it may be acting as a negative regulator to dampen the immune response upon bacterial infection.

The mechanisms of ligand recognition by TLRs have not been completely investigated. The extracellular TLR2 domain directly binds to agonists that have vastly different chemical structures, e.g. lipopeptides (Vasselon et al., 2004), peptidoglycan derived from *Staphylococcus aureus* (Iwaki et al., 2002) and zymosan (Sato et al., 2003)

to name a few. The elucidation of the crystal structure of human TLR2 bound to either TLR1 or TLR6 and their respective synthetic lipopeptide agonists provided detailed insights into TLR heterodimerization and lipopeptide binding (Jin et al., 2007; Kang et al., 2009). The triacylated lipopeptide bridges the two receptors together to form an m-shaped ternary complex with two acyl chains of Pam_3CSK_4 bound by the TLR2 hydrophobic pocket found at the central LRR domain and the amide-linked lipid chain accommodated by a narrow hydrophobic channel in the convex side of TLR1 (Jin et al., 2007). Despite knowledge of the final TLR1/TLR2/Pam_3CSK_4 crystal structure, no information is available with regard to the order of assembly, binding affinity, and kinetics of TLR1/TLR2/Pam_3CSK_4 ternary complex formation. There are also conflicting reports on the existence of pre-formed TLR2 homodimers or heterodimers (Triantafilou et al., 2006) in contrast to ligand-induced ternary complex formation.

In this study, we aimed to examine the mechanism of TLR2 complex formation following recognition of microbial agonists by performing biochemical and biophysical experiments on functional soluble forms of TLR1, TLR2, and TLR10 extracellular domains (ECDs). Specifically, we defined the ligand recognition and physical interactions leading to the formation of cell-activating complexes by measuring receptor-receptor interactions in the presence or absence of the synthetic lipopeptides. Since TLR1 and TLR10 share interactions with TLR2 and common microbial agonists, we also assessed competition between these two receptors for those common components.

Materials and Methods

Reagents

The synthetic bacterial lipopeptides N-Palmitoyl-S-[2,3-bis(palmitoyloxy)-(2*R*)-propyl]-(*R*)-cysteinyl-(*S*)-seryl-(*S*)-lysyl-(*S*)-lysyl-(*S*)-lysyl-(*S*)-lysine x 3 CF_3COOH (R-Pam_3CSK_4) and the non-acylated synthetic peptide S-[2,3-bis(acetyloxy)-(2RS)-propyl]-[R]-cysteinyl-[S]-seryl-[S]-lysyl-[S]-lysyl-[S]-lysyl-[S]-lysine x 3 CF_3COOH (Ac_2CSK_4) were purchased from EMC Microcollections (Tuebingen, Germany). The Macrophage-activating lipopeptide-2, *S*-[2,3-bis(Palmityloxy)-(2*R*)-propyl-cysteinyl-GNNDESNISFKEK] (MALP-2) was purchased from Enzo Life Sciences (formerly Alexis Biochemicals; Plymouth Meeting, PA).

HRP-conjugated anti-FLAG (clone M2) monoclonal Ab was purchased from Sigma Aldrich (St. Louis, MO), while the HRP-conjugated anti-hemagglutinin (HA) monoclonal antibody was purchased from Miltenyi Biotec Inc. (Auburn, CA). The unconjugated anti-human TLR1 mAb (clone GD2.F4, CD281) and anti-human TLR2 mAb (clone T2.5, CD282) were obtained from eBioscience (San Diego, CA).

Cloning

Soluble extracellular domains of FLAG-tagged TLR2, HA-tagged TLR1, HA-tagged $TLR1_{P315L}$, and HA-tagged TLR10 were produced using the hybrid LRR technique described by Jin, MS *et al*.(Jin et al., 2007). The soluble TLR-Fc fusion expression vectors were constructed by overlap extension PCR using primers and methods described previously (Guan et al., 2010). Briefly, coding regions for the extracellular domains of TLR1 (both wild-type and a P315L mutant), TLR2, TLR6, or TLR10 (aa 22-476, 17-508, 25-481, and 20-474 respectively) were fused to the highly

conserved LRR C-terminal capping module of a hagfish variable lymphocyte receptor (VLRB.61) by overlap extension PCR and subsequently cloned as *Bgl*II/*Nhe*I fragments into a modified pDisplay vector (kindly provided by Dr. David M. Kranz, Department of Biochemistry, University of Illinois at Urbana Champaign). This vector contains the Fc domain of human IgG1 downstream of the NheI site, and the sequence for either the FLAG or HA tag upstream of the *Bgl*II site. A thrombin cleavage site (LVPRGS) was added at the 3'-end of the TLRvlr hybrid to allow cleavage of the soluble TLR from the Fc fusion protein. Recombinant DNA plasmids were verified by DNA sequencing (UIUC Core Sequencing Facility).

Cell Culture

Freestyle HEK 293F cells (Invitrogen Life Technologies) adapted to grow in Freestyle serum-free expression medium (Invitrogen Life Technologies) were cultured at 37˚C in a humidified environment containing 8% CO_2. Stable HEK 293F cell lines expressing soluble TLR1, $TLR1_{P315L}$, TLR2, TLR6, and TLR10 were generated by transfection followed by G418 selection and limiting dilution as previously described (Guan et al., 2010). Stable cell lines were grown in Freestyle serum-free expression medium containing 0.25 mg/ml G418 and cultured in suspension at 37^{o}C with continuous shaking at 125 rpm in a humidified environment containing 8% CO_2.

Protein Purification

Soluble TLR-Fc fusion proteins were purified from stable HEK 293F cell supernatant by affinity chromatography using Protein G sepharose for fast flow (GE Healthcare; Piscataway, NJ) on an AKTA prime purification system (GE Healthcare), as previously described (Guan et al., 2010). The Fc tag was removed after the first round of

purification by adding restriction grade thrombin protease (Novagen; Madison, WI) at a concentration of 1U thrombin per 0.25mg TLR-ECD-Fc protein. After 18 hours incubation at room temperature, the TLR extracellular domain was separated from the Fc fragments by another round of affinity chromatography in the AKTA prime system using a 1ml pre-packed protein A column (Pierce, Rockford, IL) and PBS pH 7.4 running buffer. The TLRs were concentrated from the flow-through using an Amicon Ultra-4 centrifugal device (Millipore) and centrifuged at 2500xg for 15-25 minutes at 4^{o}C, to a volume of 0.5ml. The concentrated protein was then loaded on a Superdex 200 10/300GL gel filtration column (GE Healthcare) in PBS pH 7.4 running buffer at a flow rate of 0.5 ml/min. The eluted fractions containing monomeric TLR extracellular domains were pooled and concentrated using size exclusion centrifugation (Amicon). Final protein concentration after three rounds of purification was measured using the Pierce BCA protein assay kit (Rockford, IL). Protein purity was determined by mass spectrometry (Mass Spectrometry Laboratory, School of Chemical Sciences, University of Illinois at Urbana-Champaign) using MALDI as the ionization technique and sinapinic acid as a calibration matrix.

Receptor binding assays using microtiter plates

HA-tagged TLR1 and TLR10 purified proteins (10 μg/ml in PBS pH 7.4) were coated onto 96-well microtiter plates at 4^{o}C overnight. For all ELISAs, binding steps were performed at room temperature in 2-(N-morpholino)ethanesulfonic acid (MES) buffer pH 7.5, and wells were washed with PBS containing 0.05% Tween-20. Non-specific binding was blocked with a commercially available blocking buffer (Pierce, Rockford, IL) for 2 hours. The wells were then washed and incubated for 2 hours with an

equimolar amount of FLAG-tagged TLR2 that had been pre-incubated for 2 h at 25°C with various concentrations of the synthetic ligands Pam_3CSK_4, MALP-2, and Ac_2CSK_4 in MES buffer pH 7.5. One set of pre-incubation reactions contained 20 μg/ml blocking anti-TLR2 mAb (T2.5). Binding of soluble TLR2 to either TLR1 or TLR10 immobilized on the wells was detected using HRP conjugated anti-FLAG antibody, followed by the addition of o-phenylenediamine (OPD) substrate dissolved in 0.05 M phosphate-citrate buffer pH 5.0 containing 0.05% H_2O_2. The colorimetric detection was quantified by measuring absorbance at 490 nm using an ELISA plate reader.

Surface plasmon resonance using BIAcore

Interactions between the triacylated synthetic lipopeptide Pam_3CSK and each of the TLR receptors 1, 2, and 10 were measured by surface plasmon resonance using the BIAcore X system (GE Healthcare). All experiments were conducted at 25^{o}C. Pam_3CSK_4 were immobilized on a carboxymethyldextran (CM5) biosensor chip using standard amine-coupling procedure through EDC [1-Ethyl-3-(3-dimethylaminopropyl) carbodiimide hydrochloride] and NHS (N-hydroxysuccinimide). Briefly, a continuous flow of 5 μl/min was maintained over the sensor in HBS-EP buffer (10 mM HEPES, 150 mM NaCl, 3 mM EDTA, and 0.005% Tween-20). The matrix of the chip was activated by a 10 min injection of 50uL of 1:1 mixture of EDC and NHS, followed by a 6 min injection of 20ug/ml Pam_3CSK_4 in 10 mM sodium acetate pH 5.5 in one flow cell, and 20ug/ml Ac_2CSK_4 in 10mM sodium acetate pH 5.5 in another flow cell. The procedure was completed by a 7-min exposure to 50ul of 1.0 M ethanolamine hydrochloride pH 8.5 to inactivate residual esters. Using MES pH 7.5 as the binding buffer, monomeric TLRs 1, 2, and 10 were injected at a flow rate of 10 μl/min over the immobilized Pam_3CSK_4

and Ac_2CSK_4 in Flow Cells 2 and 1, respectively. Varying concentration of TLRs (at 0.2uM, 0.4uM, 0.6uM, 0.8uM, 1.0uM, 2.0uM, and 4.0uM) was injected to the flow cells in each cycle for 2 minutes, followed by a dissociation time of 5 minutes. Sensors were regenerated after each cycle by sequential injection of 40ul of 1M NaCl (5 pulses) and 0.1% SDS (2 pulses) at a flow rate of 100ul/min to dissociate the analyte from the ligand and regenerate the surface back to the original baseline. The final sensograms were calculated by subtracting the signal of the control (Flow Cell 1) from that of the test (Flow Cell 2), and the results expressed in response units. The BIAcore 3.0 evaluation software was used to analyze data and generate dissociation constants for the analyte-ligand interaction.

Purification of Lipoprotein (Lip12) from E. coli

An *E. coli* Lip 12 gene cloned into pET28b vector and expressed in *E. coli* BL21 (DE3) strain were kindly provided by Dr. Peter Tobias and Dr. Hyun-Ku Lee (The Scripps Research Institute, La Jolla, CA). A 1 liter culture of Lip12-expressing *E. coli* BL21 cells (OD_{600} = 0.6) grown in LB broth supplemented with 30mM Kanamycin were induced for 3 hours with 1mM IPTG. The cell pellet obtained after centrifugation at 10,000xg for 10mins were lysed using the BugBuster Master Mix (Novagen) following the manufacturer's protocol. The expressed proteins with a COOH-terminal 6× histidine tag were batch-purified from the cell lysate by cobalt affinity chromatography using Pierce His-Pur Cobalt resin (Fisher Scientific) on a gravity column. After letting the cell lysate flow through the column, the resin was washed with a high-salt wash buffer (300mM NaCl + 50mM Na_2HPO_4 + 20mM imidazole, pH 8.0). His-tagged Lip12 proteins were eluted using a gradient elution buffer (300mM NaCl + 50mM Na_2HPO_4 +

50mM-500mM imidazole, pH 7.4). The eluted fractions containing the purified Lip 12 proteins were pooled and concentrated using a size exclusion centrifugation (Amicon), and the buffer was dialyzed to PBS pH 7.4. The final protein concentration was measured using the Pierce BCA protein assay kit (Rockford, IL).

Kinetic analysis using ForteBio Octet

The Octet analysis was performed at 37°C in PBS pH 7.4 running buffer. The buffer and samples to be analyzed were placed on a 96-well black, flat-bottom, polypropylene microplate (Greiner Bio-One) and agitated at 1000 rpm. Protein A sensor tips were equilibrated in the running buffer for 120 sec, followed by saturation with 30 μg/mL Fc-tagged TLRs for 900 sec. Unbound Fc-tagged TLRs were washed in the running buffer for another 900 sec. The sensors containing the immobilized Fc-tagged TLRs were then dipped onto wells containing Lip12 purified from *E. coli* and prepared in varying concentrations (0.0uM, 2.0uM, 5.0uM, 10.0uM, and 20.0uM). Association between the Fc-tagged TLRs and the Lip12 ligand was monitored for 900 sec and dissociation into the buffer was followed for another 900 sec. Data analysis was performed using the Octet software.

Cell stimulation assays

SW620 cells were co-transfected with various combinations of TLRs (or the empty vector pFLAG-CMV) together with a firefly luciferase gene driven by the IL-8 promoter and a Renilla luciferase gene driven by a basal promoter (pRL-null) as a transfection control (Promega; Madison, WI). Transfections were performed using a cationic lipid agent, Fugene-6 (Roche), at a 4:1 lipid:DNA ratio. Forty-eight hours post-transfection, the cells were stimulated for 6 hours with the indicated synthetic or purified

agonists. Following the manufacturer's protocol for the dual luciferase assay (Promega), cell lysates were collected 6 hours post-stimulation and analyzed for firefly and Renilla luciferase activity using a BioTek Synergy HT plate reader (BioTek; Winooski, VT). The transfection efficiency across different wells was normalized by dividing the firefly luciferase activity by the Renilla luciferase control. After correcting for transfection efficiency, all values were normalized to those of unstimulated cells transfected with the empty pFLAG-CMV vector.

Results

In order to measure protein-protein interactions in solution using biochemical and biophysical assays, we purified the extracellular domain of TLRs. As described in detail in Chapter 2, we engineered the ECD of TLRs 1, 2, 6, and 10 fused to an Fc fragment and expressed the recombinant proteins in human embryonic kidney (HEK) 293F cells. Proteins were purified from the culture supernatant of cells stably expressing the fusion proteins by affinity chromatography on a protein G column. Monomeric HA-tagged TLRs 1 (both wild-type and a P315L mutant), 2, 6, and 10, together with a FLAG-tagged TLR2, were generated after cleavage of the Fc tag and were verified to be properly folded using monoclonal antibodies that only recognize the native form of TLRs. The purified proteins were loaded on a Coomassie-stained gel to determine relative molecular weight (Figure 3.1A), and were also submitted for mass spectrometry analysis to determine their purity and molecular mass (Figure 3.1B). The protein yield from 1L of culture supernatant of TLR1, TLR2, and TLR10 is typically ~630ug, ~215ug, and ~319ug, respectively. Due to the low protein yield for TLR6, we decided not to include this TLR in this study (Figure 3.1A).

Binding of TLR2 to either TLR1 or TLR10 is induced by Pam_3CSK_4 and is specific

We performed preliminary binding studies using microtiter plate assays to optimize buffer conditions and qualitatively examine ligand-induced TLR heterodimerization. By comparing different buffers and pH of solution, we observed that TLR complex formation in the presence of Pam_3CSK_4 was optimal under MES buffer pH 7.5. Having optimized the conditions for microtiter plate assays, we proceeded to vary the order in which we form the ternary complex. We performed sequential addition of proteins by immobilizing one receptor on the plate, followed by addition of the lipopeptide or the co-receptor (in succession or together), and assayed for the formation of the ternary complex by measuring the binding of the receptor that was in solution. We observed formation of a stable complex when the co-receptor and lipopeptide agonist were added together, but not when they were sequentially added to the plate, suggesting that all three components of the ternary complex have to be present in close proximity in order to assemble a stable complex.

Addition of increasing concentrations of triacylated agonist Pam_3CSK_4 but not a diacylated or non-acylated synthetic lipopeptides increased TLR2 binding to either TLR1 or TLR10 coated on microtiter plates (Figure 3.2 A and B). To further show specificity, TLR2 binding was reduced in the presence of a neutralizing monoclonal antibody to TLR2 (T2.5). Binding was also found to be saturable upon addition of increasing concentrations of TLR2 to a TLR1-coated plate in the presence of Pam_3CSK_4 at a constant molar ratio of TLR2:Pam_3CSK_4 = 1:5 (Figure 3.3A). We also observed that TLR1 formed a ternary complex with Pam_3CSK_4 at lower TLR2 concentrations compared to TLR10 (Figure 3.3 A and B). In contrast, TLR2 pre-incubated with MALP-

2, the diacylated lipopeptide agonist for TLR2/TLR6, did not form complexes with either TLR1 or TLR10 on the plate. Similarly, the non-stimulatory compound Ac_2CSK_4, which lacks the acyl- and amide-bound fatty acid chain of Pam_3CSK_4, did not enhance the binding of TLR2 to either TLR1 or TLR10, showing that the lipid chains are required for the formation of a stable heterodimer (Figure 3.2 and 3.3).

We also performed complex formation in the reverse order, where we added TLR1 pre-incubated with different agonists to TLR2 immobilized on the plate. In this order of addition, we observed that binding is more efficient (i.e. higher absorbance values) if TLR1 pre-incubated with Pam_3CSK_4 is added to TLR2 on the plate (Figure 3.4). Time course experiments suggest that a stable TLR1/TLR2/Pam_3CSK_4 complex forms in 30 minutes on microtiter plates but can form at a faster rate (about 5 minutes) if TLR1 is in solution (i.e., TLR2 is coated onto microtiter plates, while TLR1 and Pam_3CSK_4 are added in solution), suggesting that TLR1 may undergo conformational changes upon binding to the agonist and/or the co-receptor. In contrast, a stable TLR2/ TLR10/Pam_3CSK_4 complex formed in 30 minutes irrespective of order of addition to the plate (data not shown).

Quantitative measurement of protein-ligand interaction using BIAcore and Octet

Based on the crystal structure (Jin et al., 2007), both TLR1 and TLR2 directly interact with Pam_3CSK_4. To quantitatively measure the kinetics of ternary complex formation in real time, surface plasmon resonance studies using BIAcore were performed. We started by measuring the interaction of a two-component system, i.e. the interaction between two TLRs in the absence of any agonists or the interaction between a TLR and Pam_3CSK_4. Using a carboxymethylated sensor (CM5 chip), we immobilized

TLR1 on the chip surface via amine coupling. We then added the co-receptor TLR2 in solution at varying concentrations. We observed that even at high concentrations of TLR2, there was no detectable interaction between two TLRs in the absence of any agonist (Table 3.1). When we measured the interaction between TLR1 on the sensor and Pam_3CSK_4 in solution, we encountered two problems: (1) the lipopeptide is a relatively small molecule (1.5kDa), and its binding could not be detected by the machine very well; and (2) Pam_3CSK_4 has a tendency to form aggregates or micelles in solution and exhibit non-specific hydrophobic interactions with the carboxymethylated matrix of the sensor chip. However, since Pam_3CSK_4 has a series of lysine residues in its peptide component, we were able to immobilize Pam_3CSK_4 on the CM5 sensor chip via amine coupling. In theory, this may have allowed the acyl chains of the lipopeptide to be freely exposed to the aqueous environment. Using this approach, we added varying concentration of TLRs 1, 2, and 10. All three TLRs were observed to directly bind to Pam_3CSK_4 immobilized on a sensor chip. TLR1 exhibited a fast on-rate as well as a fast off-rate, suggesting that TLR1-Pam_3CSK_4 interaction is weak. Both TLR2 and TLR10, on the other hand, exhibited relatively slower on- and off-rates, suggesting that they bind more tightly to Pam_3CSK_4 compared to TLR1. The dissociation constants, K_D, were measured between TLR1-Pam_3CSK_4, TLR2-Pam_3CSK_4, and TLR10-Pam_3CSK_4, and were found to be $1x10^{-6}$M, $7.57x10^{-9}$M, and $1.68x10^{-8}$M, respectively (Table 3.1).

Measuring the K_D in a three-component system to quantitatively measure ternary complex formation remains a big challenge in this study, mostly due to the difficulties in handling Pam_3CSK_4 in solution, regenerating sensor chips, and TLR protein aggregation as the cycle number increases. As mentioned above, upon dilution in polar solvents,

Pam_3CSK_4 has a greater tendency to form aggregates and exhibit non-specific binding with the carboxymethylated matrix of the sensor chip due to hydrophobic interactions. The surface regeneration steps (using 0.1% SDS buffer) after each binding cycle affected the population of active ligand (Pam_3CSK_4) reacting with the analyte (TLRs). Even in a 2-component system, we have encountered difficulties replicating the binding data for TLR binding to Pam_3CSK_4 immobilized on the sensor chip. The non-uniformity of the ligand population at each binding event or cycle leads to an inconsistent binding curve and a high chi^2 value for the computed K_D after curve fitting. We also observed non-specific binding of either TLR1 or TLR2 to an "empty" or reference CM5 sensor, which masks actual binding to the co-receptor that is immobilized on another sensor, thus giving a negative binding curve upon subtraction of the data from the reference cell. Furthermore, we noticed that the TLRs immobilized on the sensor chip are only active for the first few rounds of injection cycle, and are easily denatured by the regeneration buffer used (1M NaCl + 0.1% SDS). Collectively, our data suggest that the use of Pam_3CSK_4 as agonist in a simplified 3-component system (i.e. in the absence of either LBP or CD14), as well as the non-uniformity of successive binding events brought about by the regeneration steps in the protocol, are the two major hurdles that need to be overcome in order to achieve the objectives of this study.

To address the sensor chip regeneration problem, we decided to switch from Biacore to the ForteBio Octet QK System. Although both systems rely on biolayer interferometry, the ForteBio Octet sensors are designed for single use and can be loaded on a multichannel holder that can simultaneously run eight biosensors, thus eliminating the need for regeneration steps as well as achieving uniformity of binding conditions.

Proteins are immobilized on the biosensors, which are dipped in the wells of a microtiter plate containing the analyte(s) of interest. The Octet instrument passes a white light through the biosensor and measures the interference patterns of the light that is reflected back. The binding event is recorded as a plot of wavelength change versus time. We initially started our experiments using amine reactive sensors to covalently link one TLR to the sensor. Although we were able to immobilize all TLRs on the sensor, when we checked for proper protein folding using anti-TLR mAbs, only TLR1 was recognized by the anti-TLR1 monoclonal antibody (GD2.F4). TLR2, TLR10, and TLR4 (as a control) were weakly recognized by corresponding monoclonal antibodies, suggesting that either the immobilization steps may have rendered the mAb binding site inaccessible or the immobilization steps may have denatured the proteins.

To overcome the above sensor coupling problem, we decided to switch to a protein A sensor to immobilize our Fc-tagged TLR (TLR-Fc) proteins directly on the surface, taking advantage of the tight interaction (~10^{-10} - 10^{-11} M K_D) between protein A and the human IgG1 Fc fragment. In this way, we were able to orient the TLRs uniformly, making the active sites available for binding. The caveat to this approach is that the Fc tag in the TLR-Fc proteins causes the proteins to dimerize in an unknown conformation, and only the removal of the Fc tag after thrombin cleavage yields monomeric TLRs. Using the monoclonal antibodies anti-TLR1 (GD2F4) and anti-TLR2 (T2.5), the epitopes of which are known to be at or close to the active site of TLR1 and TLR2, respectively), we verified that the proteins are folded properly and that the active site of the dimeric proteins remains accessible for ligand recognition (Figure 3.5). To establish the reliability of the Octet system, we measured the interaction between the

TLRs and their respective mAbs (Table 3.2) and calculated dissociation constants in the sub-nanomolar range for TLR1, TLR2, and TLR10 binding to anti-TLR1 mAb (GD2.F4), anti-TLR2 mAb (T2.5), and anti-TLR10 mAb (3C10C5), respectively. All the chi^2 values for the association and dissociation curves were low and statistically significant (Table 3.2). As expected, the anti-TLR1 mAb (GD2.F4) did not bind stably with the $TLR1_{P315L}$ mutant and exhibited a thirty-fold lower dissociation constant compared to the wild-type TLR1.

To address the aggregation of Pam_3CSK_4, we decided to use a larger and more soluble agonist for TLR1/TLR2. We performed the microtiter plate assay to screen for naturally-occurring agonists that were reported to induce TLR1/TLR2 activation, such as LTIIbB5 from *E. coli* (Liang et al., 2009), Neisserial PorB (Massari et al., 2006), *Treponema denticola* periplasmic flagella (Ruby et al., 2007), and mannosylated lipoarabinomannan (Elass et al., 2007; Tapping & Tobias, 2003). None of these agonists induced the formation of a stable TLR1/TLR2 heterodimer in plate assays (data not shown). This observation, coupled with the fact that these agonists are less potent cell activators than lipoproteins, suggests that the binding affinity of TLR1 and TLR2 towards these agonists is lower compared to that of lipopeptides and lipoproteins. Alternatively, it is also possible that the agonists used in original reports were contaminated with minute amounts of lipoproteins. Another possibility is that these agonists may require an accessory molecule in order for them to be recognized by TLR1 and TLR2.

In efforts to examine a larger more soluble lipoprotein agonist, we acquired a 12 kDa lipoprotein (Lip12) from *E. coli*, expressed as a recombinant protein in *E. coli* BL21 cells with a histidine tag at the C-terminus of the protein (a gift from Dr. Peter Tobias and

Dr. Hyun-Ku Lee), which has been shown to play a role in TLR2-mediated cell activation (Lee et al., 2002). This 12kDa triacylated lipoprotein was isolated from commercial preparations of LPS that were found to activate cells through TLR2 as well as TLR4 (Lee et al., 2002). We purified his-tagged Lip12 using a cobalt column, and dialyzed the proteins in PBS buffer (Figure 3.6A). We tested the activity of this lipoprotein by stimulating SW620 epithelial cells transfected with various TLRs and an IL-8/luciferase reported gene. Lip12 was shown to stimulate SW620 cells transfected with TLR1/TLR2 but not TLR2/TLR6 (Figure 3.6B).

To assess Lip12 binding, we added varying concentrations of Lip12 (2 uM, 5 uM, 10 uM, and 20 uM) to TLR1, TLR2, TLR10, and TLR4 immobilized on different protein A sensors. As shown in Figure 3.7, Fc-tagged TLRs immobilized on a protein A sensor interacted with Lip 12 and produced a binding curve with a fast on-rate (k_{on}) and a slow off-rate (k_{off}). Using the Octet software to compute for the K_D of the interaction between TLRs and Lip 12 based on a 1:1 Langmuir binding model, the dissociation constants of wild-type TLR1, $TLR1_{P315L}$, TLR2, and TLR10 to Lip12 was measured to be $7.45x10^{-7}$ M (chi^2: 0.0193), $1.13x10^{-6}$ M (chi^2: 0.01747), $1.58x10^{-6}$ M (chi^2: 0.02892), and $3.34x10^{-7}$ M (chi^2: 0.07317), respectively (Table 3.3). As a negative control, we measured the binding of TLR4 to Lip12, and we were not able to measure any interaction. Furthermore, pre-incubation of either TLR1 or TLR2 with a known blocking antibody prevented interaction with Lip12 on the sensor, suggesting that the binding events were real and specific (data not shown).

Discussion

In Chapter 2, we established that LBP and CD14 are two accessory proteins that independently and transiently deliver a triacylated lipoprotein to TLRs 1 and 2 to enhance ternary complex formation. In this chapter, we aimed to define the order of events that lead to the formation of the final TLR1/TLR2/Pam_3CSK_4 complex and to gain further insights into the competition between TLR1 and TLR10 both for their agonist and co-receptor TLR2. Our qualitative measurements of protein-protein interactions using microtiter plate assays demonstrated that the triacylated lipopeptide Pam_3CSK_4 induces the formation of the TLR1/TLR2 and TLR2/TLR10 heterodimeric complexes. We have further shown that ternary complex formation is ligand-specific and can be blocked by monoclonal antibodies against TLR2. In this system, where one of the TLR receptors is immobilized on the plate, we have observed formation of a stable complex only when the co-receptor and lipopeptide agonist are present at the same time, but not when they are sequentially added and washed off, suggesting that all three components of the ternary complex need to be present in order to assemble a stable complex.

This study defines, for the first time, the binding kinetics of TLRs 1, 2, and 10 to immobilized lipopeptides or lipoproteins using both surface plasmon resonance (SPR, BIAcore) and biolayer interferometry (Octet). We found that the Octet system proved to be a more reliable and repeatable method compared to SPR. Prior to this study, there was limited information on TLR2-related binding kinetics. One of these studies examined the interaction between TLR2 and an early secreted antigenic target protein 6 (ESAT-6) from *Mycobacterium tuberculosis* (Pathak et al., 2007). ESAT-6 has a six-residue polypeptide found at the C-terminal domain that is sufficient for interaction with TLR2. Using SPR,

this same group later demonstrated that this short ESAT-6 polypeptide binds to TLR2, but not TLR4 immobilized on a sensor chip (Chambers et al., 2010). In addition, this group also reported that an acylated glycoprotein (MPB83) from *Mycobacterium bovis* is able to activate TLR2. However, a recombinant non-acylated form of the *M. bovis* glycoprotein (RecMPB83), which activates TLR2 more weakly compared to the acylated form, was used to demonstrate TLR2 binding in their SPR experiments (Chambers et al., 2010). In 2009, a different group looking at TLR2-peptidoglycan interaction reported binding kinetics between TLR2 immobilized on sensors and different forms of highly-purified synthetic peptidoglycan derived from both Gram-positive and Gram-negative bacteria (Asong et al., 2009). In all studies mentioned, it is noteworthy that the agonists chosen in their SPR studies are soluble in nature and lack the typical acyl chains observed in most TLR2 agonists including the more potent lipopeptides. Our study is the first to address the kinetics of interaction between TLRs and triacylated lipoproteins, which are amphipathic in nature.

Other notable SPR studies did not directly involve TLR2, and instead looked at the direct interaction between the accessory protein CD14 and microbial agonists. CD14 was among the first recognized so-called pattern recognition receptors, and plays an important role in the recognition of cell wall structures of Gram-positive as well as Gram-negative microbes (Pugin et al., 1993). CD14 is an accessory protein known to enhance the sensitivity of TLR4-expressing cells to LPS and TLR1/TLR2-expressing cells to a variety of lipidated agonists. Among these agonists, mycobacterial lipomannans (LM) and lipoarabinomannans (LAMs) isolated from *M. kansaii* were shown to interact with CD14 immobilized on a sensor (Elass et al., 2007). In chapter 2, we described in detail

the direct role of CD14 in the delivery of Pam_3CSK_4 to TLR1/TLR2. Using SPR, Nakata *et al.* (Nakata et al., 2006) reported a K_D of $5.7x10^{-6}$ M for the interaction between Pam_3CSK_4 and CD14 immobilized on the sensor. One of the limitations of this study is the lack of appropriate controls for their SPR experiment. They showed Pam_3CSK_4 binding to CD14 immobilized on the sensor, but they did not have any positive control such as LPS binding to CD14 for comparison. Another limitation in this experiment is that they used the 1.5 kDa Pam_3CSK_4 as the analyte in solution. The binding of a small molecule such as Pam_3CSK_4 is too small to be detected in BIAcore, and most likely, what the group was able to measure was the binding of Pam_3CSK_4 aggregates to CD14 on the sensor. Nevertheless, if the measured CD14-Pam_3CSK_4 dissociation constant is real, then a low K_D is consistent with the delivery function of CD14. CD14 is most likely going to transfer Pam_3CSK_4 to a receptor with a higher affinity for the lipopeptide.

Based on the crystal structure, two acyl chains of the triacylated lipopeptide Pam_3CSK_4 are bound by TLR2 in its hydrophobic pocket, while the remaining acyl chain interacts with TLR1. Since a TLR2-Pam_3CSK_4 complex has one less exposed acyl chain in solution compared to a TLR1-Pam_3CSK_4 complex, we hypothesized that TLR2 initially binds to the triacylated lipopeptide, and subsequently delivers the agonist to its partner receptor (either TLR1 or TLR10) to confer specificity and initiate appropriate cellular responses. In our BIAcore experiments, all three TLRs exhibited direct binding to Pam_3CSK_4 immobilized on an amine-reactive sensor chip (CM5). The K_D values were measured based on a 1:1 Langmuir Model for TLR1-Pam_3CSK_4, TLR2-Pam_3CSK_4, and TLR10-Pam_3CSK_4 interaction, and were found to be $1.0x10^{-7}$ M, $7.57x10^{-9}$ M, and

$1.68x10^{-8}$ M, respectively. However, we have very low confidence with these calculated K_D values since the chi^2 values for the global curve fitting were in the range of 35.5-600.

In the Octet system, we used a purified 12kDa triacylated lipoprotein (Lip12) that is bigger compared to Pam_3CKS_4 (1.5kDa). The K_D values that we were able to calculate for TLR1-Lip12, TLR2-Lip12, and TLR10-Lip12 interaction were $7.45x10^{-7}$ M, $1.58x10^{-6}$ M, and $3.34x10^{-7}$ M, respectively. The K_D values that were obtained from Octet are notably different from those measured using SPR, but the low chi^2 values suggest that the Octet was a more reliable measure compared to SPR. Surprisingly, the affinity of TLR2 to Lip12 was lower compared to that of TLR1-lipoprotein, as well as that reported for CD14-Pam_3CSK_4 (Nakata et al., 2006). Taken together, our data suggests that CD14 delivers a lipopeptide/lipoprotein to TLR1 and that the resulting TLR1-lipopeptide complex then binds to TLR2 to form the final ternary complex. It should be noted though that the N-terminal region of CD14 has been reported to directly bind to TLR2, and this interaction can be prevented using a monoclonal antibody against CD14 that also blocks CD14-mediated LPS/endotoxin binding (Iwaki et al., 2005). Further studies are required to fully elucidate the sequence of events leading to the formation of the final ternary complex.

Several attempts and approaches were made to measure the affinity constants of a 3-component system using both SPR and the Octet system. Our SPR data suggest that the aggregation state of the Pam_3CSK_4 agonist as well as the regeneration steps in the protocol are major concerns. Using the Octet system, our attempts to measure the kinetics of ternary complex formation involved immobilizing an Fc-tagged TLR, and exposing this sensor to Lip12 followed by (or together with) the monomeric TLR co-receptor.

However, aggregation of both lipoproteins and the monomeric TLRs was encountered and a significant binding curve was not observed. It is possible that the dimeric nature of the Fc-tagged TLRs on the sensors causes steric hindrance that prevents formation of a stable ternary complex with a soluble monomeric TLR and Lip12. We showed in Chapter 2 that either LBP or CD14 can independently deliver Pam_3CSK_4 to TLR1 and TLR2. Addition of LBP and/or CD14 to this system did not improve the binding curve; rather, these accessory proteins further complicated the results due to non-specific aggregation to the sensors.

TLR1 P315L is a naturally-occurring but rare TLR1 single nucleotide polymorphism that exhibits attenuated responses towards the synthetic lipopeptide Pam_3CSK_4 as well as a variety of other microbial cell wall components known to stimulate TLR1/TLR2 (Omueti et al. , 2007). Additionally, a purified TLR1 ECD with a mutation at this amino acid position failed to form a ternary complex with TLR2 upon addition of Pam_3CSK_4 in solution (Chapter 2) This point mutation in TLR1 is located in the outer loop of leucine-rich repeat motif 11, which is close to the entrance of the hydrophobic lipid-binding pocket of TLR1 and at the interface that interacts with TLR2. Interestingly, the $TLR1_{P315L}$ mutant, exhibited only a 1.5-fold lower binding affinity towards Lip12 compared to the wild-type TLR1 (Table 3.3), suggesting that the mutation at this position weakens but does not significantly alter the ability of TLR1 to bind to a lipoprotein. More importantly, this data suggests that proline at position 315 may be important for the formation of a dimer interface with TLR2, and a L315 mutation may have affected ternary complex formation, thus leading to an attenuated response in cells stimulated with Pam_3CSK_4. The next chapter of this dissertation takes a closer look at the

important regions of the TLR1 extracellular domain that are required for interaction with TLR2 upon formation of a ternary complex with an agonist.

TLRs are differentially expressed in myeloid and non-myeloid cells (Kawai & Akira, 2010). In some cell populations such as B cells, high levels of TLR1, TLR2, and TLR10 mRNA have been detected (Bourke et al., 2003) and it is highly likely that they are expressed together on the cell surface. The functional role of TLR10 is still largely unknown mainly because it does not signal via the known TLR-mediated signaling pathways. Additional data from other colleagues in our lab who are looking at TLR10 suggest that this receptor may be independently acting as a global suppressor to dampen the cell's immune response (Jiang, Li, Hess, and Tapping, unpublished results). However, TLR10 shares agonists with TLR1 and like TLR1, uses TLR2 as a co-receptor (Guan et al., 2010). Our SPR and Octet systems reveal that both TLR1 and TLR10 can bind to triacylated lipopeptides/lipoproteins. Thus, TLR10 may be acting as a negative regulator to dampen the immune response by competing with TLR1. Our microtiter plate assays show that TLR1 requires less TLR2 to form a ternary complex with Pam_3CSK_4 compared to TLR10. Moreover, when we formed the complexes in solution, we were able to observe a TLR1/TLR2/Pam_3CSK_4 ternary complex as measured by size exclusion chromatography (see Chapter 2) but not a TLR2/TLR10/Pam_3CSK_4 complex, even with the addition of LBP and CD14 (data not shown). This suggests that the affinity of TLR2 for TLR10 is weaker compared to that of TLR1. Our preliminary competition experiments on microtiter plates show that TLR2/Pam_3CSK_4 binding to TLR1 coated on microtiter plates gradually decreased when TLR2/Pam_3CSK_4 is pre-incubated with an increasing concentration of TLR10 prior to addition to the TLR1-coated plates (data not

shown). Further investigation is needed to determine whether there is a competition between TLR1 and TLR10. Given their different expression pattern and dissimilarity in signaling output (Guan et al., 2010), the ability of TLR1 and TLR10 to compete for TLR2 and/or the agonist is likely to have significant functional consequences.

Figures

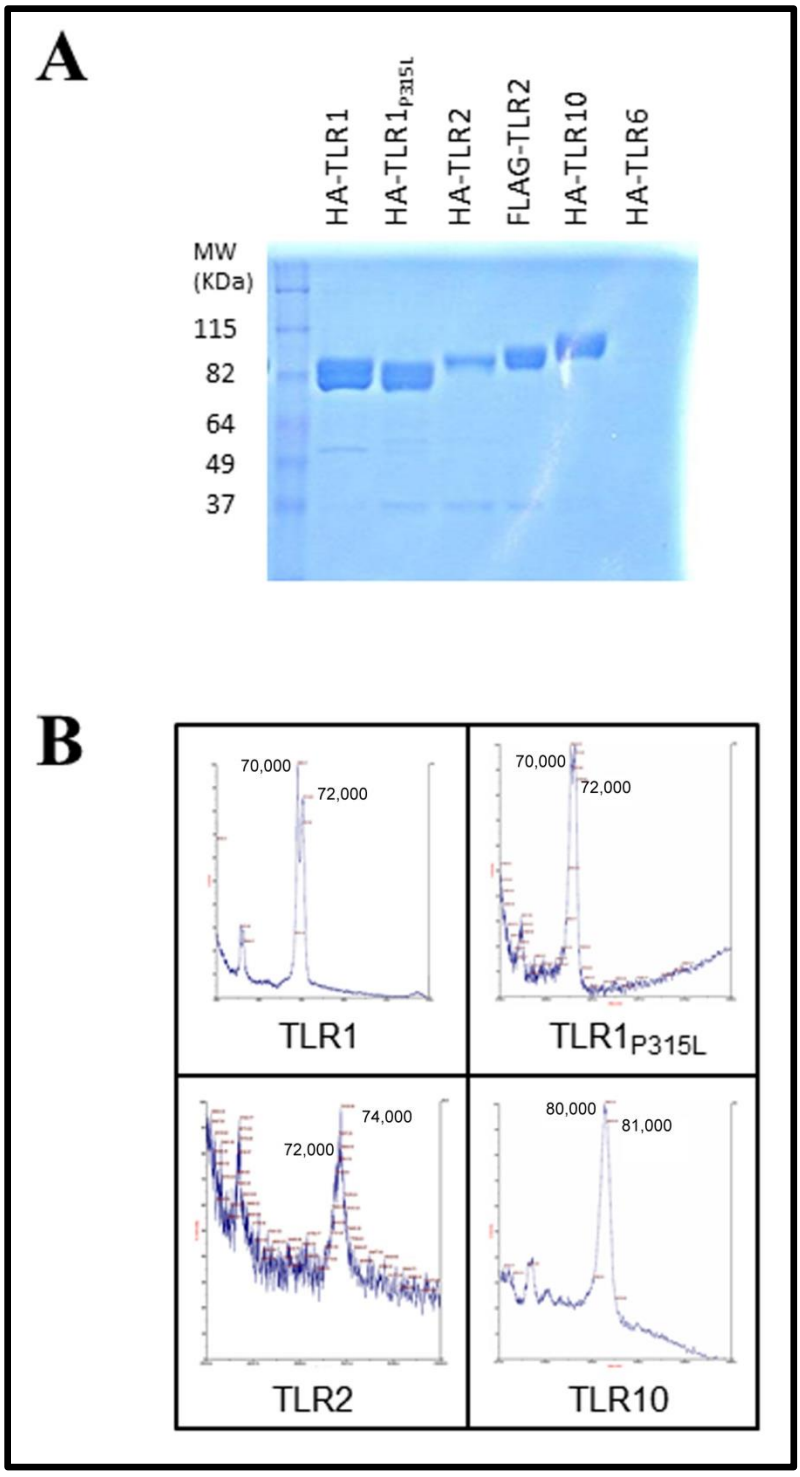

Figure 3.1. Purified TLR ECDs are monomeric. (A) Purified TLR ECD proteins loaded onto 7.5% acrylamide gel and stained with Coomassie blue dye. (B) The purity and actual molecular mass of the purified proteins were determined by mass spectrometry using MALDI as the ionization technique and sinapinic acid as the calibration matrix.

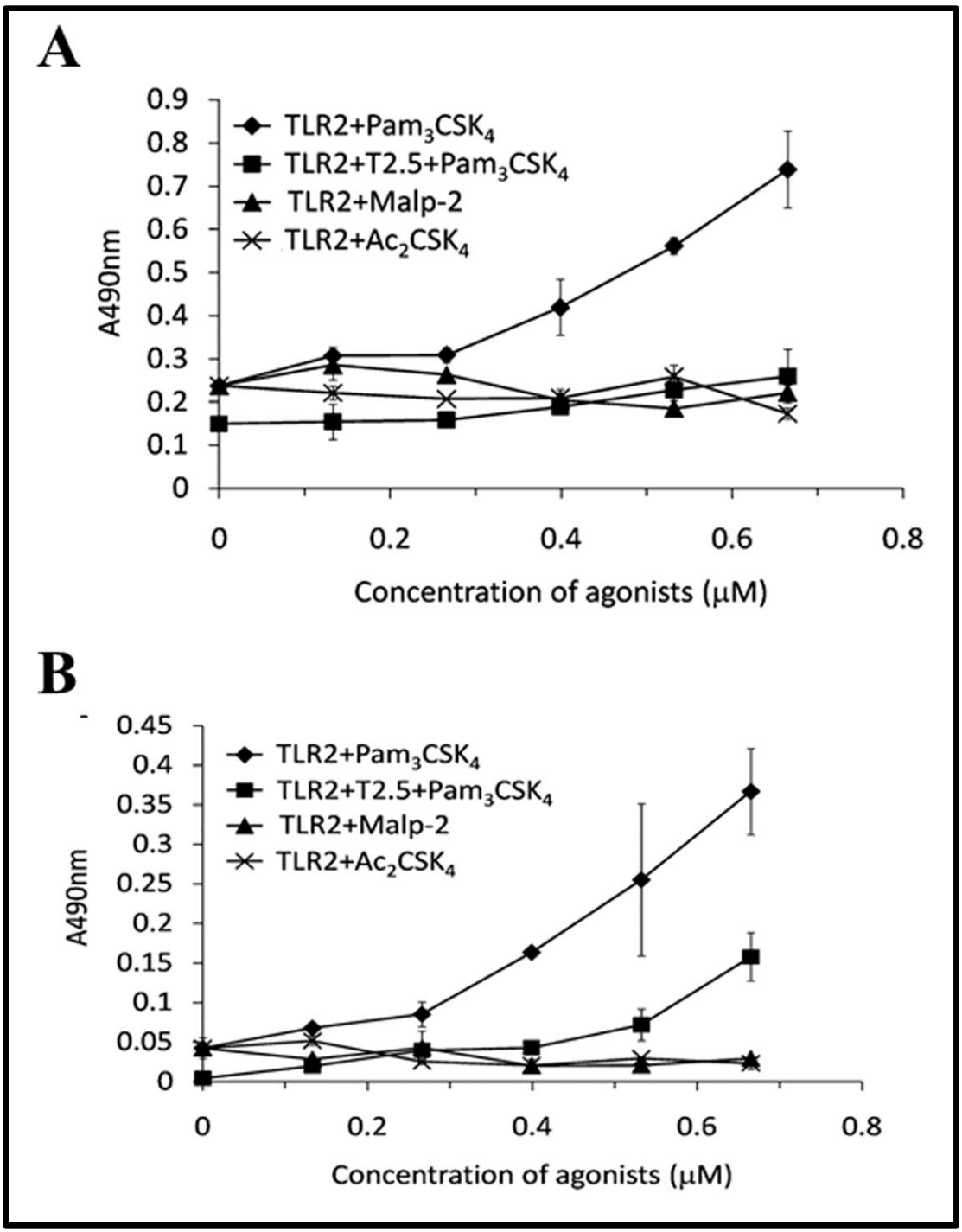

Figure 3.2. Binding of TLR2 to either TLR1 or TLR10 is ligand-induced and specific. (A) HA-tagged TLR1 ECD or (B) HA-tagged TLR10 ECD immobilized on microtiter plates were incubated with FLAG-tagged TLR2 pre-incubated with increasing concentrations of Pam_3CSK_4 (with or without T2.5 mAb), MALP-2, or Ac_2CSK_4 as indicated. Protein binding was detected through an HRP-conjugated anti-Flag antibody. Data are representative of a least three independent replicates.

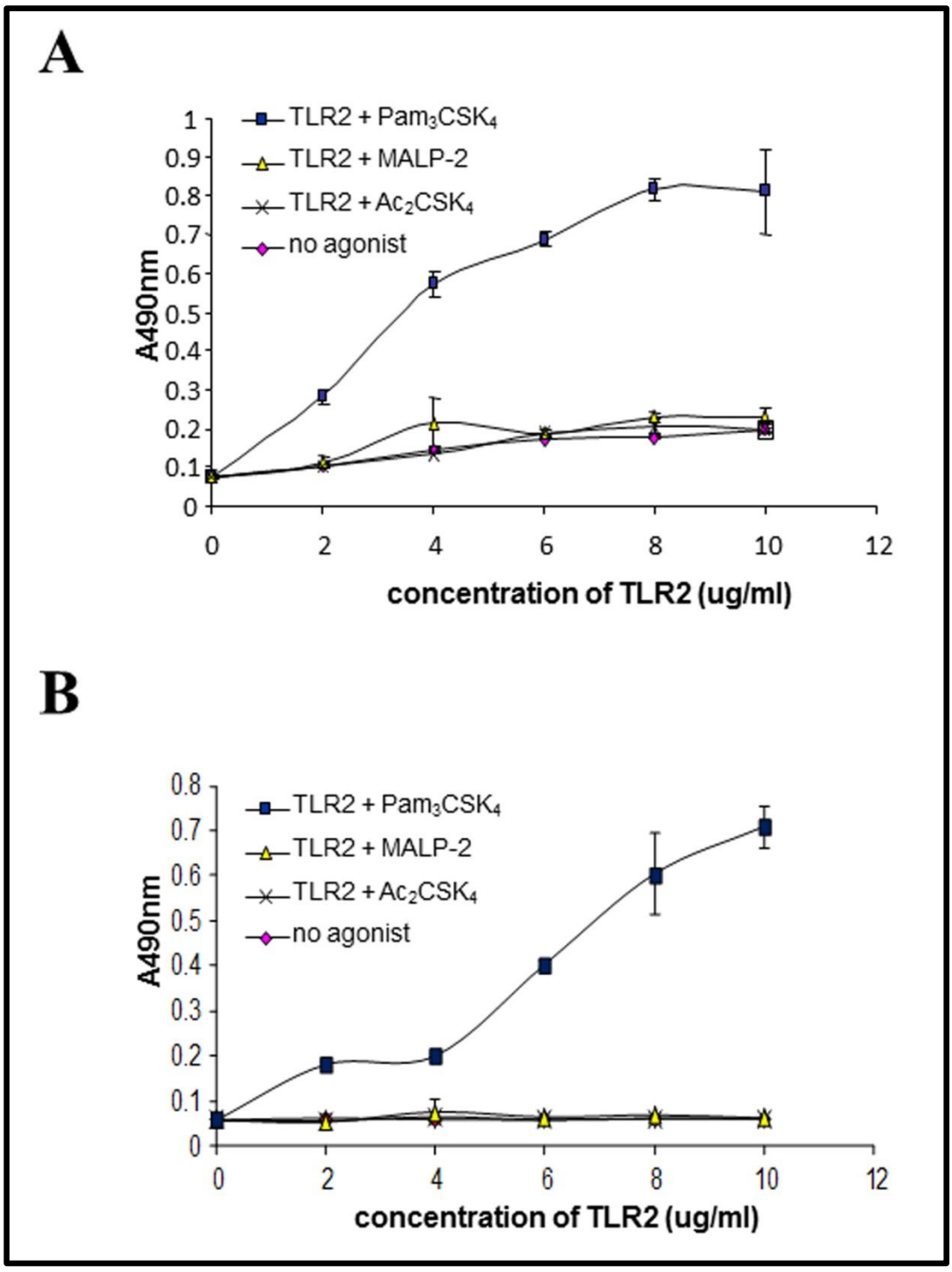

Figure 3.3. Binding of TLR2 to TLR1 is saturable and more efficient compared to TLR10. (A) HA-tagged TLR1 ECD or (B) HA-tagged TLR10 ECD immobilized on microtiter plates were incubated with increasing concentrations of FLAG-tagged TLR2 together with a 5-fold molar excess of Pam_3CSK_4, MALP-2, and Ac_2CSK_4. Protein binding was detected through an HRP-conjugated anti-Flag antibody. Data are representative of a least three independent replicates.

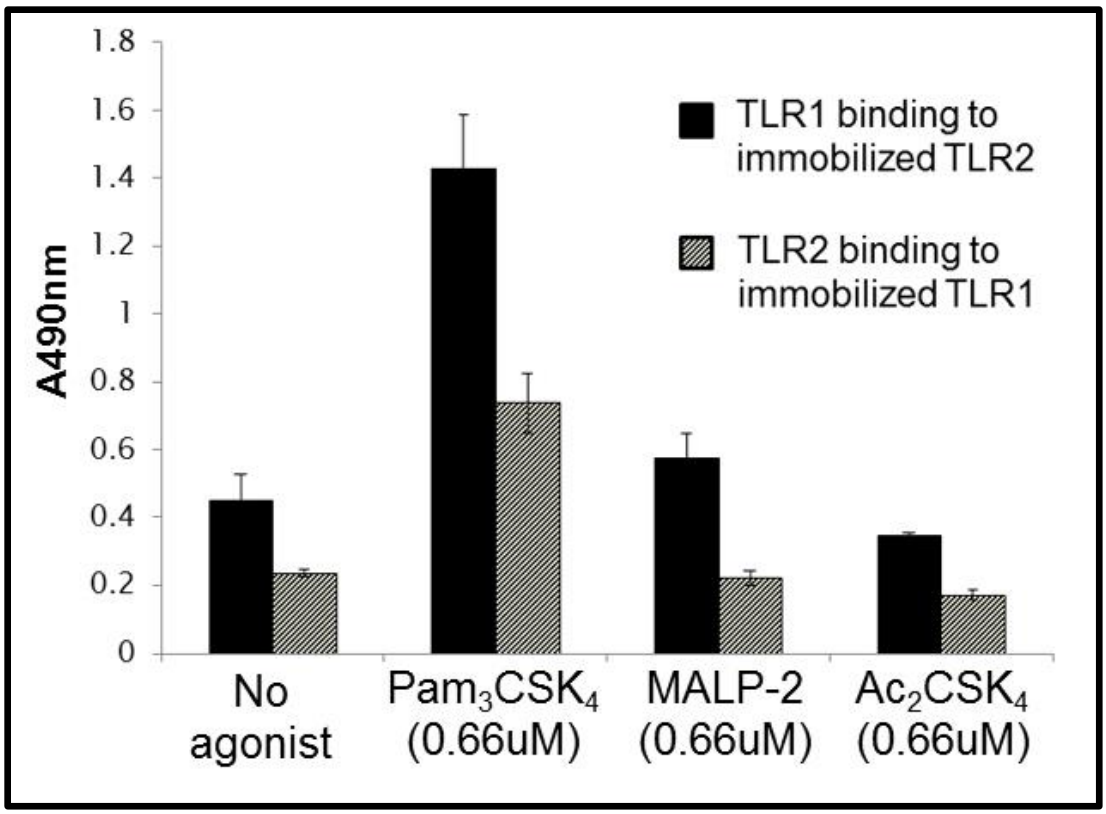

Figure 3.4. Order-of-addition experiment show that binding is more efficient if TLR1-Pam_3CSK_4 is added to TLR2 immobilized on a plate. HA-tagged TLR1 ECD pre-incubated with Pam_3CSK_4, MALP-2, or Ac_2CSK_4 were added to Flag-tagged TLR2 immobilized on a microtiter plate (blue bars), and compared to the addition of TLR2 pre-incubated with the same set of agonists to TLR1 immobilized on a plate (orange bars). Protein binding was detected through an HRP-conjugated anti-Flag antibody. Data are representative of a least three independent replicates.

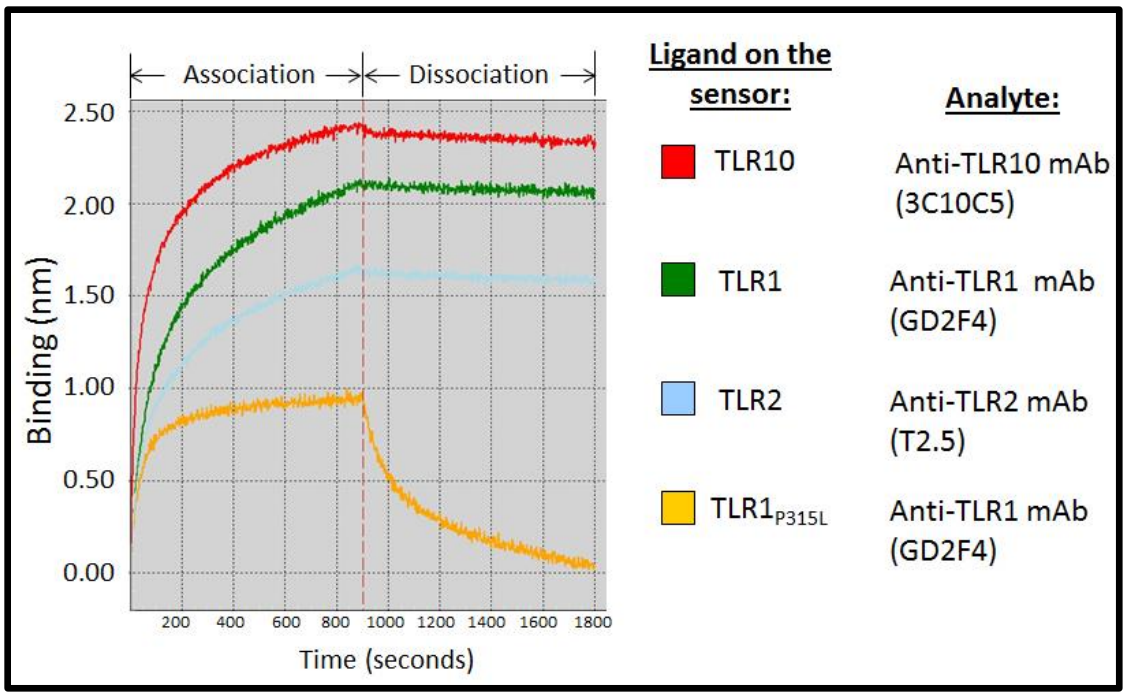

Figure 3.5. Fc-tagged TLR ECD proteins are recognized by their respective mAbs. Fc-tagged TLRs immobilized on protein A sensor tips and allowed to react with their respective mAbs in PBS pH 7.4 binding buffer as indicated. The incubation period of the TLRs with the antibodies (association phase) was set for 900 seconds (15 minutes). The sensors were then dipped on a different well containing PBS buffer to wash the unbound antibodies. This dissociation phase was also set for another 900 sec (15 min).

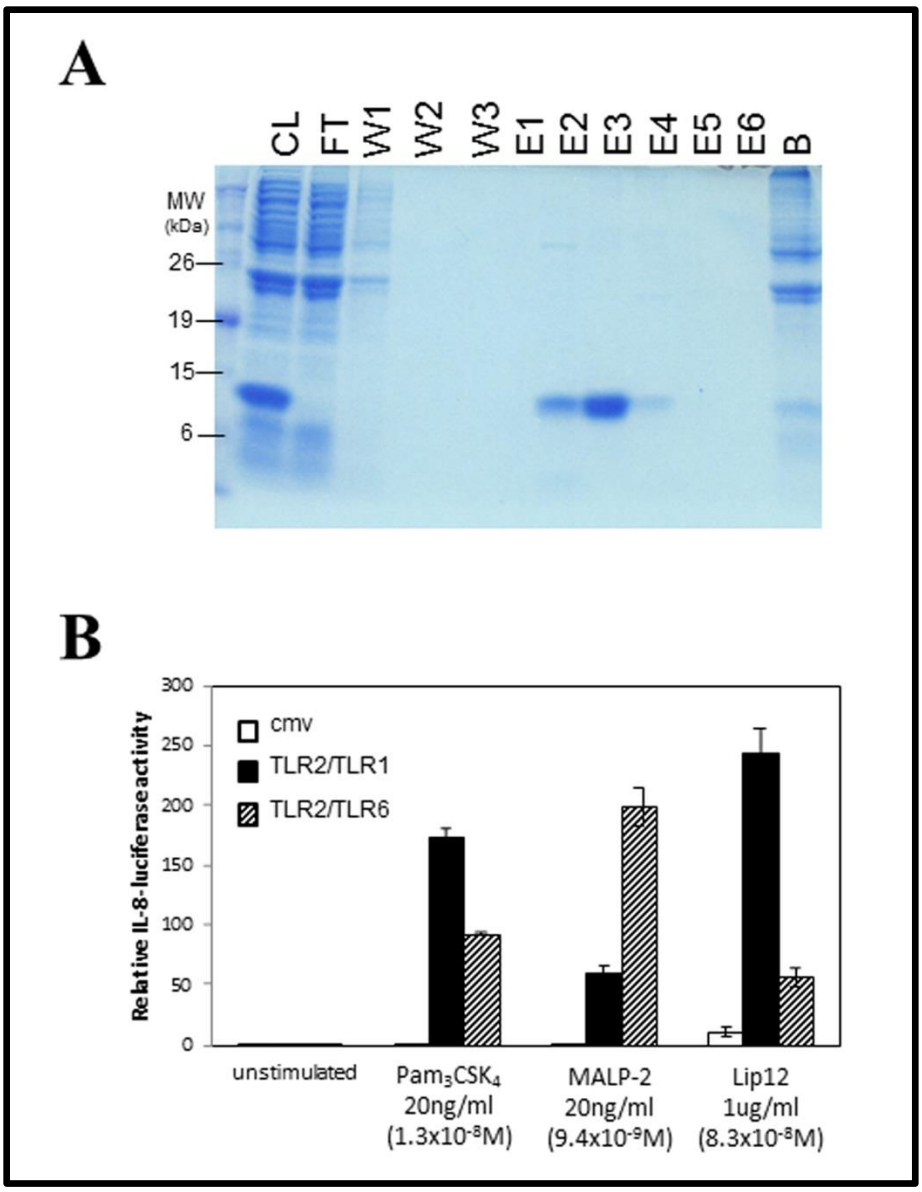

Figure 3.6. A 12kDa triacylated lipoprotein from E.coli stimulates TLR1/TLR2-transfected human epithelial cells. (A) His-tagged Lip12 protein from *E. coli* cell lysate was purified on a cobalt resin by affinity chromatography. Following a stringent wash step, the protein was eluted using a gradient elution buffer (containing 50-500mM imidazole). Legends: CL – cell lysate, FT – flow through, W – wash step, E1-E6 – elution with 50, 100, 200, 300, 400, and 500mM imidazole, B – beads. (B) SW620 cells were co-transfected with vectors expressing full length TLR1/TLR2, TLR2/TLR6, or empty CMV control vector as indicated, together with an IL-8-promoter driven luciferase reporter gene and a Renilla luciferase reporter gene. About 48-hours post transfection cells were stimulated with Lip12 or the controls Pam_3CSK_4, and MALP-2. Firefly luciferase activities were normalized to that of the Renilla luciferase control. These values were normalized to that of empty CMV vector whose value was taken as 1. Error bars represent the standard deviation of three independent events.

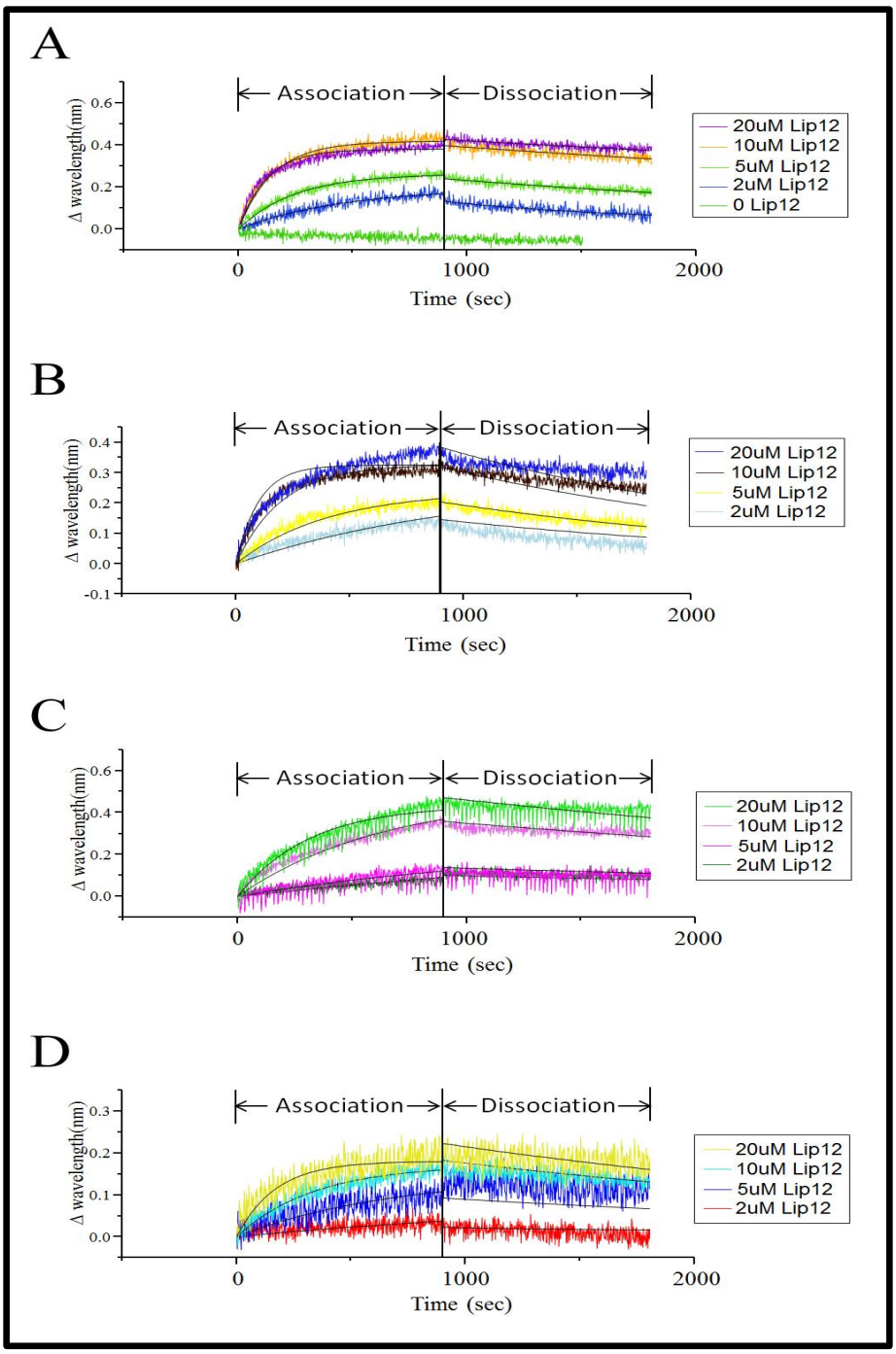

Figure 3.7. Fc-tagged TLR ECDs bind to triacylated Lip12 lipoprotein. Fc-tagged TLR1 (A), $TLR1_{P315L}$ (B), TLR2 (C), and TLR10 (D) immobilized on protein A sensor tips were incubated with increasing concentrations of purified Lip12 in PBS pH 7.4 binding buffer as indicated. The association phase was set for 900 sec. During the dissociation phase, the sensors were then dipped for another 900 sec on a different well containing PBS buffer to wash the unbound Lip12 proteins. The solid black curves represent the calculated Global Fit following a 1:1 Langmuir binding model.

Tables

Table 3.1. TLR1, TLR2, and TLR10 have different affinities for Pam_3CSK_4 based on surface plasmon resonance (BIAcore instrument).

Ligand (immobilized on the sensor)	**Analyte** (injected in solution)	k_{on} ($M^{-1}s^{-1}$)	k_{off} (s^{-1})	K_D (M)
TLR1	TLR2	Not detectable	Not detectable	Not detectable
Pam_3CSK_4	TLR1	4.6×10^{4}	4.7×10^{-3}	1.0×10^{-7}
Pam_3CSK_4	TLR2	2.08×10^{4}	1.58×10^{-4}	7.57×10^{-9}
Pam_3CSK_4	TLR10	1.94×10^{4}	3.27×10^{-4}	1.68×10^{-8}

Table 3.2. The binding affinities of TLR1, TLR2, and TLR10 to their respective monoclonal antibodies based on biolayer interferometry (Octet instrument).

Ligand	**Analyte**	k_{on} ($M^{-1}s^{-1}$)	k_{off} (s^{-1})	K_D (M)	**Assoc chi²**	**Dissoc chi²**
TLR1	Anti-TLR1 GD2F4	3.75×10^{-4}	1.44×10^{-5}	3.83×10^{-10}	0.01318	2.296×10^{-4}
$TLR1_{P315L}$	Anti-TLR1 GD2F4	7.87×10^{-4}	9.97×10^{-4}	1.27×10^{-8}	0.00521	0.00623
TLR2	Anti-TLR2 T2.5	5.39×10^{4}	7.83×10^{-6}	1.45×10^{-10}	0.02546	1.174×10^{-4}
TLR10	Anti-TLR10 3C10C5	6.75×10^{4}	3.44×10^{-5}	5.09×10^{-10}	0.02485	8.34×10^{-4}

Table 3.3. TLR1, TLR2, and TLR10 have different affinities for Lip12WT based on biolayer interferometry (Octet instrument).

Ligand (on Protein A sensor)	**Analyte** (in solution)	k_{on} ($M^{-1}s^{-1}$)	k_{off} (s^{-1})	K_D (M)	**Dissoc. Chi²**
TLR1	Lip12	$6.01x10^{2}$	$4.48x10^{-4}$	**$7.45x10^{-7}$**	0.0193
$TLR1_{P315L}$	Lip12	$5.01x10^{2}$	$5.66x10^{-4}$	**$1.13x10^{-6}$**	0.01747
TLR2	Lip12	$1.59x10^{2}$	$2.52x10^{-4}$	**$1.58x10^{-6}$**	0.02892
TLR10	Lip12	$2.95x10^{2}$	$9.86x10^{-5}$	**$3.34x10^{-7}$**	0.07317
TLR4	Lip12	No binding observed	No binding observed	No binding observed	No binding observed

CHAPTER FOUR

A COMMON EXTRACELLULAR REGION OF HUMAN TOLL-LIKE RECEPTOR 1 (TLR1) IS REQUIRED FOR CELLULAR RESPONSES TO A VARIETY OF MICROBIAL CELL WALL COMPONENTS[5]

Introduction

Toll-like receptors are central to the initiation of the innate immune responses in animal cells upon recognition of distinct bacterial, viral, and fungal components. Currently, there are ten known Toll-like receptors in humans, designated as TLR1 to TLR10, expressed either on the cell surface or in endosomal compartments (Takeda & Akira, 2005). These TLRs are able to sense the presence of microbe-associated molecular structures such as lipopolysaccharide (TLR4), flagellin (TLR5), double-stranded RNA (TLR3), single-stranded RNA (TLR7 or TLR8), or unmethylated double-stranded DNA (TLR9) [Reviewed in (Akira & Hemmi, 2003)].

Studies on knock-out mice have shown that TLR2 recognizes triacylated and diacylated lipopeptides/lipoproteins by pairing with TLR1 or TLR6, respectively (Takeuchi et al., 2001; Takeuchi et al., 2002). The unique ability of TLR2 to heterodimerize with either TLR1 or TLR6 contributes to expanding the diversity of molecules that they can recognize. In addition to triacylated lipoproteins, the TLR1/TLR2 pair is able to recognize other microbial cell wall components that differ in molecular structure such as atypical lipopolysaccharide (LPS) from non-enteric bacteria, peptidoglycan and lipoteichoic acid (LTA) from Gram-positive bacteria, lipomannans and lipoarabinomannans from mycobacteria, and zymosan from yeast to name a few

[5] Ranoa, DRE, Omueti KO, Mazur DJ, Weber BR, and Tapping RI. *Manuscript in Progress.*

(Darveau et al., 2004; Iwaki et al., 2002; Liang et al., 2009; Massari et al., 2006; Quesniaux et al., 2004a; Sato et al., 2003; Tapping & Tobias, 2003).

TLR2, together with TLR1 and TLR6, are predominantly expressed on the surface of myeloid-derived cells including monocytes, macrophages and dendritic cells, as well as on non-myeloid cells (Muzio et al., 2000; Zarember & Godowski, 2002). The genes for all three are located in human chromosome 4 (Roach et al., 2005). Evolutionary studies have shown that TLR1 and TLR6 are highly related and may have arisen as a product of gene duplication events (Roach et al., 2005). The greatest amount of variability between TLR1 and TLR6 occurs in the ECD, which is the region responsible for ligand recognition. The TLR ECD forms an evolutionarily conserved structure called the leucine rich repeat (LRR) motif, each made up of 22-29 amino acid residues with a consensus sequence of LxxLxLxxN (Bell et al., 2003; Botos et al., 2011; Kang & Lee, 2011). The TLR1, TLR2, and TLR6 ECD each have 20 LRRs stacked in a bent solenoid-shaped structure, and capped at both ends with an LRR-NT and LRR-CT capping modules (Jin et al., 2007; Kang et al., 2009). Crystal structure analyses revealed that the ectodomain of TLRs 1, 2, and 6 can be divided into three sub-domains: the N-terminal, central, and C-terminal domain. The N-terminal sub-domain, made up of the LRR-NT capping module and LRRs 1-4, have the asparagine ladder and the phenylalanine spine observed in typical LRR consensus motifs (Jin et al., 2007; Kang et al., 2009). In contrast, the LRR motifs seen in the central and C-terminal sub-domain contain atypical sequences and have no asparagine and phenylalanine spine, resulting in a conformation that deviates from the standard LRRs (Jin et al., 2007; Kang et al., 2009). More importantly, the boundary between the central and the C-terminal sub-domain of the

TLR1 and TLR2 ectodomain (LRRs 9-12) opens into a hydrophobic binding pocket where the prototypical triacylated lipopeptide ligand can be accommodated (Jin et al., 2007). The crystal structure of human TLR1 and TLR2 bound to Pam_3CSK_4 reveals that the lipopeptide coordinately binds to both receptors at this central region to form a stable TLR1/TLR2/Pam_3CSK_4 ternary signaling complex, with the N-terminal ends facing away from each other and the C-terminal ends brought together in closer proximity (Jin et al., 2007). Once this "m-shaped" conformation is assembled, the TLRs initiate a series of intracellular signaling cascades through their intracellular Toll-Interleukin Receptor (TIR) signaling domain that leads to the activation and expression of proinflammatory cytokines, chemokines and co-stimulatory molecules (Jin et al., 2007).

The objective of this study is to identify the molecular basis of interaction between non-lipoprotein microbial cell wall components and the TLR1/TLR2 heterodimer through mutational studies on TLR1. We have previously demonstrated that LRRs 9 through 12 in both TLR1 and TLR6 are essential for enabling TLR2 to recognize and discriminate between synthetic triacylated and diacylated lipopeptides (Omueti et al., 2005). We found that the same region in TLR1 is required for recognition of various microbial components. Through random mutagenesis, we generated a library of clones with single amino acid substitutions within the LRRs 9-12 region of TLR1. We identified the same set of key residues in the TLR1 LRRs 11 and 12 that are responsible for recognizing different microbial components regardless of their molecular structures, suggesting that these amino acids in the TLR1 ECD are important for the formation of a dimer interface with the co-receptor TLR2 in order to achieve the final m-shaped ternary complex. In addition, we have also identified the putative conformational epitope of an

anti-TLR1 blocking mAb, GD2.F4 to specific residues found in LRRs 10-12 of TLR1. These studies contribute to the knowledge needed for accurately designing small inhibitory molecules or developing therapeutic strategies to dampen the immune response via TLR1/TLR2 activation upon microbial infection.

Materials and Methods

Reagents

The synthetic bacterial lipopeptides N-Palmitoyl-S-[2,3-bis(palmitoyloxy)-(2*R*)-propyl]-(*R*)-cysteinyl-(*S*)-seryl-(*S*)-lysyl-(*S*)-lysyl-(*S*)-lysyl-(*S*)-lysine x 3 CF_3COOH (R-Pam_3CSK_4) and N-Acetyl-S-[2,3-bis(palmitoyloxy)-(2*RS*)-propyl]-(*R*)-cysteinyl-(*S*)-seryl-(*S*)-lysyl-(*S*)-lysyl-(*S*)-lysyl-(*S*)-lysine x 3 CF_3COOH (Pam_2AcCSK_4) were purchased from EMC Microcollections (Tuebingen, Germany). The Macrophage-activating lipopeptide-2, *S*-[2,3-bis(Palmityloxy)-(2*R*)-propyl-cysteinyl-GNNDESNISFKEK] (MALP-2) was purchased from Enzo Life Sciences (formerly Alexis Biochemicals; Plymouth Meeting, PA). The natural TLR2 agonists used in these experiments are whole or particulate components of pathogens. They include: heat killed *Listeria monocytogenes* (HKLM) from InvivoGen (San Diego, CA), LPS from *Porphyromonas gingivalis (P. gingivalis* LPS) from InvivoGen (San Diego, CA), Mycobacterial Membrane Fractions (NIAID contract N01 AI-75320 entitled *Tuberculosis Research Materials and Vaccine Testing*), heat killed *Staphylocccus aureus* (HKSA) from Invitrogen (Carlsbad, CA), non-mannose-capped lipoarabinomannan (ARALAM) from the cell wall of *M. smegmatis* obtained from Dr. J.T. Belisle (Department of Microbiology, Colorado State University), and Zymosan-A yeast particles from Invitrogen (Carlsbad, CA).

The unconjugated mouse anti-human TLR1 mAb (clone GD2.F4, CD281) and the isotype control, a mouse IgG1 mAb, were obtained from eBioscience (San Diego, CA). A mouse anti-FLAG mAB was purchased from Sigma (St. Louis, MO). A biotin-conjugated donkey anti-mouse secondary Ab and a streptavidin-phycoerythin (PE)-conjugated tertiary antibody were acquired from Jackson ImmunoResearch Laboratories, Inc. (West Grove, PA). HRP-conjugated anti-FLAG (clone M2) monoclonal Ab was purchased from Sigma Aldrich (St. Louis, MO), while the HRP-conjugated anti-hemagglutinin (HA) monoclonal antibody was purchased from Miltenyi Biotec Inc. (Auburn, CA). Unconjugated polyclonal anti-human LBP and anti-human CD14 goat IgG antibodies were kind gifts from Dr. Peter Tobias (The Scripps Research Institute, La Jolla, CA). The secondary antibodies, HRP-conjugated rabbit anti-goat IgG and HRP-conjugated goat anti-rabbit IgG were purchased from Jackson ImmunoResearch Laboratories (West Grove, PA).

Cell Culture

SW620 cells, a human colonic epithelial cell line (American Type Culture Collection no. CCL-227), were cultured in RPMI 1640 media containing 10% heat-inactivated FBS (Hyclone, Logan, UT), 2mM L-glutamine, 100 U/ml penicillin, and 100 µg/ml streptomycin (Invitrogen). Human embryonic kidney 293T cells were cultured in DMEM containing 10% heat-inactivated FBS, and 2mM L-glutamine. Cells were maintained in a 37˚C in a humidified environment containing 5% CO_2.

Construction of the TLR1 and TLR6 chimeras

The TLR1 and TLR6 ECD chimeras used in this study were generated as N-terminal FLAG-tagged constructs within a pFLAG-CMV vector using the techniques

described in (Omueti et al., 2005). Briefly, we engineered different restriction sites at the end of LRRs 5, 8, and 12 of both TLR1 and TLR6. The T6(1-5)/T1, T6(1-8)/T1, T6(1-12)/T1, T1(1-5)/T6, T1(1-8)/T6, and T1(1-12)/T6 chimeric receptors were constructed by digesting the modified TLR1 and TLR6 with the appropriate restriction enzymes followed by re-ligation reactions. On the other hand, the T6(1-17)/T1 and T1(1-17)/T6 chimeric receptors were generated from wild-type TLR1 and TLR6 using a natural HindIII site present at the end of the LRR 17 of both receptors. Recombinant DNA plasmids were verified by DNA sequencing (UIUC Core Sequencing Facility). All clones were tested and found to be expressed on the surface of transfected HEK 293T cells (Omueti et al., 2005).

Random mutagenesis of the TLR1 ECD LRRs 9-12

A library of TLR1 clones was generated by random mutagenesis by PCR. To this end, we engineered XbaI restriction sites flanking the LRRs 9-12 region of TLR1 cloned on a pFLAG-CMV vector, and subsequently excised this 300bp region by XbaI digestion for one hour at 37^{o}C. Excision was confirmed by running the digest on a 1% agarose gel, and this region was purified using Qiagen gel extraction kit. Error prone PCR as described in (Wilson & Keefe, 2001) was conducted on this fragment using the following primers: Forward [CCAATCTAGAAACAACTTGGAATTCTTTCATTAGGATCC] and Reverse [CCAATCTAGATTGTTTAAGGTAAGACTTGATAAGTTTGG] (The *Xba I* sites have been underlined). PCR products were ligated into the modified TLR1 pFLAG-CMV vector which had been previously digested with *Xba I* to remove the original LRRs 9-12. Clone Checker (Invitrogen, Carlsbad, CA) was used in accordance with the manufacturer's instructions to screen the library generated for clones which contained the

insert in the correct orientation. Unique clones were identified by DNA sequencing (UIUC Core Sequencing Facility).

Cell Activation Assays

SW620 cells were co-transfected with various combinations of TLRs together with a firefly luciferase gene driven by the IL-8 promoter and a Renilla luciferase gene driven by a basal promoter (pRL-null) as a transfection control (Promega; Madison, WI). Transfections were performed using a cationic lipid agent, Fugene-6 (Roche), at a 4:1 lipid:DNA ratio. The total amount of transfected plasmid DNA was equalized by supplementing with empty vector, pFLAG-CMV. Forty-eight hours post-transfection, the cells were stimulated for 6 hours with the indicated agonists. Following the manufacturer's protocol for the dual luciferase assay (Promega), cell lysates were collected 6 hours post-stimulation and analyzed for firefly and Renilla luciferase activity using a BioTek Synergy HT plate reader (BioTek; Winooski, VT). The transfection efficiency across different wells was normalized by dividing the firefly luciferase activity by the Renilla luciferase control. After correcting for transfection efficiency, all values were normalized to those of unstimulated cells transfected with reporters and empty pFLAG-CMV vector.

Flow cytometry

Human embryonic kidney (HEK) 293T cells were transfected with 3.0 μg of FLAG-tagged TLR constructs or empty vector. Fugene-6 (Roche Inc., Indianapolis, IN) was used as the transfection reagent to introduce the DNA vectors into the cells. Cell media was changed 6 hours post-transfection. 48 hours post-transfection, cells were removed from the plate with chilled PBS (pH 7.4) and these cell suspensions were

transferred to 1.5ml microcentrifuge tubes. These cells were incubated with either a mouse anti-FLAG M2 antibody or anti-TLR1 (GD2.F4) mAb, followed by a biotinylated donkey anti-mouse secondary antibody, and finally a streptavidin PE-conjugated tertiary antibody. The cells were then washed, fixed, and then quantified for surface fluorescence using a Coulter Epics XL instrument. Overlays were created using the Summit software program.

Size exclusion chromatography assays

The TLR1-TLR2-lipopeptide ternary complex was formed by pre-incubating 0.25uM TLR2, 0.25uM TLR1, and 2.5uM Pam_3CSK_4 (with or without 0.05uM LBP and/or 0.25uM sCD14) in PBS pH 7.4 buffer to a final volume of 0.5ml. The mixture was incubated in a 37^{o}C water-bath for 2 hours and injected into a Superdex 200 10/300GL gel filtration column (GE Healthcare) at a flow rate of 0.5 ml/min in PBS pH 7.4 running buffer. Twenty minutes after injection of the sample, 0.5ml fractions were collected covering one column bed volume (about 24ml, 48 min). The chromatogram was recorded using a manual UV recorder. The data was then re-plotted using the xyExtract v5.1 graph digitizer software (Wilton and Cleide Pereira da Silva; Campina Grande, Paraíba, Brazil).

Eluted fractions were separated on a 7.5% SDS-PAGE gel and transferred to an Immobilon-P PVDF membrane (Millipore). The membranes were blocked with 5% non-fat dry milk (NFDM) in TBS buffer containing 0.05% Tween-20. Western blotting was performed to detect TLR1 and TLR2 using HRP-conjugated anti-HA and anti-FLAG antibodies (both diluted at 1:1000 in 5% NFDM), respectively. LBP and/or CD14 was detected using either a polyclonal goat anti-LBP or goat anti-CD14 (diluted 1:500 in 5% NFDM), followed by a HRP-conjugated rabbit anti-goat IgG polyclonal antibody (diluted

1:5000 in 5% NFDM). Chemiluminescence was detected using the Pierce ECL Western blotting substrate (Rockford, IL). Membranes were then exposed to a HyBlot CL autoradiograpy film (Denville Scientific Inc.; Metuchen, NJ) and developed.

Visualization and structural analysis of the TLR1 ECD

The TLR1 structure visualization was carried out using the information from the solved crystal structure of TLR1/TLR2/Pam_3CSK_4 (Jin et al., 2007) uploaded at the RCSB Protein Data Bank (template PDB 2Z7X), and were analyzed using the Visual Molecular Dynamics (VMD) software developed at the University of Illinois at Urbana-Champaign (Humphrey et al., 1996).

Results

LRRs 9-12 of TLR1 are essential to cellular responses to synthetic and naturally-occurring TLR1-TLR2 agonists

Previous studies in our lab have shown that the LRRs 9-12 of TLR1 and TLR6 ECD are important for distinguishing a triacylated from a diacylated lipopeptide (Omueti et al., 2005). To determine if the same region of TLR1 is required for recognition of other TLR1/TLR2 natural microbial agonists, we used the same reconstitution experiments to test different TLR1 and TLR6 chimeric receptors for their ability to recognize a variety of microbial products. SW620 cell lines, a human epithelial carcinoma line, were transfected with TLR2 together with different TLR1 and TLR6 chimeras as previously described (Omueti et al., 2005). SW620 cells are deficient in TLR1 and TLR2, and express very little TLR6. Consistent with our previous studies, TLR1 in partnership with TLR2, recognized the triacylated synthetic agonist Pam_3CSK_4, while the TLR6/TLR2 pair responded to the diacylated MALP-2, as measured by the relative IL-8-luciferase reporter

activity (Figure 4.1, top panel). There are eight different N-terminal chimeras with domain exchanges between TLR1 and TLR6 at LRRs 1-5, 1-8, 1-12, and 1-17. All of these FLAG-tagged chimeric receptors were shown to be expressed on the surface of transfected SW620 cells by flow cytometry using an anti-FLAG mAb. With the exception of T1(1-8)/T6, all other N-terminal chimeras appear to be properly folded and biologically active. As TLR1 was gradually replaced with TLR6 ECDs at the N-terminal domain, the response to Pam_3CSK_4 diminished. Relative to wild-type TLR1, a TLR1 chimera whose LRRs 1-5 were replaced with that of TLR6 [T6(1-5)/T1] only exhibited about 50% IL-8 luciferase activity towards Pam_3CSK_4, while a TLR1 chimera that has TLR6 LRRs 1-8 at the N-terminal region [T6(1-8)/T1] have shown only 20% activity upon Pam_3CSK_4 stimulation. When this N-terminal replacement was extended to LRR 12 [T6(1-12)/T1], the IL-8-luciferase activity in response to Pam_3CSK_4 was almost completely lost, but was able to exhibit MALP-2 activity at about 44% relative to wild-type TLR6. The TLR1 chimera whose LRRs 1-17 have been replaced with TLR6 [T6(1-17)/T1] also exhibited diminished activity towards Pam_3CSK_4, but was able to recognize MALP-2 at similar levels compared to wild-type TLR6. On the other hand, the reverse chimeras demonstrated that when the LRRs 1-12 or 1-17 of TLR6 were replaced with that of TLR1 [T1(1-12)/T6 and T1(1-17)/T6, respectively], the ability to recognize Pam_3CSK_4 was restored. Consistent with our previous resport (Omueti et al., 2005), the LRRs 9-12 of TLR1 and TLR6 were shown to be important for recognition of their respective synthetic agonists.

Using the same chimeric receptors, we tested various known naturally-occurring TLR1/TLR2 agonists (Figure 4.1, middle and bottom panels). We observed that *P.*

gingivalis LPS activated cells transfected with TLR1/TLR2, but not TLR2/TLR6. The data also demonstrated that when the wild-type TLR1 was replaced with increasing amounts TLR6 at the N-terminal domain, the IL-8-luciferase activity of cells in response to *P. gingivalis* LPS decreased. The T6(1-5)/T1 and T6(1-8)/T1 chimeric receptors exhibited 60% and 55% luciferase activity, respectively, compared to wild-type TLR1. More importantly, when the domain exchange was extended to LRRs 1-12 and 1-17 [constructs T6(1-12)/T1 and T6(1-17)/T1], the transfected cells were no longer able to respond to *P. gingivalis* LPS. This suggests that the residues in LRRs 9-12 of TLR1 play a role in mediating recognition of *P. gingivalis* LPS. In support of this, the TLR6 chimera whose N-terminal domain was replaced with LRRs 1-12 and LRRs 1-17 of TLR1 [constructs T1(1-12)/T6 and T1(1-17)/T6] exhibited greater than 60% IL-8-luciferase activity upon stimulation with *P. gingivalis* LPS, comparable to that of wild-type TLR1.

Both the non-mannose capped lipoarabinomannan (AraLAM) from mycobacterial cell walls as well as a preparation of mycobacterial membrane fractions (Mtb mem) activate cells transfected with TLR2 and wild-type TLR1. Not surprisingly, we did observe TLR2/TLR6-mediated activity (about 45% relative to TLR1/TLR2 activity) in cells stimulated with mycobacterial membrane fractions, since the preparation of this agonist may contain some TLR2/6 agonists such as diacylated lipoproteins. Similar to what has been observed with *P. gingivalis LPS*, cells that were transfected with a chimeric TLR1 whose LRRs 1-12 and 1-17 have been replaced with the that of TLR6 [constructs T6(1-12)/T1 and T6(1-17)/T1, respectively] and stimulated with either AraLAM or mycobacterial membrane fractions exhibited an IL-8 luciferase activity was less than 20% relative to wild-type TLR1. This suggests that LRRs 9-12 of TLR1 are also

required for their recognition. However, in the reverse construct where TLR1 LRRs 1-12 were placed in TLR6 [construct T1(1-12)/T6], the cell response towards the two agonists was not rescued. Only when the substitution was extended to TLR1 LRRs 1-17 [construct T1(1-17)/T6] did we observe a greater than 65% IL-8-luciferase activity in stimulated cells, suggesting that a larger region of the TLR1 region may be necessary for full recognition of AraLAM and mycobacterial membrane fractions.

The next agonists that we tested were a derivative of yeast cell wall (Zymosan-A particles) and preparations of heat-killed *Staphylococcus aureus* (HKSA), both of which preferentially activate TLR1/TLR2 (Figure 4.1, bottom panel). Like all TLR1/2 microbial agonists tested thus far, TLR2 co-transfected with either T6(1-12)/T1 or T6(1-17)/T1 have very low IL-8-luciferase activity upon stimulation with Zymosan-A and HKSA. This activity was rescued in cells co-transfected with TLR2 and T1(1-17)/T6. These results are consistent with our previous data from other TLR1/TLR2 agonists, suggesting that the same critical regions which include LRRs 9-12 of TLR1 are required for cellular sensing of these different types of agonists.

Finally we tested heat-killed *Listeria monocytogenes* (HKLM) in our system (Figure 4.1, bottom panel). This agonist preferentially activates cells transfected with TLR2 and TLR6. TLR6-mediated activity was still observed after replacement of the first five LRRs with that of TLR1 [T1(1-5)/T6]. However, this activity was lost when the domain replacement from TLR6 to TLR1 was extended to LRR 8 [T1(1-8)/T6], LRR 12 [T1(1-12)/T6], and LRR 17 [T1(1-17)/T6]. Furthermore, in the reciprocal experiment, the response to HKLM was only restored when LRRs 1-17 of TLR6 are substituted in the TLR1 chimera [T6(1-17)/T1], suggesting that a large region of TLR6 is necessary, an

area that covers LRRs 6-17 of TLR6, for mediating TLR6 response to this microbial agonist. However, it is important to note that LRRs 9 through 12 still falls within the region needed to stimulate activity to HKLM.

The epitope of anti-TLR1 blocking mAb, clone GD2.F4, maps to the central region (LRR 11) of TLR1

When we generated our FLAG-tagged TLR1 chimeric constructs and the TLR1 single point mutants, we tested for their expression on the surface of HEK 293T cells using an anti-FLAG antibody as evidenced by the data we previously reported in 2005 (Omueti et al., 2005). To test for proper protein folding, we used an anti-TLR1 mAb (clone GD2.F4), which is known to bind endogenous TLR1 expressed on the surface of human monocytes (Wyllie et al., 2000). To this end, we show that GD2.F4 binds to wild-type TLR1 but not TLR6, and as we gradually replaced the N-terminal region of TLR1 with that of TLR6, we observed that the GD2.F4 mAb was not able to recognize the chimeric TLR1 whose N-terminal LRRs 1-12 and 1-17 have been replaced with that of TLR6 [constructs T6(1-12)/T1 and T6(1-17)/T1, respectively] (Figure 4.2). Moreover, when we tested the TLR6 chimeric constructs, the antibody bound to the constructs T1(1-12)/T6 and T1(1-17)/T6 but not to T1(1-5)/T6 and T1(1-8)/T6. Taken altogether, the data revealed that only the chimeras that contain LRRs 9-12 of TLR1 are recognized by the GD2.F4 mAb, suggesting that the epitope of the anti-TLR1 monoclonal antibody lies within this region of TLR1.

To map the epitope of the anti-TLR1 mAb, we performed random mutagenesis on the LRRs 9-12 of TLR1. We generated fifty-nine single point mutants, expressed them on HEK 293T cells, and analyzed for their binding to the anti-FLAG and the anti-TLR1

(clone GD2.F4) mAbs (Figure 4.3 and Table 4.1 columns 2 and 3). Any TLR1 mutants that fall below 50% mean fluorescence intensity (MFI) relative to the wild-type TLR1 upon anti-Flag mAb staining were deemed poorly expressed on the surface and were removed from the data set. Using this set criteria, we found a total of 41 point mutants (11 of which are located in LRR 10, 23 are in LRR 11, and 7 are in LRR 12) that exhibited good surface expression (Figure 4.3). When we stained the cells with GD2.F4, fourteen single point mutants had an MFI that is less than 50% relative to that of the wild-type TLR1, suggesting that these mutants were poorly recognized by the anti-TLR1 mAb (Figure 4.3). Those that have <5% MFI relative to wild-type fluorescence were the point mutants S309N, D310V, F312S, F314L, P315L, and Q316K. We mapped these residues on the variable loop of LRR 11 of the TLR1 ECD using the PDB structure reported by Jin *et al.* in 2007 (Jin et al., 2007) and the VMD software to illustrate the possible binding site of the GD2.F4 mAb. Interestingly, GD2.F4 inhibits agonist-induced activation of TLR1 (Omueti et al., 2007), suggesting a crucial role for LRR 11 in receptor function.

Figure 4.4A shows the ribbon diagram of TLR1 ECD (in blue) highlighting its LRRs 9-12, while Figure 4.4B shows the space-filling model of TLR1 with the LRRs 9-12 in an alternating color scheme (blue and light gray). Pam_3CSK_4 is also included in both figures 4.4A and 4.4B to demonstrate that one of its acyl chains inserts into the hydrophobic channel located between LRRs 11 and 12 of TLR1. Figures 4.4C and 4.4D show the location of the 41 critical residues in the TLR1 ECD in the ribbon and space-filling model, respectively. The amino acid residues S309, D310, F312, F314, P315, Q316, S317, and Y320 are all found in the variable loop of LRR 11, which line the

entrance of the hydrophobic channel of TLR1. L287 and R290 are mapped at the periphery of the convex surface, flanking F314 and P315. On the other hand, S279 and V307 are found on concave side, lining part of the β-sheet structures. Finally, F331 is buried inside the hydrophobic pocket. Taken together, data suggests that the putative conformational epitope of the GD2.F4 mAb encompasses the region where amino acid residues S309, D310, F312, F314, P315, Q316, S317, and Y320 from the variable loop of LRR 11 are located, and that mutations in S279, V307, and F331 may have changed the over-all folding of the LRRs 10-12, thus indirectly affecting binding of the GD2.F4 antibody (Figure 4.4D).

Amino acid residues located at LRRs 11 and 12 of the TLR1 ECD contribute to cellular responses to triacylated lipopeptide (Pam_3CSK_4)

The data presented thus far have highlighted the importance of LRRs 9-12 of TLR1 in sensing various TLR1/TLR2 agonists. To identify the important residues in this region, we generated a mutant library by random mutagenesis. As previously mentioned, we screened our FLAG-tagged single-point mutants for surface expression and their ability to bind to the anti-TLR1 mAb GD2.F4 (see Table 4.1). Based on our surface expression data, point mutants that were poorly expressed on the cell surface were excluded from our data analysis (see Table 4.1). Using our cell-based reconstitution assay, we further screened our mutant library for function by transfecting SW620 cells with the different TLR1 point mutants together with TLR2, a luciferase reporter gene under the control of an IL-8 promoter, and a Renilla transfection control. This was followed by stimulation with the potent synthetic triacylated lipopeptide agonist Pam_3CSK_4. To analyze the functional data, mutants displaying $\leq 20\%$ of wild-type TLR1

activity are considered poorly responsive to Pam_3CSK_4. This cut-off was based on the relative IL-8-luciferase activity of SW620 cells transfected with TLR2 alone and stimulated with Pam_3CSK_4.

For most of the clones we isolated, the single amino acid change did not affect their expression on the cell surface or their ability to recognize the triacylated agonist Pam_3CSK_4. Figure 4.5 summarizes selected TLR1 single point mutants that are found in LRRs 11 and 12 and their response to Pam_3CSK_4 as measured by the relative IL-8 – luciferase activity in our cell-based reconstitution assay. Comparing this data with the results from the GD2.F4 mAb binding experiment, most of the single point mutants that failed to bind to the GD2.F4 mAb (S309N, D310V, F312S, F312Y, S317G, and Y320N) exhibited normal response to the agonist Pam_3CSK_4. In contrast, we identified three clones in the variable loop of LRR11 (F314L, P315L, and Q316K) and one in LRR12 (V339D) that strikingly did not respond to Pam_3CSK_4 even though they were all expressed on the cell surface as measured by the anti-FLAG mAb (Table 4.1). This data suggests that the four amino acids at positions 314, 315, 316, and 339 are important for TLR1 recognition of Pam_3CSK_4 and the formation of a dimer interface with the co-receptor TLR2. This region was also identified to be important for binding the amide-linked acyl chain of Pam_3CSK_4 as revealed by the crystal structure (Jin et al., 2007). The TLR1/TLR2/Pam_3CSK_4 crystal structure also shows that the oxygen in the amide group of the Cysteine residue in Pam_3CSK_4 forms H-bonds with the side chain of Q316 in TLR1 (Jin et al., 2007). Thus a mutation from glutamine to lysine at position 316 may have altered this interaction between TLR1 and Pam_3CSK_4.

We have previously demonstrated that $TLR1_{P315L}$, which is a rare but naturally-occurring single nucleotide polymorphism observed in individuals of African descent, confers a greatly attenuated response to lipopeptide agonists (Omueti et al., 2007). We have also previously shown by gel filtration chromatography that the formation of the final TLR1/TLR2/Pam_3CSK_4 ternary complex is ligand-induced and requires the assistance of either LBP or soluble CD14 for the efficient delivery of the monomeric agonist to the TLRs (Ranoa et al., 2013; Chapter 2). Using purified, monomeric, and functional TLR1 and TLR2 extracellular domains, we compared the ability of wild-type TLR1 and $TLR1_{P315L}$ to form the ternary complex with TLR2 and the triacylated agonist Pam_3CSK_4 in solution. In contrast to wild type TLR1, $TLR1_{P315L}$ did not form a stable ternary complex with TLR2 and Pam_3CSK_4, as indicated by the presence of a smaller peak with a calculated relative molecular weight of 183kDa (Figures 4.6A and 4.6B, left panel). The bigger peak that came out at a later time represents the protein monomers, which have a calculated relative molecular weight of 70kDa and 80kDa for TLR1 and TLR2, respectively. When we analyzed the eluted fractions by Western blot, both wild-type TLR1 and TLR2 were detected in earlier eluted fractions containing the ternary complex (Figure 4.6A, right panel), whereas $TLR1_{P315L}$ incubated with TLR2 both came out in the later fractions containing the monomeric proteins (Figure 4.6B, right panel). The fact that TLR1 proline at amino acid position 315 is critical for ternary complex formation explains the highly attenuated responses of this naturally occurring TLR1 variant to triacylated lipopeptides. As an additional control, we show in Figure 4.3C that a diacylated synthetic agonist Pam_2AcCSK_4 does not induce complex formation between

wild-type TLR1 and TLR2 suggesting that the third acyl chain of the lipopeptide is necessary for conferring specificity to TLR1/TLR2-mediated responses.

The critical amino acids of TLR1 at LRRs 11-12 required for receptor function are strikingly similar across all naturally occurring TLR1/TLR2 agonists, irrespective of their chemical nature

Similar to what we did with the TLR1 chimeric receptors, we also tested our single point mutants in their ability to sense naturally-occurring agonists such as *P. gingivalis* LPS, mycobacterial membrane fractions, and Zymosan particles from yeast cells (Figure 4.7). We transfected SW620 cells with TLR2 together with the different TLR1 point mutants, and measured the relative IL-8 – luciferase activity after stimulation with the aforementioned agonists. The summarized data from single point mutants shown in Figure 4.7 are mapped in LRRs 11 and 12 of the TLR1 ECD. When transfected cells were stimulated with *P. gingivalis* LPS, the F314D, P315L, Q316K, and V339D mutants were highly attenuated, showing less than 20% IL-8 – luciferase activity. The V311E and E321V mutants were weakly attenuated in sensing *P. gingivalis* LPS, with about 40-60% IL-8 – luciferase activity. The mutated residues that conferred a highly attenuated response to *P. gingivalis* LPS are strikingly similar to what was observed with Pam_3CSK_4 (Figure 4.5), suggesting that the same region in TLR1 may be required for binding to or recognizing one of the acyl chains of *P. gingivalis* LPS.

Similarly, we also observed that the response of SW620 cells expressing the TLR1 mutants F314D, P315L, Q316K, and V339D mutants were also highly attenuated when stimulated with mycobacterial membrane fraction and Zymosan particles, while the mutants V311E, Y320N, and E321V exhibited a weakly attenuated response. These

suggest that even with a heterogeneous mixture of agonist whose structures may differ from the typical lipidated TLR1/TLR2 agonists, the region required for TLR1 recognition remains the same.

Using the information from the TLR1/TLR2/Pam_3CSK_4 crystal structure uploaded at the Protein Data Bank (PDB 2Z7x) and the VMD software, we mapped these important residues on the TLR1 ECD. Figure 4.8A shows the ribbon diagram of the TLR1 LRRs 10-12 and the relative position of the residues V311, F314, P315, Q316, Y320, E321, and V339 on the flexible loops on the convex surface of LRRs 11 and 12. Figure 4.8B shows the same information, with the critical residues illustrated in space-filling model to demonstrate that the residues V311, F314, P315, Q316, Y320, and V339 all line the entrance of the hydrophobic pocket of TLR1 formed between LRRs 11 and 12, and where the third acyl chain of Pam_3CSK_4 binds in the crystal structure. This explains why the mutants F314D, P315L, Q316K, and V339D were unresponsive to Pam_3CSK_4, *P.gingivalis* LPS, mycobacterial membrane fraction, and Zymosan particles (Figures 4.5 and 4.7). More importantly, these residues may be critical for the formation of a dimer interface with the co-receptor TLR2.

Figure 4.8C reveals the dimer interface between LRRs 10*-13* of TLR2 (left side, shaded in gray) and LRRs 10-12 of TLR1 (right side, shaded in blue), as viewed from the top of the ternary TLR1/TLR2/Pam_3CSK_4 ternary complex structure. For orientation, two of the acyl chains of Pam_3CSK_4 are inserted inside the hydrophobic pocket of TLR2 formed between LRRs 12* and 13*, while the third acyl chain of Pam_3CSK_4 is inserted inside the hydropobic channel formed by LRRs 11 and 12 of TLR1. The hydrophobic/non-polar, polar, acidic, and basic residues are shaded in yellow,

green, red, and blue, respectively. The side chains of the TLR1 amino acid residues V311, P315, Y320, and V339 are all predicted to have hydrophobic interactions with some residues in TLR2 (Jin et al., 2007). For example, the hydrophobic V311 residue of TLR1 is predicted to interact with the residues L350*, P352*, and Y376* of TLR2. The P315 residue of TLR1 is predicted to interact with the TLR2 Y323*. The polar Y320 of TLR1 is predicted to interact with TLR2's F322*, Y323*, and L324*. Finally, V339 of TLR1 is predicted to interact with F322*, F349*, and L371* of TLR2. On the other hand, the acidic amino acid residue E321 found at the periphery of the convex surface of TLR1 is predicted to form ionic bonds with the basic residues H318* and R321* found in the flexible loop of LRR11* of TLR2.

Taken altogether, the critical residues important for recognition of a variety of TLR1/TLR2 agonists that we have identified in our random mutagenesis studies are located in regions of the TLR1 ECD that are important for formation of dimer interface with TLR2. Our data were found to be consistent with the published TLR1/TLR2/Pam_3CSK_4 crystal structure and provides strong support to most of the predicted important interacting residues in TLR1 (Jin et al., 2007).

Discussion

Lipoproteins or lipopeptides are potent agonists of TLR2 and its co-receptors (Aliprantis et al., 1999; Brightbill et al., 1999; Takeuchi et al., 2000). Through the reciprocal domain exchange of two homologous TLRs, TLR1 and TLR6, our previous studies have shown that the residues of LRRs 9-12 of TLR1 and TLR6, though not sufficient, are required for discriminating between triacylated and diacylated lipopeptides (Omueti et al., 2005). Other researchers such as (Grabiec et al., 2004) and (Andersen-

Nissen et al., 2007) have demonstrated the role of central LRRs of TLR2 and TLR5 in mediating species-specific agonist specificity to different lipopeptides and flagellin, respectively.

This study aims to further define the specific region(s) in the TLR1 ECD that is required for recognition of various microbial cell wall components that are known to activate the TLR1/TLR2 receptor pair. The first purified microbial component that we tested on SW620 epithelial cells were purified atypical LPS from *Porphyromonas gingivalis* (*P. gingivalis*). This Gram-negative bacterium is the causative agent of chronic oral inflammation that leads to periodontal disease (Holt et al., 1999). It has been demonstrated that a preparation of *P.gingivalis* LPS may contain various Lipid A species, some of which are recognized by TLR4, while others are sensed by TLR1/TLR2; but stringent purification procedures can separate the different Lipid A species (Darveau et al., 2004; Hirschfeld et al., 2001).

In addition to *P. gingivalis* LPS, we also used other heat-killed microbial preparations or microbial products previously demonstrated to be TLR2 dependent agonists, which include arabinose lipoarabinomannan (ARALAM) from mycobacterial sp. (Means et al., 1999); zymosan yeast particles (Sato et al., 2003; Underhill et al., 1999); mycobacteria membrane fractions; heat killed *Staphylococcus aureus* (HKSA); and heat-killed *Listeria monocytogenes* (HKLM). Mycobacterial membrane fractions are rich in TLR2 agonists such as lipomannans, lipoarabinomannans, glycolipids, and various species of lipoproteins (Gehring et al., 2004; Gilleron et al., 2003; Means et al., 1999; Noss et al., 2001; Pecora et al., 2006; Quesniaux et al., 2004). *S. aureus* and *L. monocytogenes* are both Gram-positive organisms. The cell wall of gram positive

organisms is known to be rich in peptidoglycan and lipoteichoic acids (Dziarski & Gupta, 2005; Schwandner et al., 1999). It has been shown that heat-killed whole cell preparation of *S. aureus* induced NF-kB activation in TLR2-transfected CHO cells (Yoshimura et al., 1999). It has also been observed that TLR2-deficient mice are highly susceptible to *S. aureus*, whereas TLR4-deficient mice are not (Takeuchi et al., 2000).

All the microbial agonists that we tested in this study require LRRs 9-12 of TLR1 to be involved in their recognition. Interestingly, the heat-killed microbial agonists and particulates, showed a requirement for not only LRRs 9 through 12 but for a larger region extending before or after this LRR region. The reason for this observation is currently not known. A possibility is that these particulate agonists do need a larger contact surface area of TLR1 in order to be recognized by the receptor. Regardless of the surface area required, a theme that emerges from the N-terminal and internal chimera results is that when the TLR1 LRRs 9-12 are missing, or not part of the chimeric receptor, the cell activation observed upon stimulation is very minimal.

Since LRRs 9-12 of TLR1 were repeatedly shown to be the smallest region of importance in the recognition of various microbial agonists, a library of clones with single amino acid substitutions within this region of TLR1 was created. We tested for cell surface expression and the ability of the single point mutants to bind to an anti-TLR1 mAb GD2.F4.We have previously shown that GD2.F4 is a neutralizing anti-TLR1 mAb that failed to bind to the $TLR1_{P315L}$ mutant (Omueti et al., 2007). In this study, we have demonstrated that the putative epitope of the anti-TLR1 blocking mAb, GD2.F4, maps to the flexible loop of LRR 11of TLR1 and includes the amino acid positions S309, D310, F312, F314, P315, Q316, S317, and Y320. The knowledge of the antibody epitope could

potentially lead to the design of therapeutic inhibitory compounds that could either serve as an antagonist to TLR1/TLR2 or as a competitive inhibitor to the natural microbial agonists.

More importantly, by combining our results from the GD2.F4 binding experiments and the screening of TLR1 single point TLR1 mutants for their response to various agonists such as Pam_3CSK_4, *P. gingivalis* LPS, mycobacterial membrane fraction, and yeast Zymosan, our data demonstrate that the amino acid residues F314, P315, Q316, and V339 of TLR1 are required for sensing various microbial components known to activate TLR1/TLR2 regardless of the microbial component's chemical structure. Interestingly, three of the amino acids (F314, P315, and Q316) that lay side-by-side in the outer loop of LRR11 lining the entrance of the TLR1 hydrophobic pocket, was also identified to be a part of the putative epitope of the GD2.F4 mAb. The mutants F314L, P315L, Q316K failed to bind to GD2.F4 and also failed to respond to the microbial agonists used in this study. The V339D mutant, on the other hand, was unresponsive to the microbial agonists tested but was able to bind to the GD2.F4 mAb. While it is possible that the mutations at F314L, P315L, and Q316K simply destroyed or altered the structure of the TLR1 extracellular domain, the V339D mutant demonstrate that our results are real and add to the argument that collectively, these regions are important specifically for the formation of a dimer interface with TLR2. V339 lies within the outer loop of LRR12 just below the three residues in LRR11, also part of the hydrophobic residues lining the entrance of the TLR1 binding pocket (Figure 4.5). The physical proximity of F314, P315, Q316 and V339 to the hydrophobic binding pocket of TLR1 combined with the loss-of-function data resulting from mutations of these residues

suggests a functional patch that may affect the interaction of TLR1 with both the agonist and the co-receptor TLR2. Based on the TLR1/TLR2/Pam_3CSK_4 crystal structure (Jin et al., 2007), the amino acid residues P315 and V339 of TLR1 are predicted to form hydrophobic interactions with several amino acid residues from TLR2 (Figure 4.8.C).

Kinetic measurements performed on soluble wild-type TLR1 and the $TLR1_{P315L}$ extracellular domain binding to lipoproteins reveal that there is only a 1.5-fold difference in their affinity for the agonist, where TLR1-lipoprotein $K_D = 7.45x10^{-7}$ while $TLR1_{P315L}$ $K_D = 1.13x10^{-6}$ (see Chapter 3 Table 3.3). However, cells that were stimulated with $TLR1_{P315L}$ failed to respond to Pam_3CSK_4 (Omueti et al., 2007). Furthermore, purified $TLR1_{P315L}$ ECD failed to form a ternary complex with TLR2 in the presence of excess amounts of Pam_3CSK4 (Figure 4.6). All these data suggest that proline at position 315 is more important for the formation of a dimer interface with TLR2.

It is noteworthy to mention that the amino acid residues V311, P315, Y320, R337, and V339 of TLR1 were found to be necessary for the recognition of a non-lipidated protein ligand, the pentameric ganglioside-binding (B_5) sub-unit of the type IIb enterotoxin from *E. coli* (LT-IIb-B_5) (Liang et al., 2009). The molecular docking studies performed by this group suggest that the relatively huge LT-IIb-B_5 protein binds to hydrophobic residues found at the convex surface of both TLR1 and TLR2 LRRs 9-12 domain (Liang et al., 2009). This interaction leads to the formation of a similar "m-shaped" TLR1/TLR2 heterodimer, suggesting that the critical TLR1 residues identified in their mutational studies are located on the TLR1/TLR2 dimer interface region (Liang et al., 2009).

Phylogenetic studies on TLR1 reveal that the TLR1 gene has undergone positive selection over the course of evolution (Wlasiuk & Nachman, 2010). Numerous amino acid sites were predicted to be important either for ligand binding or formation of dimer interface with TLR2. Comparing our TLR1 mutational studies with their computational data, we found that only a few amino acid sites are in common, namely, amino acids at position 289, 293, 303, 313, 321, and 337 (Wlasiuk & Nachman, 2010). Computational data also suggest that amino acid position 303 and 313 are important for ligand binding, while 321 and 337 are necessary for the formation of a dimer interface with TLR2. We generated mutants F289I, D293Y, S303Y, E321V, E321K, E321D, and R337H. With the exception of R337H, all mutants were expressed well on the cell surface, however, their response to Pam_3CSK_4 as measured by the IL-8-luciferase activity is similar to wild-type TLR1 (Table 4.1), suggesting that these mutations did not affect function of TLR1 in terms of recognizing Pam_3CSK_4 nor binding with TLR2. A few evolutionary and polymorphic studies have also suggested amino acid positions located in other LRRs of TLR1 that may be important for the formation of dimer interface. This includes the SNPs L443I, V542A, and T565S that are found in LRR17 and the C-terminal capping region of the TLR1 ECD (Georgel et al., 2009; Jin et al., 2007). However, these regions are outside the scope of our random mutagenesis study.

Taken altogether, our data suggest that irrespective of their assumed chemical nature, the microbial agonist induces the formation of an "m-shaped" TLR1/TLR2/agonist ternary complex. To date, the crystal structures of seven TLRs in complex with their respective ligands have already been solved: TLR1/TLR2/Pam_3CSK_4 (Jin et al., 2007), TLR2/TLR6/Pam_2CSK_4 (Kang et al., 2009), TLR4/MD2/LPS (Park et

al., 2009), TLR3/double-stranded RNA (Liu et al., 2008), TLR5/FliC flagellin (Yoon et al., 2012), and TLR8/single-stranded RNA (Tanji et al., 2013). The unifying theme taken from all these available TLR-ligand crystal structures is the fact that upon ligand binding, the TLRs undergo conformational changes to form a stable "m-shaped" complex that allows the C-terminal regions, and consequently the TIR cytoplasmic domain of the two interacting TLRs, to come into close proximity with one another thus setting up the stage that allows a signaling cascade to occur. [Reviewed in (Akira et al., 2006; O'Neill, 2008)].

Figures

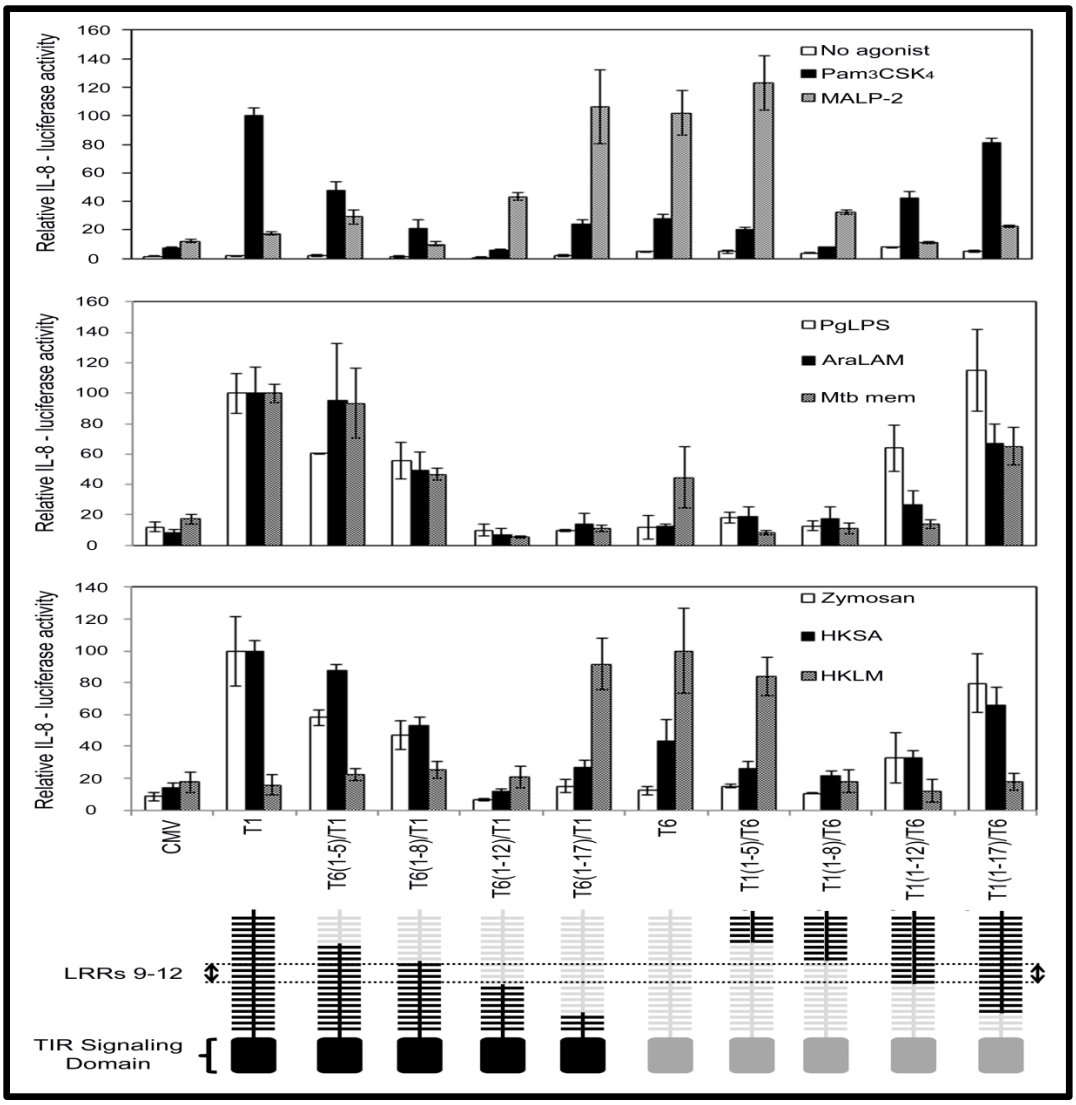

Figure 4.1. The LRRs 9-12 of TLR1 are important for recognition of a variety of microbial agonists. SW620 epithelial cells were co-transfected with TLR2 and either a TLR1 or a TLR6 N-terminal chimera, an IL-8-driven luciferase gene, and a *Renilla* transfection control. Cells were then stimulated with 20ng/ml Pam_3CSK_4, 20ng/ml MALP-2, 100ng/ml *P. gingivalis* LPS (Pg LPS), 10μg/ml of non-mannose-capped lipoarabinomannan (AraLAM) from Mycobacterial cell walls, 6μg/ml of Mycobacterial membrane fraction (Mtb mem), $1x10^7$ particles/ml of Zymosan particles, 200μg/ml of heat-killed *Staphylococcus aureus* (HKSA), and $1x10^8$ cells/ml of heat-killed *Listeria monocytogenes* (HKLM). Six hours post-stimulation, the luciferase activity was measured following manufacturer's protocol. Firefly luciferase activities were normalized to that of the Renilla luciferase control. These values were normalized to that of empty CMV vector whose value was taken as 1. Error bars represent the standard deviation of three independent events. Chimeric constructs are indicated at the bottom, with black areas indicating regions of TLR1 and gray areas indicating regions of TLR6.

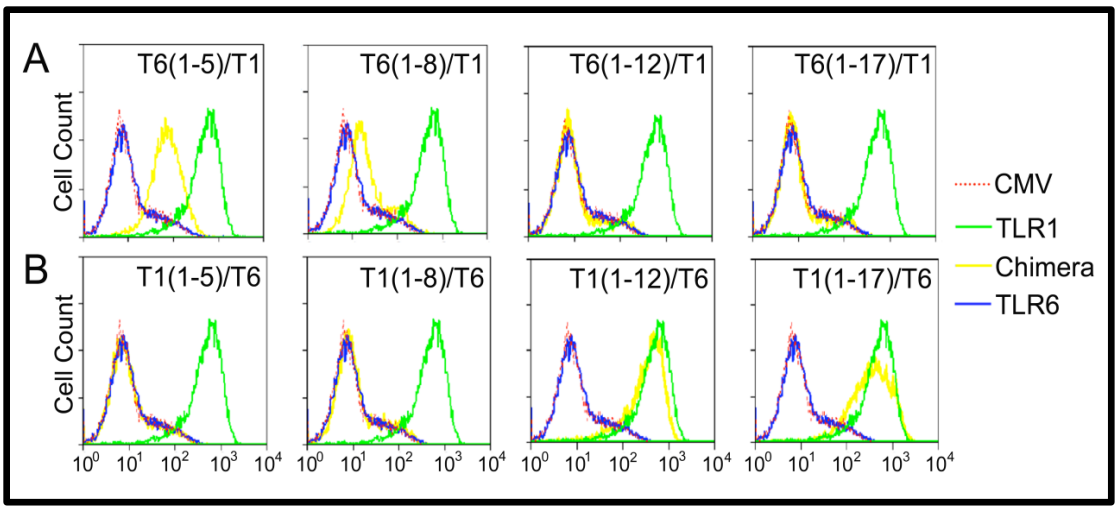

Figure 4.2. N-terminal TLR1 and TLR6 chimeras demonstrate that the epitope of anti-TLR1 mAb, GD2.F4, maps to the central LRRs 9-12 of TLR1. HEK 293T cells were transfected with either FLAG-tagged empty CMV vector (red-dotted line), FLAG-tagged TLR1 (green), FLAG-tagged TLR1 chimera (yellow) labeled specifically in each box, or FLAG-tagged TLR6 (blue). After 48 hours, cells were removed from the plate and incubated sequentially with anti-TLR1 mAb, GD2.F4, followed by biotinylated donkey anti-mouse secondary Ab, and a streptavidin-PE-conjugated tertiary antibody. After labeling, the cells were washed, fixed, and analyzed by flow cytometry for surface expression of TLRs.

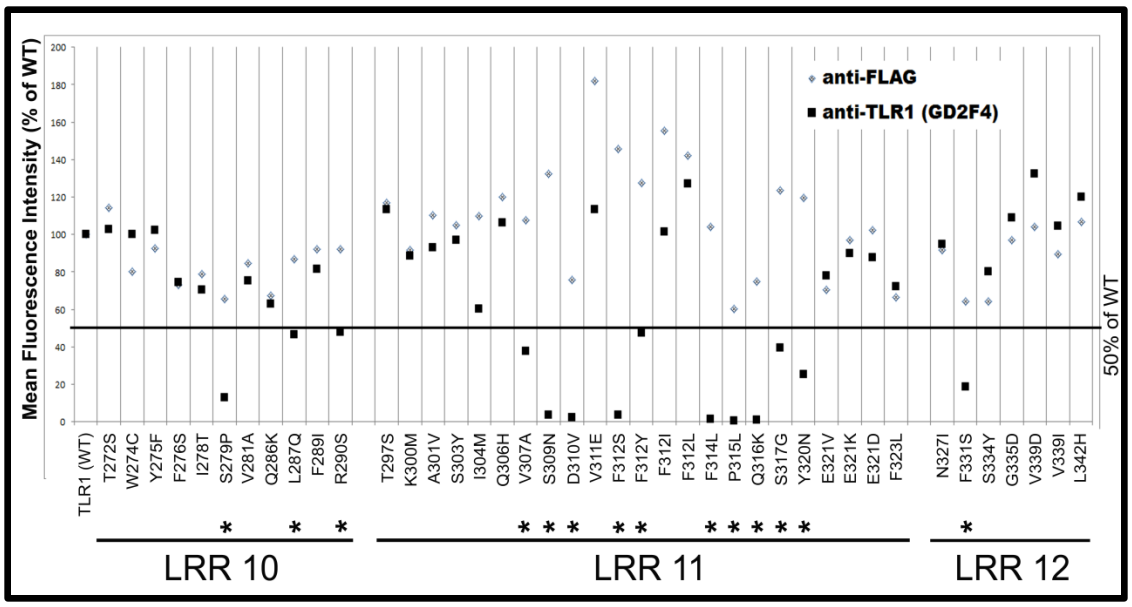

Figure 4.3. The putative epitope of anti-TLR1 mAb (GD2.F4), a blocking antibody against TLR1, extends from S279P to F331S. HEK 293T cells were transfected with either FLAG-tagged wild-type TLR1 or any of the fifty-nine single-point TLR1 mutants. After 48 hours, cells were removed from the plate and incubated sequentially with either an anti-FLAG (A) or an anti-TLR1 mAb, GD2.F4 (B) as the primary antibody, followed by biotinylated donkey anti-mouse secondary Ab, and a streptavidin-PE-conjugated tertiary antibody. After labeling, the cells were washed, fixed, and analyzed by flow cytometry for surface expression of TLRs. The data were normalized to that of the wild-type TLR1 whose value was set at 100% mean fluorescence intensity (MFI). Single point mutants that had less than 50% MFI relative to wild-type TLR1 upon staining with the anti-TLR1 monoclonal antibody (GD2.F4) were marked with *****.

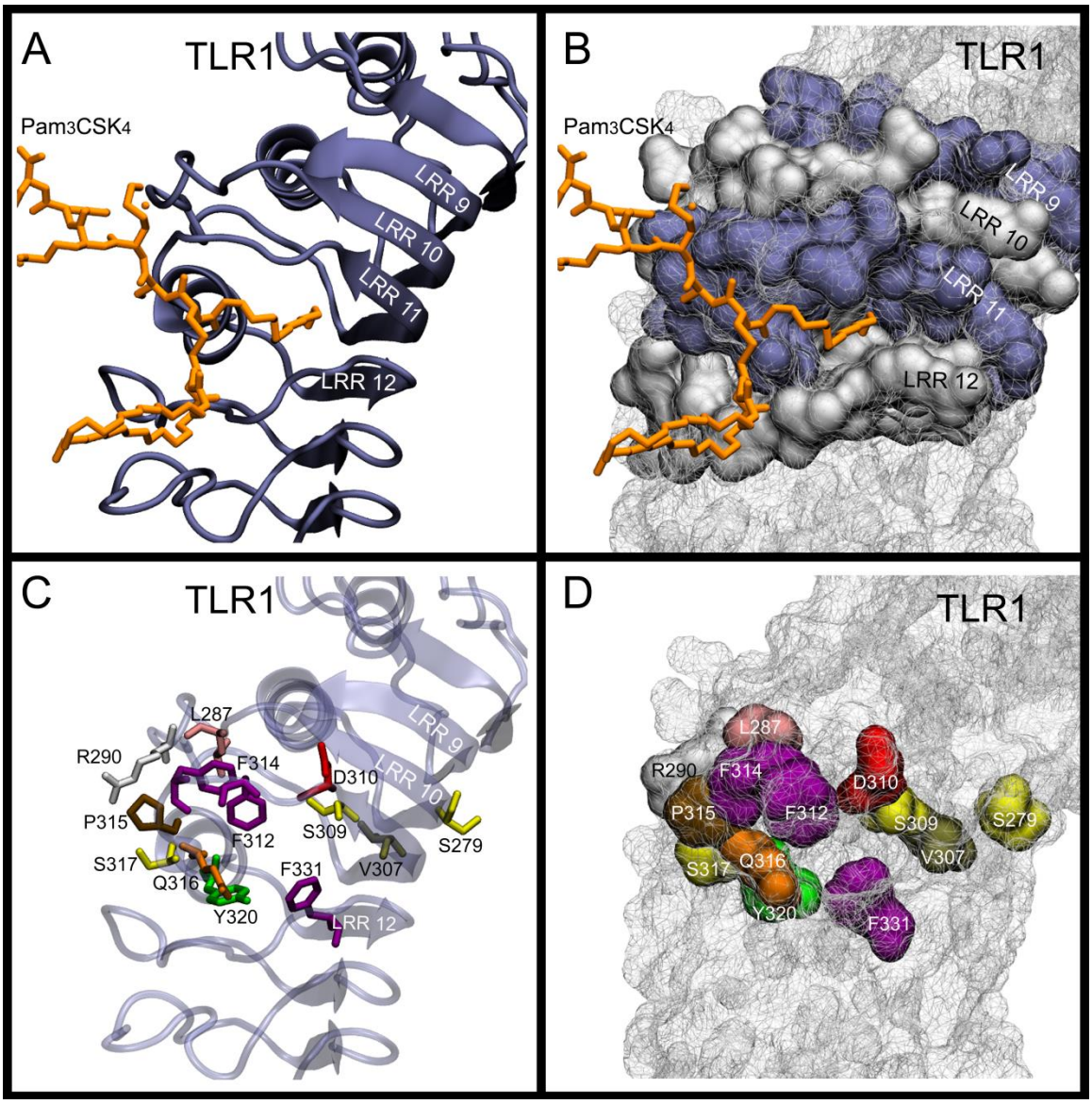

Figure 4.4. Structural model for the conformational epitope of the anti-TLR1 mAb (GD2.F4) using the PDB file 2Z7X and the VMD software. (A) Ribbon diagram of TLR1 LRRs 9-12 (in dark blue), together with Pam_3CSK_4 (in orange). One of the acyl chains of Pam_3CSK_4 in inserted between LRRs 11 and 12 of TLR1. (B) Space-filling model of the same region shown in (A), with the LRRs in alternating color. LRRs 9 and 11 are in blue, while LRRs 10 and 12 are in light gray. The hydrophobic pocket of TLR1 formed between LRRs 11 and 12 is the area where one of the acyl chains in Pam_3CSK_4 (orange) is inserted. (C) Ribbon diagram of TLR1 together with the different amino acid residues that were found to be critical for binding the anti-TLR1 mAb: S279, L287, R290, V307, S309, D310, F312, F314, P315, Q316, S317, Y320, and F331. The amino acids are colored according to their name (ser: yellow, leu: pink, arg: grayish-white, val: tan, asp: red, phe: purple, pro: ochre, gln: orange, and tyr: green). (D) Space-filling model of the same region shown in (C).

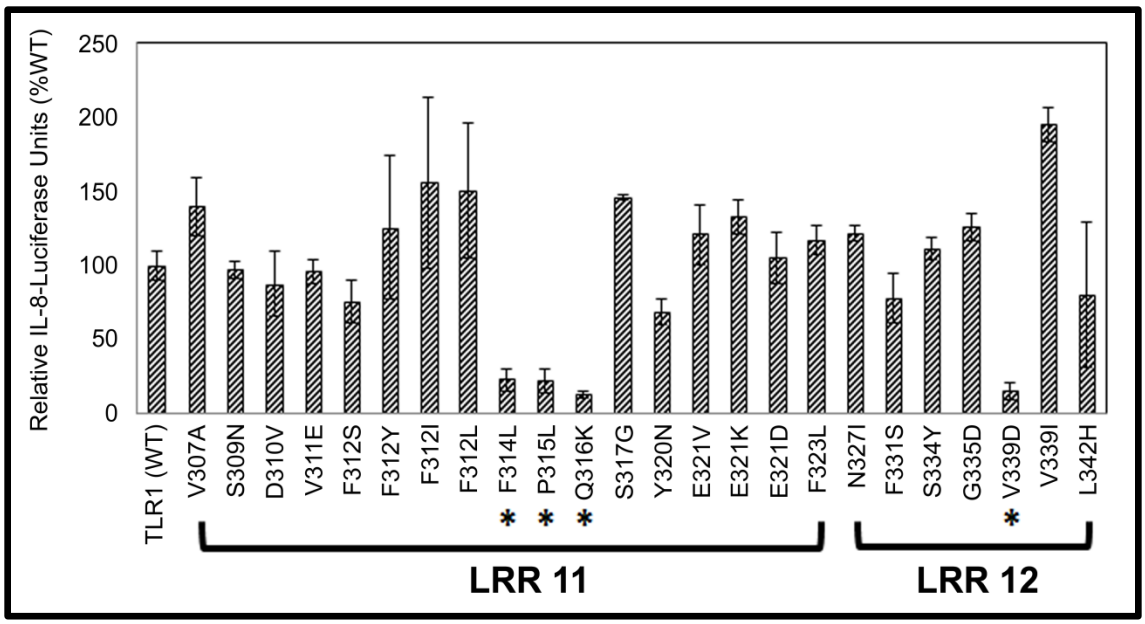

Figure 4.5. The TLR1 single-point mutants F314L, P315L, Q316K, and V339D exhibit highly-attenuated responses to the triacylated lipopeptide Pam_3CSK_4. SW620 epithelial cells were co-transfected with TLR2 and different TLR1 single-point mutants, an IL-8-driven luciferase gene, and a *Renilla* transfection control. Cells were then stimulated with 20ng/ml Pam_3CSK_4. Six hours post-stimulation, the luciferase activity was measured following manufacturer's protocol. Firefly luciferase activities were normalized to that of the Renilla luciferase control. These values were normalized to that of empty CMV vector whose value was taken as 1. Error bars represent the standard deviation of three independent events.

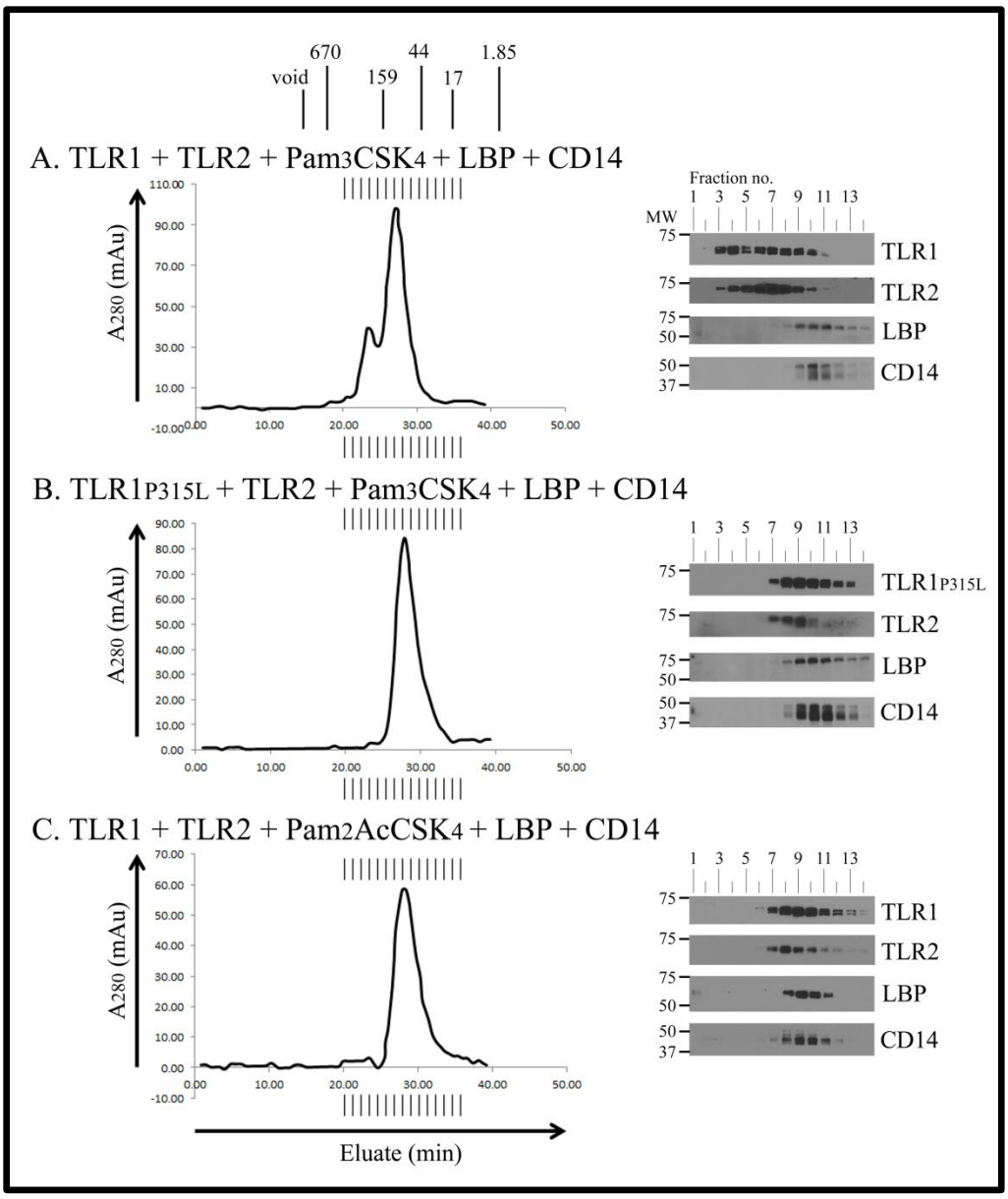

Figure 4.6. $TLR1_{P315L}$ does not form a ternary complex with TLR2 and Pam_3CSK_4 in solution. 0.5uM wild-type TLR1 (A) or 0.5uM $TLR1_{P315L}$ (B) were pre-incubated with 0.5uM TLR2, a 5 fold molar excess of Pam_3CSK_4 (2.5uM), 0.05uM LBP, and 0.25uM sCD14 in PBS pH 7.4 buffer for two hours at 37°C in a 500ul reaction volume. In (C), 2.5uM Pam_2AcCSK_4 was added to wild-type TLR1, TLR2, LBP and CD14 instead of Pam_3CSK_4. Protein complexes were separated by size exclusion chromatography. The expected molecular weight of the TLR monomers and dimers was estimated by column calibration using known molecular weight standards including bovine thyrogloblulin (670 kDa), bovine γ-globulin (158 kDa), ovalbumin (44 kDa), myoglobin (17 kDa), and vitamin B-12 (1.35 kDa). Proteins in eluted fractions were separated on a 7.5% SDS-PAGE gel, transferred by Western blotting, and TLR1, TLR2, LBP or sCD14 were detected using suitable antibodies and HRP conjugates (see Materials and Methods). The results shown are representative of at least three independent experiments.

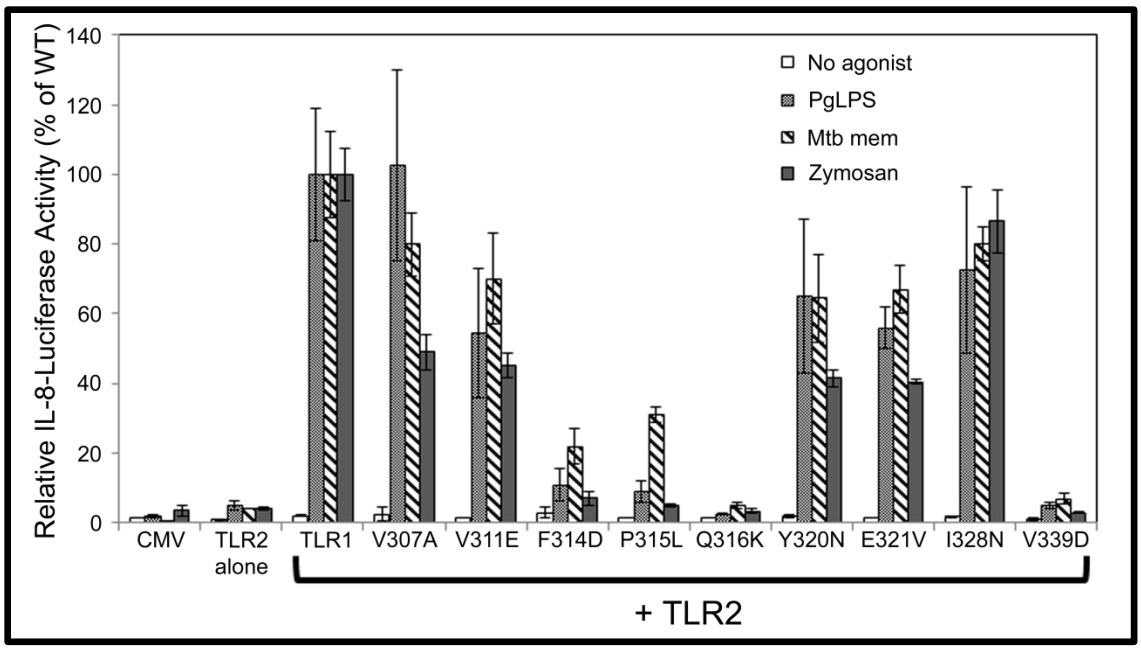

Figure 4.7. The same single-point TLR1 mutants F314L, P315L, Q316K, and V339D exhibited highly attenuated responses to a variety of microbial agonists. SW620 epithelial cells were co-transfected with TLR2 and different TLR1 single-point mutants, an IL-8-driven luciferase gene, and a *Renilla* transfection control. Cells were then stimulated with 100ng/ml *P. gingivalis* LPS (Pg LPS), 6μg/ml of Mycobacterial membrane fraction (Mtb mem), and $1x10^7$ particles/ml of Zymosan particles. Six hours post-stimulation, the luciferase activity was measured following manufacturer's protocol. Firefly luciferase activities were normalized to that of the Renilla luciferase control. These values were normalized to that of empty CMV vector whose value was taken as 1. Error bars represent the standard deviation of three independent events.

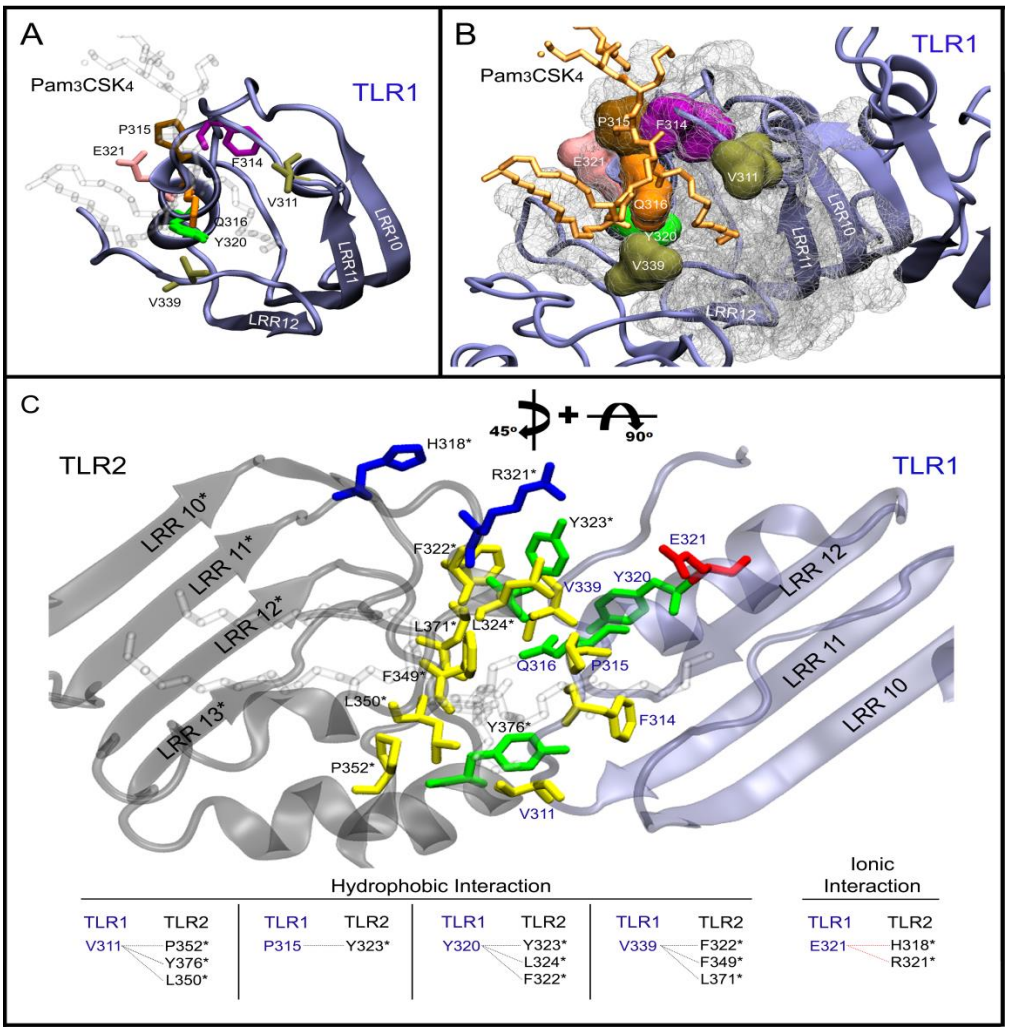

Figure 4.8. Structural model of the critical residues found in LRRs 11 and 12 of TLR1 required for recognition of different microbial agonists using the PDB file 2Z7X and the VMD software. (A) Ribbon diagram of TLR1 LRRs 10-12 (in dark blue), together with the amino acid residues V311, F314, P315, Q316, Y320, E321, and V339 colored according to amino acid name (val: tan, phe: purple, pro: ochre, gln: orange, and tyr: green). A gray sketch of Pam_3CSK_4 was included for orientation purposes. (B) Space-filling model of the same region shown in (A). (C) Ribbon diagram of the top view of the TLR1/TLR2/Pam_3CSK_4 ternary complex (PDB 2Z7X) highlighting the critical interacting amino residues between TLR1 and TLR2. TLR1 LRRs 10-12 are shown in blue on the right, while TLR2 LRRs 10*-13* are shown in gray on the left. The critical amino acid residues in TLR1 are shown in blue font, while those of TLR2 are shown in black font marked with a *. The residues were color-coded according to amino acid properties: non-polar is yellow, polar is green, acidic is red, and basic is blue. The predicted hydrophobic and ionic interactions between specific TLR1 and TLR2 residues are summarized at the bottom of the figure. Pam_3CSK_4 is partly shown in light gray sketch with two of its acyl chain inserted between LRRs 12* and 13* of TLR2, and the third acyl chain inserted between LRR 11 and 12 of TLR1.

Table

Table 4.1. TLR1 clones with single amino acid substitution within LRRs 9-12. The first column indicates the amino acid change of the clone. Columns two and three summarize the data obtained from HEK 293T cells transfected with the clones and their relative mean fluorescence intensity with respect to wild-type TLR1 upon staining with anti-FLAG and anti-TLR1 mAb, respectively. The fourth column shows the IL-8-luciferase data from SW620 cells transfected with the clone and TLR2 and stimulated with 20ng/ml Pam_3CSK_4 (as described in Materials and Methods section), while the fifth column reflects the standard deviation calculated from three independent trials.

AMINO ACID CHANGE	**%WT Fluorescence (anti-FLAG)**	**%WT Fluorescence (anti-TLR1)**	**Pam_3CSK_4**	**(+/-) Error**
TLR2 ALONE	-	-	10.53	(7.09)
TLR1	100.00	100.00	100.00	(10.23)
LRR 9				
V268G	8.9	2.69	10.44	(4.97)
V268I	84.85	84.46	131.73	(31.70)
LRR 10				
H270Y	109.00	103.23	92.55	(12.40)
H270R	60.94	55.41	74.37	(73.65)
T271I	50.62	56.73	205.64	(6.60)
T272S	114.38	102.58	102.98	(18.07)
V273E	28.50	10.90	33.79	(5.77)
W274R	24.79	5.37	98.53	(33.20)
W274C	80.10	99.98	78.14	(68.20)
Y275F	92.74	102.22	199.84	(47.14)
F276S	73.13	74.23	93.72	(35.27)
I278T	79.03	70.46	213.36	(29.08)
S279P	65.57	12.87	59.82	(28.37)
S279T	77.54	89.96	103.19	(35.30)
V281M	75.29	86.87	73.74	(52.20)
V281A	84.56	75.48	136.67	(12.77)
G285K	35.29	26.99	120.22	(8.52)
Q286P	112.50	120.17	94.38	(55.84)
Q286K	67.16	62.75	116.29	(16.40)
L287Q	86.61	46.66	167.66	(56.60)
F289I	92.17	81.44	107.15	(2.56)
R290S	92.26	47.96	152.64	(9.02)
D293Y	61.66	65.64	117.33	(2.43)
LRR 11				
T297S	116.98	113.32	133.83	(3.83)
K300M	91.73	88.56	84.95	(48.90)
A301V	110.10	92.86	158.29	(27.81)

Table 4.1. (continued)

S303Y	104.80	96.90	110.57	(39.30)
I304M	109.88	60.33	94.77	(27.50)
I304K	4.90	3.69	36.34	(9.90)
Q306H	120.21	106.10	84.60	(30.50)
V307A	107.39	37.59	139.48	(19.68)
S309N	132.25	3.61	97.35	(5.83)
D310V	75.95	2.44	87.39	(22.10)
V311E	181.96	113.17	95.55	(8.25)
F312S	145.74	3.76	75.42	(14.40)
F312Y	127.57	47.36	125.39	(48.40)
F312I	155.34	101.56	155.83	(57.90)
F312L	142.05	127.02	150.68	(45.10)
F314L	103.93	1.56	23.08	(7.45)
P315L[6]	60.03	0.65	21.85	(8.04)
Q316K	75.03	1.03	12.74	(2.81)
S317G	123.44	39.35	145.97	(1.29)
Y320N	119.48	25.32	68.58	(8.74)
E321V	70.63	77.83	120.89	(20.41)
E321K	96.86	89.85	132.99	(11.76)
E321D	102.24	87.62	105.32	(17.35)
F323L	66.66	72.27	117.32	(9.96)
LRR 12				
N327Y	58.28	61.57	95.45	(27.14)
N327I	91.56	94.61	121.89	(5.02)
I328N	49.68	46.55	29.07	(4.56)
F331S	64.20	18.55	78.01	(16.92)
S334Y	64.19	80.02	111.58	(7.88)
G335D	96.79	109.12	125.88	(9.38)
G335S	93.06	128.43	93.60	(53.50)
R337H	27.76	5.80	131.71	(30.64)
V339D	104.02	132.59	14.99	(6.05)
V339L	109.92	134.35	100.46	(7.70)
V339I	89.40	104.73	195.01	(11.36)
L342H	106.83	119.98	80.32	(48.95)

[6] From Omueti KO, Mazur DJ, Thompson KS, Lyle EA, Tapping RI. J Immunol. 2007 May 15; 178 (10): 6387-6394.

CHAPTER FIVE

CONCLUSION

Summary

Through recognition of specific microbe-associated molecular patterns (MAMPs), including bacterial lipoproteins, the TLR1 and TLR2 receptor pair plays a pivotal role in the induction of host inflammatory responses following infection. TLR2 is an extensively studied receptor in innate immunity. Its importance in host inflammatory responses to infection has been demonstrated in studies using knockout mice. However, these types of studies do not provide insights into the structure/function relationship or in the interactions with actual ligands and/or co-receptors. The availability of the crystal structure of TLR1/TLR2/Pam_3CSK_4 has been a tremendous contribution to the knowledge on structure/function relation, and provided validation to numerous mutational and overexpression studies performed to understand TLR2 interaction with TLR1. This dissertation sought to gain further insights on the order of events that lead to TLR1/TLR2/Pam_3CSK_4 ternary complex formation as well as to identify critical regions in the TLR1 ECD that are required for ligand recognition and/or interaction with TLR2.

The most commonly studied TLR2 ligands are the synthetic tri- and diacylated lipopeptides Pam_3CSK_4 and Pam_2CSK_4, as well as the Mycoplasma-derived lipoproteins macrophage-activating lipopeptide-2 (MALP2) and FSL-1. Bacterial lipoproteins are characterized by a diacyl-glycerol that is connected to the sulfur atom of the N-terminal cysteine. Depending on the microbe and whether or not it is producing a certain type of enzyme, an additional lipid chain is added to the cysteine amino terminus via an amide bond (Nakayama et al., 2012). Stimulation of cells by soluble bacterial triacylated

lipoproteins involves formation of a ternary TLR1/TLR2/lipoprotein complex. However, even though the TLR1/TLR2 pair is able to recognize soluble lipoproteins, in the intact cell wall of microbes, the lipoproteins are anchored in the microbial membrane and therefore inaccessible to the receptors (Underhill & Gantner, 2004). Chapter 2 described how cell stimulation is enhanced by either serum LBP or sCD14, two pattern recognition receptors which were demonstrated to act by catalytically delivering lipopeptides directly to TLR1/TLR2. Using purified proteins that are monomeric, properly folded, and biologically functional, we were able to demonstrate by size exclusion chromatography that LBP and sCD14 enhance TLR1/TLR2/Pam_3CSK_4 formation but are not part of the stable ternary complex. Either LBP or sCD14 were shown to independently deliver Pam_3CSK_4 to TLR1 and TLR2. This is the first report demonstrating that LBP can deliver agonists directly to TLR1/TLR2 independent of CD14. Unlike the TLR4 system, our data suggests that there is a redundancy of function between LBP and CD14 in terms of presenting lipopeptides directly to TLR1 and TLR2. Likewise, we were also able to show that cellular responses of epithelial cells to microbial lipoproteins are enhanced by either LBP or sCD14, but sCD14 requires a longer time to bind to triacylated lipopeptides compared to LBP.

The question of whether or not TLRs form pre-formed homodimers or heterodimers were also addressed in Chapter 2. In the absence of any agonists, pre-incubation of TLR1 either with itself or with TLR2 did not lead to the formation of stable homodimers and/or heterodimers. We also have physical evidence showing that the triacylated lipopeptide Pam_3CSK_4 induces the formation of TLR1/TLR2 heterodimers but not homodimers. Our data supports the numerous findings demonstrating that TLR2 must

heterodimerize with its co-receptors upon ligand recognition to initiate the appropriate signaling response (Ozinsky et al., 2000; Takeuchi et al., 2001; Wyllie et al., 2000). We acknowledge that our studies mainly involved the use of soluble TLR ECDs, and that the TLR transmembrane and/or the TIR domains may contribute to the homodimerization or heterodimerization observed by other groups (Triantafilou et al., 2006).

Chapter three described the biophysical measurements we performed to address a possible competition between TLR1 and TLR10 for microbial agonists and the co-receptor TLR2. It is noteworthy to take a closer look at the TLR2/10 interaction and compare that with the TLR1/2 pair, given that we have previously reported that TLR10 is able to interact with TLR2 in response to agonists that are shared with TLR1 (Guan et al., 2010). It is also interesting to note that TLR10 expression is high in B cells, but very low in macrophages and plasmacytoid dendritic cells [Reviewed in (Janssens & Beyaert, 2003]. Knowing that TLR10 does not signal via the known TLR2-mediated signaling pathway leading to the expression of pro-inflammatory cytokines and chemokines, we believe that TLR10 competes with TLR1 in recognizing TLR1/TLR2 agonists leading to a different, yet unknown, cellular response. Additional data from other colleagues in our lab who are looking at TLR10 suggest that this receptor may be independently acting as a global suppressor to dampen the cell's immune response (Jiang, Li, Hess, and Tapping, unpublished results).

Our qualitative experiments using microtiter plate assays demonstrated that TLR2 binding to either TLR1 or TLR10 is ligand-induced, saturable and agonist-specific. Compared to TLR1, TLR10 required more TLR2 to form a complex with Pam_3CSK_4 in microtiter plates. We were able to demonstrate in Chapter 2 that we could form the

TLR1/TLR2/Pam_3CSK_4 ternary complex in solution. However, using the same size exclusion chromatography assay, we were not able to observe a stable TLR2/TLR10/Pam_3CSK_4 complex formation in solution. The results of our microtiter plate assays and the size exclusion chromatography column suggest that the affinity of TLR2 to TLR10 is weaker compared to that of TLR1.

To measure kinetics of interaction between the receptors and the agonist, we performed biolayer interferometry on an Octet instrument, which was shown to be a more reliable method for measuring protein interactions in a two-component system compared to surface plasmon resonance on a BIAcore machine. We have evidence showing that Fc-tagged TLRs 1, 2, and 10 all directly bind to a 12kDa lipoprotein (Lip12) purified from *E. coli* that has been previously verified to stimulate TLR1/TLR2- but not TLR2/TLR6-transfected cells. Amongst the three TLRs tested, TLR1 showed the highest affinity or lowest dissociation constant for the lipoprotein ($K_D = 7.45x10^{-7}$ M), followed by the TLR10-Lip12 ($K_D = 3.34x10^{-7}$M), and finally by TLR2-Lip12 ($K_D = 1.58x10^{-6}$M). To our knowledge, this is the first time that the interactions between TLRs and lipoprotein have been quantitatively measured. All previous available data showed the interaction of TLR2 towards soluble agonists such as peptidoglycan (Asong et al., 2009). However, the limitation of this experiment is the use of Fc-tagged TLRs immobilized on protein A sensors. We found that Fc-tagged TLRs are forming non-specific dimers due to the Fc protein domain. We think that this dimerization of TLRs provides a conformational steric hindrance that interferes with the formation of a ternary complex upon addition of the monomeric co-receptors. Our attempts to measure the ternary complex formation by addition of the co-receptor to these pre-formed TLR-Lip12 complexes using either the

Octet system or BIAcore failed to give consistent, quantifiable, and reliable results due to technical difficulties encountered with the dimeric nature of the Fc-tagged TLRs immobilized on the sensor as well as the aggregation of the lipoproteins in solution. We also found that the TLRs could not be immobilized on amine-reactive sensors via chemical coupling due to the sensitive nature of the purified TLR ECDs.

Even though we were not able to measure the kinetics of ternary complex formation in solution, one important finding that emerged from our TLR-lipoprotein measurements was additional insight into the order of events that lead to complex formation. Since TLR1 exhibited the highest affinity towards Lip12 compared to TLR2 and TLR10, our data suggest that lipoproteins will be delivered to TLR1 first, followed by a TLR1-lipoprotein binding to the co-receptor TLR2. If the reported dissociation constant for a CD14-Pam_3CSK_4 interaction ($K_D = 5.7x10^{-6}M$) is correct (Nakata et al., 2006), one could deduce based on the K_D values that CD14 will preferably deliver Pam_3CSK_4 to TLR1 over TLR2.

Interestingly, in the absence of TLR2 we observed that both CD14 and TLR1 eluted in earlier fractions in our size exclusion chromatography column (see Chapter 2, figure 2.3A), while in the presence of TLR2, sCD14 eluted in later fractions as a monomeric protein (figure 2.3B right panel). This suggests that sCD14 and TLR1 interact in a Pam_3CSK_4-dependent fashion. Since sCD14 was shown to not be a part of the final ternary complex, Figure 2.3C suggests that the binding of TLR2 to the sCD14-TLR1-Pam_3CSK_4 complex displaces sCD14 leading to formation of the final ternary TLR1-TLR2-Pam_3CSK_4 ternary complex. This observation supports a model where, upon binding lipopeptide, sCD14 stably interacts with TLR1 but is then displaced by TLR2

during formation of the final ternary complex. This is in contrast to what has been previously suggested by other groups that CD14 might be interacting with soluble TLR2, which as a decoy receptor, would prevent CD14 from delivering lipopeptides to membrane-bound TLR2 (LeBouder et al., 2003). CD14 has previously been demonstrated to interact directly with TLR2 using immunoblot assays (Iwaki et al., 2002; Iwaki et al., 2005) and this interaction was blocked by a monoclonal antibody against CD14 that is known to block CD14-mediated LPS loading (Iwaki et al., 2005). However, the group did not look at any interaction between CD14 and TLR1.

Chapter 4 provided an in-depth analysis of the important regions in the TLR1 ECD that is required for ligand binding and formation of a dimer with the co-receptor TLR2. We also gained insights as to how the TLR1/TLR2 pair recognizes various microbial components other than lipoproteins. We have shown that LRRs 9-12 of TLR1 are required for discrimination of all TLR1/TLR2 microbial agonists that we tested in this study. Random mutagenesis of TLR1 LRRs 9-12 residues resulted in single point mutants that are not recognized by anti-TLR1 antibody clone GD2.F4, thus revealing the putative epitope of this neutralizing antibody, which maps close to the entrance of the hydrophobic binding pocket of TLR1. Amino acid residues found at the entrance of the hydrophobic binding pocket of TLR1 at LRRs 11 and 12 are important for recognition of the triacylated lipoptide Pam_3CSK_4. The same TLR1 point mutants fail to respond to Pam_3CSK_4 and other TLR1/TLR2 microbial agonists. Taken together, the critical amino acids of TLR1 required for receptor function are strikingly similar across all naturally occurring TLR1/2 agonists, irrespective of their assumed chemical nature, suggesting that

TLR1 uses the same contact points to form a dimer interface with TLR2 regardless of the agonist type.

We have also demonstrated in Chapter 4 that a naturally occurring polymorphic variant of TLR1, with proline at position 315 mutated to leucine (P315L), exhibited impaired responses to a variety of TLR1/2 agonists including lipoproteins. Additionally, a purified TLR1 ECD with a mutation at this amino acid position failed to form a ternary complex with TLR2 upon addition of Pam_3CSK_4 in solution (Chapter 2 and 4). Interestingly, this SNP is relatively rare in human populations. Although no individuals homozygous for the L315 allele have been found to date, a small percentage (3.4% allele frequency) of heterozygous individuals of African-American descent, and a much smaller population (0.8% allele frequency) of individuals with European ancestry, has been observed (www.ncbi.nlm.nih.gov/SNP). It is not known whether the impaired response of heterozygotes to TLR1/2 agonist is due to a dominant negative effect or a gene dosage effect. Our results in Chapter 4, together with the crystal structure of TLR1/TLR2/Pam_3CSK_4, suggest that the proline at amino acid position 315 in TLR1 contributes to hydrophobic interactions that line the TLR1/2 dimer interface, and a mutation to leucine at this region disrupts TLR1 and TLR2 dimerization, thus preventing the formation of the ternary complex. Using the Octet system, we were able to demonstrate in Chapter 3 that $TLR1_{P315L}$ is still able to bind the lipoprotein immobilized on a sensor, with measured dissociation constant ($K_D = 1.13x10^{-6}M$) that is only 1.5-fold larger than that of the wild-type TLR1 ($K_D = 7.45x10^{-7}M$). This provides additional proof that proline at position 315 is important for the formation of a dimer interface with TLR2.

Using size exclusion chromatography, we failed to form a ternary complex of TLR1/TLR2 together with the natural microbial agonists in solution, even in the presence of LBP and CD14. It is possible that the affinity of the TLRs to these microbial agonists is much lower compared to their affinity towards lipoproteins, thus requiring a higher concentration of agonists to form a complex or to stimulate cells. It is also possible that they may require some other accessory molecules for delivery to the TLRs. There are some scavenger receptors that act like pattern recognition receptors, and although not yet well-studied, they may also assist in the delivery of some microbial ligands and/or intact microbes to the TLRs [reviewed in (van Bergenhenegouwen et al., 2013)].

Significance and Future Work

Assessing the order of events in TLR1/TLR2/Pam_3CSK_4 ternary complex formation

Due to the technical difficulties we encountered using our purified TLRs and lipoproteins, we were not able to measure the kinetics of a ternary complex formation using the Octet system in this study. What we learned from our experiments is that we could not use Fc-tagged TLRs on the sensor, and we also could not covalently immobilize TLRs on the sensor via standard amine coupling procedure. We have attempted to immobilize the TLRs indirectly on the sensor via their FLAG- or the HA-tags, however, the interaction between the FLAG(HA)-tag and the anti-FLAG(HA) mAb was not strong enough to stably hold the TLRs on the sensors. One possibility that we did not explore in this study is to generate biotinylated TLR constructs, and take advantage of the strong interaction between streptavidin and biotin.

Alternatively, we could also perform a different assay to measure kinetics of interaction. We have attempted to use a microcalorimeter to examine ternary complex formation. However, this technique requires a large amount of purified proteins, and our HEK 293F stable cell lines do not express soluble TLRs at a high enough concentration, thus limiting our protein yield. A nanocalorimeter that requires less amount of starting material would be a good alternative to try to measure complex formation.

Gaining more insights on the competition between TLRs 1 and 10 for TLR2 and/or their agonists

Based on our microtiter plate assays and the Octet kinetic measurements, we were able to show that similar to TLR1, TLR10 could also bind to lipoproteins and form a complex with TLR2, suggesting that there is a possible competition between TLR1 and TLR10. Our preliminary data show that TLR2 prefers TLR1 over TLR10 as a co-receptor. However, additional kinetic measurements are needed to be able to understand the nature of this competition. This is an important question to answer, since we know that TLR10 does not signal via the known TLR2 signaling pathway. If one of the roles of TLR10 is to act as a negative regulator to dampen immune responses towards lipoproteins, then the kinetics data that we generate for TLR10 interaction with TLR2 in comparison with TLR1 would help increase our understanding of the difference in signaling output between the two competing TLRs.

Distinguishing critical regions in the TLR1 ECD that are important for ligand recognition and formation of dimer interface with TLR2

To further study the critical regions of the TLR1 ECD, experiments that could differentiate regions that are important for ligand binding and/or formation of dimer

interface should be designed and performed. One could start by comparing our TLR1 mutational analysis with other groups' computational as well as evolutionary studies on the critical sites on TLR1 and/or TLR2. For example, a study conducted by Georgel *et al.* in 2009 revealed that 1% of the Caucasian genomic DNA that they analyzed have the L443I, V545A, and T565S SNPs in their TLR1 gene, and mutations at any of these sites may potentially impair TLR1/TLR2 heterodimer formation (Georgel et al., 2009). In addition, the group that solved the TLR1/TLR2/Pam_3CSK_4 crystal structure have predicted several important residues in TLR1 ECD that are important for interaction with the TLR2 ECD via formation of hydrogen bonds, ionic bonds, and hydrophobic interactions (Jin et al., 2007). Another group has performed computational studies to identify critical regions in TLR1 and have identified that amino acid positions 284, 303, 308, and 313 of the TLR1 ECD are important for ligand binding, while residues 321 and 337 are important for dimerization interface (Wlasiuk & Nachman, 2010). However, there has been very little experimental data available which demonstrates that these predicted amino acid sites are critical for TLR1 function. This is where the TLR1 single point mutants become valuable tools to validate the existing data generated via computational studies. We acknowledge that our random mutagenesis approach of the TLR1 ECD was not able to control the specific amino acid sites mutated or the nature of the mutation itself. For example, we may have generated single point mutants that did not affect overall function of the protein due to similarity in amino acid properties. Additional insights may be generated by performing site-directed mutagenesis of the TLR1 ECD at the predicted sites.

Investigating the biological role of the naturally-occurring soluble TLR2

In humans, there are naturally occurring soluble forms of TLR2 (sTLR2), which consist of the TLR2 extracellular domain. sTLR2 is released by monocytes and is present in plasma, breast milk (LeBouder et al., 2003), saliva (Kuroishi et al., 2007), and amniotic fluid (Dulay et al., 2009) as a product of post-translational modifications (the protein fragments vary in size). The amount of sTLR2 and the expression pattern of the different forms of sTLR2 detected in the serum vary from individual to individual and may be affected by race, ethnicity, or genetic variability, although nobody has shown this correlation yet. The full extent of sTLR2's negative regulatory capacity, the mechanism underlying it, and its biological significance in vivo has not yet been determined. One group reported that sTLR2 binds to CD14 as a decoy receptor, thus preventing the latter from binding to membrane-bound TLR2 (LeBouder et al., 2003; Raby et al., 2009). sTLR2 in human breast milk has been found to be protective against HIV-1 infection (Henrick et al., 2012), while depletion of sTLR2 from serum renders monocytes and leukocytes sensitive to lipopeptides and other known TLR2 microbial agonists (LeBouder et al., 2003; Raby et al., 2009). Interestingly, these studies did not examine how TLR1 or TLR6 might come into play in this system. A previous graduate student in the lab (Johnson and Tapping, unpublished results) have shown that upon stimulation of monocytes with synthetic ligands for TLR2, there is an upregulation of TLR2 transcription and a down-regulation of both TLR1 and TLR6. How this correlates with the production of soluble TLR2 and the latter's role in ligand selectivity and functional specificity remains to be elucidated. Other than sTLR2, no naturally occurring soluble

form of a mammalian TLR has been identified to date, although a soluble TLR4 has been reported in mice as a splicing variant (Iwami et al., 2000).

Assessing the existence of TLR2 homodimers and other co-receptors of TLR2

Another important question that needs to be addressed involves the possibility of TLR2 homodimer formation. A corollary question to this would be "Do TLR2 bind with other PRRs, without the need for either TLR1 or TLR6?" For example, CD36 is a scavenger receptor that was shown to deliver LTA and MALP2 from Gram-positive bacteria to TLR2 and TLR6 (Hoebe et al., 2005). This PRR is a glycoprotein with several functions such as lipid transport, hemostasis, and angiogenesis (Greenwalt et al., 1992). There have been reports of TLR2/TLR6 requiring additional help from CD36 for initial ligation of specific lipopeptides prior to CD14 loading (Triantafilou et al., 2006). There are also a number of other ligands that have been reported to stimulate TLR2-expressing cells, but do not appear to require the presence of TLR1 or TLR6. These include microbial components such as lipoteichoic acids (Schwandner et al., 1999) and also endogenous components or damage-associated molecular patterns (DAMPs) such as heat-shock protein 60 (Vabulas et al., 2001). However, most of these reported studies were performed on cell lines that may have endogenous expression of TLR2 co-receptors TLR1, 6, and 10, and therefore were not carefully taken into consideration. While it is possible that TLR2 may be interacting with an as yet unidentified co-receptor(s), if not forming homodimers with itself, it is imperative that careful experiments be performed to address this issue.

Testing for bonafide naturally occurring TLR2 agonists

Over the years, several agonists for TLR2, both microbial and endogenous compounds, have been identified. To our knowledge, there are very few physical data showing direct interactions between the receptors and the more recently reported agonists, especially the endogenous ones. By performing physical studies with the soluble TLRs and a wide variety of purified compounds, we should be able to address which components are *bonafide* TLR2 agonists, and be able to quantitatively measure their kinetics of interaction with the TLRs using the Octet system that we have optimized for lipoproteins. Some of the naturally-occurring microbial ligands that are commercially available in purified form are atypical LPS from *P. gingivalis*, lipoteichoic acid, and lipomannans or lipoaribomannans from mycobacterial species. Other purified microbial components that are known to stimulate TLR2 may also be obtained from other research groups through collaboration, examples of which include B subunit of type II Heat-Labile enterotoxins (LT-IIb) from *E. coli*, *Neisseria* porB from meningococcal species, and *Treponema denticola* flagella. A more interesting set of TLR2 ligands to examine are the endogenous ligands that are implicated in sterile chronic inflammation (i.e. amyloid β, serum amyloid A, β-defensins, α-synuclein, and eosinophil-derived neurotoxins) (Cheng et al., 2007; Gariboldi et al., 2008; Kim et al., 2013; Liu et al., 2012; Yang et al., 2008). To our knowledge, there is very little information available that shows direct interaction between these ligands and the TLRs. Alternatively, it is also possible that these reported agonists of TLR2 are contaminated with minute amounts of lipoproteins. To determine whether or not a given microbial component is a genuine TLR2 agonist, it is important to consider that preparation and purification of recombinant microbial components from

typical bacterial expression systems inherently produce lipoprotein contaminants. A stringent purification method or synthetic preparation of agonists would be a preferred option when designing experiments aimed to identify genuine agonists or antagonists of the TLR2 family of receptors.

Therapeutic targeting of TLR1 and TLR2

Activation of TLRs in response to microbial infection leads to the production of a variety of proinflammatory cytokines, chemokines, and costimulatory molecules, an excess of which could lead to profound deleterious effects, including septic shock and death. A number of reports have implicated TLR2 in the pathogenesis of chronic inflammatory, autoimmune, and infectious diseases [Reviewed in (van Bergenhenegouwen et al., 2013)]. A better understanding of host-microbe interaction may lead to new and improved therapeutic strategies targeting TLR2 function in health and disease. Several therapeutic approaches could be designed using humanized inhibitory TLR monoclonal antibodies (Arslan et al., 2012), antagonistic oligonucleotides (Chang et al., 2009), and recombinant soluble TLRs, all of which are capable of minimizing the activation of the TLR1/TLR2 pathway. A series of novel synthetic phospholipids and high affinity aptamers have been recently designed and were shown to be antagonists of TLR2 (Arslan et al., 2012; Spyvee et al. 2005), however, functional data are still lacking. Using our TLR1 single point mutants, we could screen these synthetic antagonists and compare the critical regions in TLR1 that differentiate a receptor's response towards an antagonistic versus an agonistic ligand. Alternatively, there have been reports on the use of synthetic agonists such as lipopeptides as adjuvants because of their ability to activate antigen-presenting cells like macrophages and

dendritic cells, thus improving the immunogenicity of an otherwise weak vaccine (Kaisho & Akira, 2002). This is consistent with Janeway's original observation that several microbial products are potent vaccine adjuvants and likely work through TLRs (Medzhitov & Janeway Jr, 1996).

REFERENCES

1. Agnese, D. M., Calvano, J. E., Hahm, S. J., Coyle, S. M., Corbett, S. A., Calvano, S. E., & Lowry, S. F. (2002). Human toll-like receptor 4 mutations but not CD14 polymorphisms are associated with an increased risk of Gram-negative infections. *Journal of Infectious Diseases, 186*(10), 1522-1525.

2. Akira, S., & Hemmi, H. (2003). Recognition of pathogen-associated molecular patterns by TLR family. *Immunology Letters, 85*(2), 85-95.

3. Akira, S., Uematsu, S., & Takeuchi, O. (2006). Pathogen recognition and innate immunity. *Cell, 124*(4), 783-801.

4. Akira, S., & Takeda, K. (2004). Toll-like receptor signaling. *Nat Rev Immunol, 4*(7), 499-511.

5. Alexopoulou, L., Thomas, V., Schnare, M., Lobet, Y., Anguita, J., Schoen, R. T., Medzhitov, R., Fikrig, E., & Flavell, R. A. (2002). Hyporesponsiveness to vaccination with borrelia burgdorferi OspA in humans and in TLR1-and TLR2-deficient mice. *Nature Medicine, 8*(8), 878-884.

6. Aliprantis, A. O., Yang, R. B., Mark, M. R., Suggett, S., Devaux, B., Radolf, J. D., Klimpel, G.R., Godowski, P., & Zychlinsky, A. (1999). Cell activation and apoptosis by bacterial lipoproteins through toll-like receptor-2. *Science, 285*(5428), 736-739.

7. Andersen-Nissen, E., Smith, K. D., Bonneau, R., Strong, R. K., & Aderem, A. (2007). A conserved surface on toll-like receptor 5 recognizes bacterial flagellin. *The Journal of Experimental Medicine, 204*(2), 393-403.

8. Anderson, K. V., Bokla, L., & Nüsslein-Volhard, C. (1985). Establishment of dorsal-ventral polarity in the drosophila embryo: The induction of polarity by the toll gene product. *Cell, 42*(3), 791-798.

9. Antal-Szalmas, P., Strijp, J., Weersink, A., Verhoef, J., & Van Kessel, K. (1997). Quantitation of surface CD14 on human monocytes and neutrophils. *Journal of Leukocyte Biology, 61*(6), 721-728.

10. Arslan, F., Houtgraaf, J. H., Keogh, B., Kazemi, K., de Jong, R., McCormack, W. J., O'Neill, L.A.J., McGuirk, P., Timmers, L., Smeets, M.B., Akeroyd, L., Reilly, M., Pasterkamp, G., & de Kleijn, D. P. V. (2012). Treatment with OPN-305, a humanized Anti–Toll-like receptor-2 antibody, reduces myocardial ischemia/reperfusion injury in pigs. *Circulation: Cardiovascular Interventions, 5*(2), 279-287.

11. Asong, J., Wolfert, M. A., Maiti, K. K., Miller, D., & Boons, G. (2009). Binding and cellular activation studies reveal that toll-like receptor 2 can differentially recognize peptidoglycan from Gram-positive and Gram-negative bacteria. *Journal of Biological Chemistry, 284*(13), 8643-8653.

12. Baeuerle, P. A., & Henkel, T. (1994). Function and activation of NF-kappaB in the immune system. *Annual Review of Immunology, 12*(1), 141-179.

13. Belisle, J. T., Brandt, M. E., Radolf, J. D., & Norgard, M. V. (1994). Fatty acids of treponema pallidum and borrelia burgdorferi lipoproteins. *Journal of Bacteriology, 176*(8), 2151-2157.

14. Bell, J. K., Mullen, G. E. D., Leifer, C. A., Mazzoni, A., Davies, D. R., & Segal, D. M. (2003). Leucine-rich repeats and pathogen recognition in toll-like receptors. *Trends in Immunology, 24*(10), 528-533.

15. Bella, J., Hindle, K. L., McEwan, P. A., & Lovell, S. C. (2008). The leucine-rich repeat structure. *Cellular and Molecular Life Sciences, 65*(15), 2307-2333.

16. Belvin, M. P., & Anderson, K. V. (1996). A conserved signaling pathway: The drosophila toll-dorsal pathway. *Annual Review of Cell and Developmental Biology, 12*(1), 393-416.

17. Beutler, B., & Rietschel, E. T. (2003). Innate immune sensing and its roots: The story of endotoxin. *Nat Rev Immunol, 3*(2), 169-176.

18. Botos, I., Segal, D., & Davies, D. (2011). The structural biology of toll-like receptors. *Structure, 19*(4), 447-459.

19. Bourke, E., Bosisio, D., Golay, J., Polentarutti, N., & Mantovani, A. (2003). The toll-like receptor repertoire of human B lymphocytes: Inducible and selective expression of TLR9 and TLR10 in normal and transformed cells. *Blood, 102*(3), 956-963.

20. Bowie, A., & O'Neill, L. A. (2000). The interleukin-1 receptor/toll-like receptor superfamily: Signal generators for pro-inflammatory interleukins and microbial products. *Journal of Leukocyte Biology, 67*(4), 508-514.

21. Brandt, M., Riley, B., Radolf, J., & Norgard, M. (1990). Immunogenic integral membrane proteins of borrelia burgdorferi are lipoproteins. *Infection and Immunity, 58*(4), 983-991.

22. Branger, J., Florquin, S., Knapp, S., Leemans, J. C., Pater, J. M., Speelman, P., Golenbock, D.T., & van der Poll, T. (2004). LPS-binding protein-deficient mice have an impaired defense against Gram-negative but not Gram-positive pneumonia. *International Immunology, 16*(11), 1605-1611.

23. Branger, J., Leemans, J. C., Florquin, S., Speelman, P., Golenbock, D. T., & van der Poll, T. (2005). Lipopolysaccharide binding protein-deficient mice have a normal defense against pulmonary mycobacterial infection. *Clinical Immunology, 116*(2), 174-181.

24. Brightbill, H. D., Libraty, D. H., Krutzik, S. R., Yang, R., Belisle, J. T., Bleharski, J. R., Maitland, M., Norgard, M.V., Plevy, S.E., Smale, S.T., Brennan, P.J., Bloom, B.R., Godowski, P.J., & Modlin, R. L. (1999). Host defense mechanisms triggered by microbial lipoproteins through toll-like receptors. *Science, 285*(5428), 732-736.

25. Carty, M., Goodbody, R., Schroder, M., Stack, J., Moynagh, P. N., & Bowie, A. G. (2006). The human adaptor SARM negatively regulates adaptor protein TRIF-dependent toll-like receptor signaling. *Nature Immunology, 7*(10), 1074-1081.

26. Chambers, M. A., Whelan, A. O., Spallek, R., Singh, M., Coddeville, B., Guerardel, Y., & Elass, E. (2010). Non-acylated mycobacterium bovis glycoprotein MPB83 binds to TLR1/2 and stimulates production of matrix metalloproteinase 9. *Biochemical and Biophysical Research Communications, 400*(3), 403-408.

27. Chang, Y., Kao, W., Wang, W., Wang, W., Yang, R., & Peck, K. (2009). Identification and characterization of oligonucleotides that inhibit toll-like receptor 2-associated immune responses. *The FASEB Journal, 23*(9), 3078-3088.

28. Cheng, N., He, R., Tian, J., Patrick, P. Y., & Richard, D. Y. (2008). Cutting edge: TLR2 is a functional receptor for acute-phase serum amyloid A. *The Journal of Immunology, 181*(1), 22-26.

29. Chuang, T., & Ulevitch, R. J. (2001). Identification of hTLR10: A novel human toll-like receptor preferentially expressed in immune cells. *Biochimica Et Biophysica Acta (BBA) - Gene Structure and Expression, 1518*(1–2), 157-161.

30. da Silva Correia, J., Soldau, K., Christen, U., Tobias, P. S., & Ulevitch, R. J. (2001). Lipopolysaccharide is in close proximity to each of the proteins in its membrane receptor complex. *Journal of Biological Chemistry, 276*(24), 21129-21135.

31. Darveau, R. P., Pham, T. T., Lemley, K., Reife, R. A., Bainbridge, B. W., Coats, S. R., Howald, W.N., Way, S.S., & Hajjar, A. M. (2004). Porphyromonas gingivalis lipopolysaccharide contains multiple lipid A species that functionally interact with both toll-like receptors 2 and 4. *Infection and Immunity, 72*(9), 5041-5051.

32. Dinarello, C. (1991). Interleukin-1 and interleukin-1 antagonism. *Blood, 77*(8), 1627-1652.

33. Dulay, A. T., Buhimschi, C. S., Zhao, G., Oliver, E. A., Mbele, A., Jing, S., & Buhimschi, I. A. (2009). Soluble TLR2 is present in human amniotic fluid and modulates the intraamniotic inflammatory response to infection. *The Journal of Immunology, 182*(11), 7244-7253.

34. Dziarski, R., & Gupta, D. (2005). Staphylococcus aureus peptidoglycan is a toll-like receptor 2 activator: A reevaluation. *Infection and Immunity, 73*(8), 5212-5216.

35. Echchannaoui, H., Frei, K., Schnell, C., Leib, S. L., Zimmerli, W., & Landmann, R. (2002). Toll-like receptor 2–Deficient mice are highly susceptible to streptococcus pneumoniae meningitis because of reduced bacterial clearing and enhanced inflammation. *Journal of Infectious Diseases, 186*(6), 798-806.

36. Ehlers, S., Reiling, N., Gangloff, S., Woltmann, A., & Goyert, S. (2001). Mycobacterium avium infection in CD14-deficient mice fails to substantiate a significant role for CD14 in antimycobacterial protection or granulomatous inflammation. *Immunology, 103*(1), 113-121.

37. Elass, E., Coddeville, B., Guérardel, Y., Kremer, L., Maes, E., Mazurier, J., & Legrand, D. (2007). Identification by surface plasmon resonance of the mycobacterial lipomannan and lipoarabinomannan domains involved in binding to CD14 and LPS-binding protein. *FEBS Letters, 581*(7), 1383-1390.

38. Erdile, L. F., Brandt, M., Warakomski, D., Westrack, G., Sadziene, A., Barbour, A., & Mays, J. (1993). Role of attached lipid in immunogenicity of borrelia burgdorferi OspA. *Infection and Immunity, 61*(1), 81-90.

39. Erdile, L. F., & Guy, B. (1997). OspA lipoprotein of borrelia burgdorferi is a mucosal immunogen and adjuvant. *Vaccine, 15*(9), 988-995.

40. Eriksson, U., Ricci, R., Hunziker, L., Kurrer, M. O., Oudit, G. Y., Watts, T. H., Sonderegger, I.,Bachmaier, K., Kopf, M., & Penninger, J. M. (2003). Dendritic cell-induced autoimmune heart failure requires cooperation between adaptive and innate immunity. *Nature Medicine, 9*(12), 1484-1490.

41. Fan, X., Stelter, F., Menzel, R., Jack, R., Spreitzer, I., Hartung, T., & Schütt, C. (1999). Structures in bacillus subtilis are recognized by CD14 in a lipopolysaccharide binding protein-dependent reaction. *Infection and Immunity, 67*(6), 2964-2968.

42. Fierer, J., Swancutt, M. A., Heumann, D., & Golenbock, D. (2002). The role of lipopolysaccharide binding protein in resistance to salmonella infections in mice. *The Journal of Immunology, 168*(12), 6396-6403.

43. Frey, E. A., Miller, D. S., Jahr, T. G., Sundan, A., Bazil, V., Espevik, T., Finlay, B.B., & Wright, S. D. (1992). Soluble CD14 participates in the response of cells to lipopolysaccharide. *The Journal of Experimental Medicine, 176*(6), 1665-1671.

44. Froon, A. H. M., Dentener, M. A., Greve, J. W. M., Ramsay, G., & Buurman, W. A. (1995). Lipopolysaccharide toxicity-regulating proteins in bacteremia. *Journal of Infectious Diseases, 171*(5), 1250-1257.

45. Funda, D. P., Tučková, L., Farré, M. A., Iwase, T., Moro, I., & Tlaskalová-Hogenová, H. (2001). CD14 is expressed and released as soluble CD14 by human intestinal epithelial cells in vitro: Lipopolysaccharide activation of epithelial cells revisited. *Infection and Immunity, 69*(6), 3772-3781.

46. Funderburg, N., Lederman, M. M., Feng, Z., Drage, M. G., Jadlowsky, J., Harding, C. V., Weinberg, A., & Sieg, S. F. (2007). Human β-defensin-3 activates professional antigen-presenting cells via toll-like receptors 1 and 2. *Proceedings of the National Academy of Sciences, 104*(47), 18631-18635.

47. Gariboldi, S., Palazzo, M., Zanobbio, L., Selleri, S., Sommariva, M., Sfondrini, L., Cavicchini, S., Balsari, A., & Rumio, C. (2008). Low molecular weight hyaluronic acid increases the self-defense of skin epithelium by induction of β-defensin 2 via TLR2 and TLR4. *The Journal of Immunology, 181*(3), 2103-2110.

48. Gay, N. J., & Keith, F. J. (1991). Drosophila toll and IL-1 receptor. *Nature, 351*(6325), 355-356.

49. Gehring, A. J., Dobos, K. M., Belisle, J. T., Harding, C. V., & Boom, W. H. (2004). Mycobacterium tuberculosis LprG (Rv1411c): A novel TLR-2 ligand that inhibits human macrophage class II MHC antigen processing. *The Journal of Immunology, 173*(4), 2660-2668.

50. Georgel, P., Macquin, C., & Bahram, S. (2009). The heterogeneous allelic repertoire of human toll-like receptor (*TLR*) genes. *PLoS ONE, 4*(11), e7803-7813.

51. Gilleron, M., Quesniaux, V. F. J., & Puzo, G. (2003). Acylation state of the phosphatidylinositol hexamannosides from mycobacterium bovis bacillus calmette guérin and mycobacterium tuberculosis H37Rv and its implication in toll-like receptor response. *Journal of Biological Chemistry, 278*(32), 29880-29889.

52. Gioannini, T. L., Teghanemt, A., Zhang, D., Levis, E. N., & Weiss, J. P. (2005). Monomeric endotoxin:Protein complexes are essential for TLR4-dependent cell activation. *Journal of Endotoxin Research, 11*(2), 117-123.

53. Gordon, S. (2008). Elie metchnikoff: Father of natural immunity. *European Journal of Immunology, 38*(12), 3257-3264.

54. Grabiec, A., Meng, G., Fichte, S., Bessler, W., Wagner, H., & Kirschning, C. J. (2004). Human but not murine toll-like receptor 2 discriminates between tri-palmitoylated and tri-lauroylated peptides. *Journal of Biological Chemistry, 279*(46), 48004-48012.

55. Greenwalt, D., Lipsky, R., Ockenhouse, C., Ikeda, H., Tandon, N., & Jamieson, G. (1992). Membrane glycoprotein CD36: A review of its roles in adherence, signal transduction, and transfusion medicine. *Blood, 80*(5), 1105-1115.

56. Guan, Y., Ranoa, D. R. E., Jiang, S., Mutha, S. K., Li, X., Baudry, J., & Tapping, R. I. (2010). Human TLRs 10 and 1 share common mechanisms of innate immune sensing but not signaling. *The Journal of Immunology, 184*(9), 5094-5103.

57. Hasan, U., Chaffois, C., Gaillard, C., Saulnier, V., Merck, E., Tancredi, S., Guiet, C., Briere, F., Vlach, J., Lebecque, S., Trinchieri, G., & Bates, E. E. M. (2005). Human TLR10 is a functional receptor, expressed by B cells and plasmacytoid dendritic cells, which activates gene transcription through MyD88. *The Journal of Immunology, 174*(5), 2942-2950.

58. Haziot, A., Chen, S., Ferrero, E., Low, M. G., Silber, R., & Goyert, S. M. (1988). The monocyte differentiation antigen, CD14, is anchored to the cell membrane by a phosphatidylinositol linkage. *The Journal of Immunology, 141*(2), 547.

59. Haziot, A., Ferrero, E., Köntgen, F., Hijiya, N., Yamamoto, S., Silver, J., Stewart, C.L., & Goyert, S. M. (1996). Resistance to endotoxin shock and reduced dissemination of Gram-negative bacteria in CD14-deficient mice. *Immunity, 4*(4), 407-414.

60. Haziot, A., Rong, G. W., Silver, J., & Goyert, S. M. (1993). Recombinant soluble CD14 mediates the activation of endothelial cells by lipopolysaccharide. *The Journal of Immunology, 151*(3), 1500-1507.

61. Haziot, A., Hijiya, N., Schultz, K., Zhang, F., Gangloff, S. C., & Goyert, S. M. (1999). CD14 plays no major role in shock induced by staphylococcus aureus but down-regulates TNF-α production. *The Journal of Immunology, 162*(8), 4801-4805.

62. Hemmi, H., Takeuchi, O., Kawai, T., Kaisho, T., Sato, S., Sanjo, H., Matsumoto, M., Hoshino, K., Wagner, H., Takeda, K., & Akira, S. (2000). A toll-like receptor recognizes bacterial DNA. *Nature, 408*(6813), 740-745.

63. Henrick, B. M., Nag, K., Yao, X., Drannik, A. G., Aldrovandi, G. M., & Rosenthal, K. L. (2012). Milk matters: Soluble toll-like receptor 2 (sTLR2) in breast milk significantly inhibits HIV-1 infection and inflammation. *PLoS ONE, 7*(7), e40138-40147.

64. Hirschfeld, M., Kirschning, C. J., Schwandner, R., Wesche, H., Weis, J. H., Wooten, R. M., & Weis, J. J. (1999). Cutting edge: Inflammatory signaling by borrelia burgdorferi lipoproteins is mediated by toll-like receptor 2. *The Journal of Immunology, 163*(5), 2382-2386.

65. Hirschfeld, M., Weis, J. J., Toshchakov, V., Salkowski, C. A., Cody, M. J., Ward, D. C., Qureshi, N., Michalek, S.M., & Vogel, S. N. (2001). Signaling by toll-like receptor 2 and 4 agonists results in differential gene expression in murine macrophages. *Infection and Immunity, 69*(3), 1477-1482.

66. Hoebe, K., Georgel, P., Rutschmann, S., Du, X., Mudd, S., Crozat, K., Sovath, S., Shamel, L., Hartung, T., Zahringer, U., & Beutler, B. (2005). CD36 is a sensor of diacylglycerides. *Nature, 433*(7025), 523-527.

67. Hoffmann, P., Heinle, S., Schade, U. F., Loppnow, H., Ulmer, A. J., Flad, H. D., Jung, G., & Bessler, W. G. (1988). Stimulation of human and murine adherent cells by bacterial lipoprotein and synthetic lipopeptide analogues. *Immunobiology, 177*(2), 158-170.

68. Holt, S. C., Kesavalu, L., Walker, S., & Genco, C. A. (1999). Virulence factors of porphyromonas gingivalis. *Periodontology 2000, 20*(1), 168-238.

69. Honda, K., Ohba, Y., Yanai, H., Negishi, H., Mizutani, T., Takaoka, A., Taya, C., & Taniguchi, T. (2005). Spatiotemporal regulation of MyD88-IRF-7 signalling for robust type-I interferon induction. *Nature, 434*(7036), 1035-1040.

70. Hoshino, K., Takeuchi, O., Kawai, T., Sanjo, H., Ogawa, T., Takeda, Y., Takeda, K., & Akira, S. (1999). Cutting edge: Toll-like receptor 4 (TLR4)-deficient mice are hyporesponsive to lipopolysaccharide: Evidence for TLR4 as the lps gene product. *The Journal of Immunology, 161*(7), 3749-3752.

71. Humphrey, W., Dalke, A., & Schulten, K. (1996). VMD: Visual molecular dynamics. *Journal of Molecular Graphics, 14*(1), 33-38.

72. Inabe, K., & Kurosaki, T. (2002). Tyrosine phosphorylation of B-cell adaptor for phosphoinositide 3-kinase is required for akt activation in response to CD19 engagement. *Blood, 99*(2), 584-589.

73. Iwaki, D., Mitsuzawa, H., Murakami, S., Sano, H., Konishi, M., Akino, T., & Kuroki, Y. (2002). The extracellular toll-like receptor 2 domain directly binds peptidoglycan derived from staphylococcus aureus. *Journal of Biological Chemistry, 277*(27), 24315-24320.

74. Iwaki, D., Nishitani, C., Mitsuzawa, H., Hyakushima, N., Sano, H., & Kuroki, Y. (2005). The CD14 region spanning amino acids 57–64 is critical for interaction with the extracellular toll-like receptor 2 domain. *Biochemical and Biophysical Research Communications, 328*(1), 173-176.

75. Iwami, K., Matsuguchi, T., Masuda, A., Kikuchi, T., Musikacharoen, T., & Yoshikai, Y. (2000). Cutting edge: Naturally occurring soluble form of mouse toll-like receptor 4 inhibits lipopolysaccharide signaling. *The Journal of Immunology, 165*(12), 6682-6686.

76. Iwasaki, A., & Medzhitov, R. (2004). Toll-like receptor control of the adaptive immune responses. *Nature Immunology, 5*(10), 987-995.

77. Jack, R. S., Fan, X., Bernheiden, M., Rune, G., Ehlers, M., Weber, A., Kirsch, G., Mentel, R., Furll, B., Freudenberg, M., Schmitz, G., Stelter, F., & Schutt, C. (1997). Lipopolysaccharide-binding protein is required to combat a murine Gram-negative bacterial infection. *Nature, 389*(6652), 742-745.

78. Janeway, C.A. Jr., Travers, P., & Walport, M. (2001). *Immunobiology: The immune system in health and disease* (5th edition ed.). New York: Garland Science.

79. Janeway, C. A. Jr. (1989). Approaching the asymptote? Evolution and revolution in immunology. *Cold Spring Harbor Symposia on Quantitative Biology, 54*, 1-13.

80. Janssens, S., & Beyaert, R. (2003). Role of toll-like receptors in pathogen recognition. *Clinical Microbiology Reviews, 16*(4), 637-646.

81. Jin, M. S., Kim, S. E., Heo, J. Y., Lee, M. E., Kim, H. M., Paik, S.G., & Lee, H., Lee, J. (2007). Crystal structure of the TLR1-TLR2 heterodimer induced by binding of a tri-acylated lipopeptide. *Cell, 130*(6), 1071-1082.

82. Jin, M. S., & Lee, J. (2008). Structures of the toll-like receptor family and its ligand complexes. *Immunity, 29*(2), 182-191.

83. Kaisho, T., & Akira, S. (2002). Toll-like receptors as adjuvant receptors. *Biochimica Et Biophysica Acta (BBA) - Molecular Cell Research, 1589*(1), 1-13.

84. Kang, J. Y., Nan, X., Jin, M. S., Youn, S. J., Ryu, Y. H., Mah, S., Han, S.H., Lee, H., Paik, S.G., & Lee, J. (2009). Recognition of lipopeptide patterns by toll-like receptor 2-toll-like receptor 6 heterodimer. *Immunity, 31*(6), 873-884.

85. Kang, J. Y., & Lee, J. (2011). Structural biology of the toll-like receptor family. *Annual Review of Biochemistry, 80*(1), 917-941.

86. Kawai, T., & Akira, S. (2010). The role of pattern-recognition receptors in innate immunity: Update on toll-like receptors. *Nature Immunology, 11*(5), 373-384.

87. Keestra, A. M., de Zoete, M. R., van Aubel, R. A. M. H., & van Putten, J. P. M. (2007). The central leucine-rich repeat region of chicken TLR16 dictates unique ligand specificity and species-specific interaction with TLR2. *The Journal of Immunology, 178*(11), 7110-7119.

88. Kelley, S. L., Lukk, T., Nair, S. K., & Tapping, R. I. (2013). The crystal structure of human soluble CD14 reveals a bent solenoid with a hydrophobic amino-terminal pocket. *The Journal of Immunology, 190*(3), 1304-1311.

89. Kiechl, S., Lorenz, E., Reindl, M., Wiedermann, C. J., Oberhollenzer, F., Bonora, E., Willeit, J., & Schwartz, D. A. (2002). Toll-like receptor 4 polymorphisms and atherogenesis. *N Engl J Med, 347*(3), 185-192.

90. Kim, C., Ho, D., Suk, J., You, S., Michael, S., Kang, J., Joong, L.S., Masliah, E., Hwang, D., Lee, H., & Lee, S. (2013). Neuron-released oligomeric α-synuclein is an endogenous agonist of TLR2 for paracrine activation of microglia. *Nature Communications, 4*, 1562-1573.

91. Kim, H. M., Park, B. S., Kim, J., Kim, S. E., Lee, J., Oh, S. C., Enkhbayar, P., Matsushima, N., Lee, H., Yoo, O.J., & Lee, J. (2007). Crystal structure of the TLR4-MD-2 complex with bound endotoxin antagonist eritoran. *Cell, 130*(5), 906-917.

92. Knapp, S., de Vos, A. F., Florquin, S., Golenbock, D. T., & van der Poll, T. (2003). Lipopolysaccharide binding protein is an essential component of the innate immune response to escherichia coli peritonitis in mice. *Infection and Immunity, 71*(12), 6747-6753.

93. Kolek, M. J., Carlquist, J. F., Muhlestein, J. B., Whiting, B. M., Horne, B. D., Bair, T. L., & Anderson, J. L. (2004). Toll–like receptor 4 gene Asp299Gly polymorphism is associated with reductions in vascular inflammation, angiographic coronary artery disease, and clinical diabetes. *American Heart Journal, 148*(6), 1034-1040.

94. Krüger, C., Schütt, C., Obertacke, U., Joka, T., Müller, F. E., Knöller, J., Köller, M., Konig, W., & Schönfeld, W. (1991). Serum CD14 levels in poly traumatized and severely burned patients. *Clinical & Experimental Immunology, 85*(2), 297-301.

95. Kuroishi, T., Tanaka, Y., Sakai, A., Sugawara, Y., Komine, K., & Sugawara, S. (2007). Human parotid saliva contains soluble toll-like receptor (TLR) 2 and modulates TLR2-mediated interleukin-8 production by monocytic cells. *Molecular Immunology, 44*(8), 1969-1976.

96. LeBouder, E., Rey-Nores, J. E., Rushmere, N. K., Grigorov, M., Lawn, S. D., Affolter, M., Griffin, G.E., Ferrara, P., Schiffrin, E.J., Morgan, B.P., & Labéta, M. O. (2003). Soluble forms of toll-like receptor (TLR)2 capable of modulating TLR2 signaling are present in human plasma and breast milk. *The Journal of Immunology, 171*(12), 6680-6689.

97. Lee, H. Y., Takeshita, T., Shimada, J., Akopyan, A., Woo, J. I., Pan, H., Moon, S., Andalibi, A., Park, R.K., & Kang, S. H. (2008). Induction of beta defensin 2 by NTHi requires TLR2 mediated MyD88 and IRAK-TRAF6-p38MAPK signaling pathway in human middle ear epithelial cells. *BMC Infectious Diseases, 8*(1), 87.

98. Lee, H., Lee, J., & Tobias, P. S. (2002). Two lipoproteins extracted from escherichia coli K-12 LCD25 lipopolysaccharide are the major components responsible for toll-like receptor 2-mediated signaling. *The Journal of Immunology, 168*(8), 4012-4017.

99. Lee, J. D., Kravchenko, V., Kirkland, T. N., Han, J., Mackman, N., Moriarty, A., Leturcq, D., Tobias, P.S., & Ulevitch, R. J. (1993). Glycosyl-phosphatidylinositol-anchored or integral membrane forms of CD14 mediate identical cellular responses to endotoxin. *Proceedings of the National Academy of Sciences, 90*(21), 9930-9934.

100. Lemaitre, B., Nicolas, E., Michaut, L., Reichhart, J., & Hoffmann, J. A. (1996). The dorsoventral regulatory gene cassette spätzle/toll/cactus controls the potent antifungal response in drosophila adults. *Cell, 86*(6), 973-983.

101. Leonard, J. N., Ghirlando, R., Askins, J., Bell, J. K., Margulies, D. H., Davies, D. R., & Segal, D. M. (2008). The TLR3 signaling complex forms by cooperative receptor dimerization. *Proceedings of the National Academy of Sciences, 105*(1), 258-263.

102. Liang, S., Hosur, K. B., Lu, S., Nawar, H. F., Weber, B. R., Tapping, R. I., Connell, T.D., & Hajishengallis, G. (2009). Mapping of a microbial protein domain involved in binding and activation of the TLR2/TLR1 heterodimer. *The Journal of Immunology, 182*(5), 2978-2985.

103. Lien, E., Sellati, T. J., Yoshimura, A., Flo, T. H., Rawadi, G., Finberg, R. W., Carroll, J.D., Espevik, T., Ingalls, R.R., & Radolf, J. D. (1999). Toll-like receptor 2 functions as a pattern recognition receptor for diverse bacterial products. *Journal of Biological Chemistry, 274*(47), 33419-33425.

104. Liew, F. Y., Xu, D., Brint, E. K., & O'Neill, L. A. J. (2005). Negative regulation of toll-like receptor-mediated immune responses. *Nat Rev Immunol, 5*(6), 446-458.

105. Liu, L., Botos, I., Wang, Y., Leonard, J. N., Shiloach, J., Segal, D. M., & Davies, D. R. (2008). Structural basis of toll-like receptor 3 signaling with double-stranded RNA. *Science, 320*(5874), 379-381.

106. Liu, S., Liu, Y., Hao, W., Wolf, L., Kiliaan, A. J., Penke, B., Rübe, C.E., Walter, J., Heneka, M.T., Hartmann, T., Menger, M.D., & Fassbender, K. (2012). TLR2 is a primary receptor for alzheimer's amyloid ß peptide to trigger neuroinflammatory activation. *The Journal of Immunology, 188*(3), 1098-1107.

107. Manukyan, M., Triantafilou, K., Triantafilou, M., Mackie, A., Nilsen, N., Espevik, T., Wiesmüller, K.H., Ulmer, A.J., & Heine, H. (2005). Binding of lipopeptide to CD14 induces physical proximity of CD14, TLR2 and TLR1. *European Journal of Immunology, 35*(3), 911-921.

108. Martin, T. R., Mathison, J. C., Tobias, P. S., Letúrcq,D.J., Moriarty, A. M., Maunder, R. J., & Ulevitch, R. J. (1992). Lipopolysaccharide binding protein enhances the responsiveness of alveolar macrophages to bacterial lipopolysaccharide. implications for cytokine production in normal and injured lungs. *The Journal of Clinical Investigation, 90*(6), 2209-2219.

109. Massari, P., Visintin, A., Gunawardana, J., Halmen, K. A., King, C. A., Golenbock, D. T., & Wetzler, L. M. (2006). Meningococcal porin PorB binds to TLR2 and requires TLR1 for signaling. *The Journal of Immunology, 176*(4), 2373-2380.

110. Means, T. K., Lien, E., Yoshimura, A., Wang, S., Golenbock, D. T., & Fenton, M. J. (1999). The CD14 ligands lipoarabinomannan and lipopolysaccharide differ in their requirement for toll-like receptors. *The Journal of Immunology, 163*(12), 6748-6755.

111. Medzhitov, R., Preston-Hurlburt, P., & Janeway, C. A. (1997). A human homologue of the drosophila toll protein signals activation of adaptive immunity. *Nature, 388*(6640), 394-397.

112. Medzhitov, R., & Janeway Jr, C. A. (1996). On the semantics of immune recognition. *Research in Immunology, 147*(4), 208-214.

113. Medzhitov, R. (2009). Approaching the asymptote: 20 years later. *Immunity, 30*(6), 766-775.

114. Meng, G., Grabiec, A., Vallon, M., Ebe, B., Hampel, S., Bessler, W., Wagner, H., & Kirschning, C. J. (2003). Cellular recognition of tri-/di-palmitoylated peptides is independent from a domain encompassing the N-terminal seven leucine-rich repeat (LRR)/LRR-like motifs of TLR2. *Journal of Biological Chemistry, 278*(41), 39822-39829.

115. Morrison, T. B., Weis, J. H., & Weis, J. J. (1997). Borrelia burgdorferi outer surface protein A (OspA) activates and primes human neutrophils. *The Journal of Immunology, 158*(10), 4838-4845.

116. Muzio, M., Polentarutti, N., Bosisio, D., Prahladan, M. K., & Mantovani, A. (2000). Toll-like receptors: A growing family of immune receptors that are differentially expressed and regulated by different leukocytes. *Journal of Leukocyte Biology, 67*(4), 450-456.

117. Nagai, Y., Akashi, S., Nagafuku, M., Ogata, M., Iwakura, Y., Akira, S., Kitamura, T., Kosugi, A., Kimoto, M., & Miyake, K. (2002). Essential role of MD-2 in LPS responsiveness and TLR4 distribution. *Nature Immunology, 3*(7), 667-672.

118. Nakata, T., Yasuda, M., Fujita, M., Kataoka, H., Kiura, K., Sano, H., & Shibata, K. (2006). CD14 directly binds to triacylated lipopeptides and facilitates recognition of the lipopeptides by the receptor complex of toll-like receptors 2 and 1 without binding to the complex. *Cellular Microbiology, 8*(12), 1899-1909.

119. Nakayama, H., Kurokawa, K., & Lee, B. L. (2012). Lipoproteins in bacteria: Structures and biosynthetic pathways. *FEBS Journal, 279*(23), 4247-4268.

120. Netea, M. G., Sutmuller, R., Hermann, C., Van der Graaf, C. A. A., Van der Meer, J. W. M., van Krieken, J. H., Hartung, T., Adema, G., & Kullberg, B. J. (2004). Toll-like receptor 2 suppresses immunity against candida albicans through induction of IL-10 and regulatory T cells. *The Journal of Immunology, 172*(6), 3712-3718.

121. Ni, M., MacFarlane, A. W., Toft, M., Lowell, C. A., Campbell, K. S., & Hamerman, J. A. (2012). B-cell adaptor for PI3K (BCAP) negatively regulates toll-like receptor signaling through activation of PI3K. *Proceedings of the National Academy of Sciences, 109*(1), 267-272.

122. Noss, E. H., Pai, R. K., Sellati, T. J., Radolf, J. D., Belisle, J., Golenbock, D. T., Boom, W.H., & Harding, C. V. (2001). Toll-like receptor 2-dependent inhibition of macrophage class II MHC expression and antigen processing by 19-kDa lipoprotein of mycobacterium tuberculosis. *The Journal of Immunology, 167*(2), 910-918.

123. O'Neill, L. A. (2006). How toll-like receptors signal: What we know and what we don't know. *Current Opinion in Immunology, 18*(1), 3-9.

124. Okada, T., Maeda, A., Iwamatsu, A., Gotoh, K., & Kurosaki, T. (2000). BCAP: The tyrosine kinase substrate that connects B cell receptor to phosphoinositide 3-kinase activation. *Immunity, 13*(6), 817-827.

125. Omueti, K. O., Beyer, J. M., Johnson, C. M., Lyle, E. A., & Tapping, R. I. (2005). Domain exchange between human toll-like receptors 1 and 6 reveals a region required for lipopeptide discrimination. *Journal of Biological Chemistry, 280*(44), 36616-36625.

126. Omueti, K. O., Mazur, D. J., Thompson, K. S., Lyle, E. A., & Tapping, R. I. (2007). The polymorphism P315L of human toll-like receptor 1 impairs innate immune sensing of microbial cell wall components. *The Journal of Immunology, 178*(10), 6387-6394.

127. O'Neill, L. A. J., Golenbock, D., & Bowie, A. G. (2013). The history of toll-like receptors mdash] redefining innate immunity. *Nat Rev Immunol, 13*(6), 453-460.

128. O'Neill, L. A. J. (2008). When signaling pathways collide: Positive and negative regulation of toll-like receptor signal transduction. *Immunity, 29*(1), 12-20.

129. Opitz, B., Schröder, N. W. J., Spreitzer, I., Michelsen, K. S., Kirschning, C. J., Hallatschek, W., Zähringer, U., Hartung, T., Göbel, U.B., & Schumann, R. R. (2001). Toll-like receptor-2 mediates treponema glycolipid and lipoteichoic acid-induced NF-κB translocation. *Journal of Biological Chemistry, 276*(25), 22041-22047.

130. Ozinsky, A., Underhill, D. M., Fontenot, J. D., Hajjar, A. M., Smith, K. D., Wilson, C. B., Schroeder, L., & Aderem, A. (2000). The repertoire for pattern recognition of pathogens by the innate immune system is defined by cooperation between toll-like receptors. *Proceedings of the National Academy of Sciences, 97*(25), 13766-13771.

131. Park, B. S., Song, D. H., Kim, H. M., Choi, B. S., Lee, H., & Lee, J. O. (2009). The structural basis of lipopolysaccharide recognition by the TLR4–MD-2 complex. *Nature, 458*(7242), 1191-1195.

132. Park, J. S., Svetkauskaite, D., He, Q., Kim, J. Y., Strassheim, D., Ishizaka, A., & Abraham, E. (2004). Involvement of toll-like receptors 2 and 4 in cellular activation by high mobility group box 1 protein. *Journal of Biological Chemistry, 279*(9), 7370.

133. Pathak, S. K., Basu, S., Basu, K. K., Banerjee, A., Pathak, S., Bhattacharyya, A., Kaisho, T., Kundu, M., & Basu, J. (2007). Direct extracellular interaction between the early secreted antigen ESAT-6 of mycobacterium tuberculosis and TLR2 inhibits TLR signaling in macrophages. *Nature Immunology, 8*(6), 610-618.

134. Pecora, N. D., Gehring, A. J., Canaday, D. H., Boom, W. H., & Harding, C. V. (2006). Mycobacterium tuberculosis LprA is a lipoprotein agonist of TLR2 that regulates innate immunity and APC function. *The Journal of Immunology, 177*(1), 422-429.

135. Piazza, M., Calabrese, V., Baruffa, C., Gioannini, T., Weiss, J., & Peri, F. (2010). The cationic amphiphile 3,4-bis(tetradecyloxy)benzylamine inhibits LPS signaling by competing with endotoxin for CD14 binding. *Biochemical Pharmacology, 80*(12), 2050-2056.

136. Picard, C., Puel, A., Bonnet, M., Ku, C., Bustamante, J., Yang, K.,Soudais, C., Dupuis, S., Feinberg, J., Fieschi, C., Elbim, C., Hitchcock, R., Lammas, D., Davies, G., Al-Ghonaium, A., Al-Rayes, H., Al-Jumaah, S., Al-Hajjar, S., Al-Mohsen, I.Z., Frayha, H.H., Rucker, R., Hawn, T.R., Aderem, A., Tufenkeji, H., Haraguchi, S., Day, N.K., Good, R.A., Gougerot-Pocidalo, M., Ozinsky, A., & Casanova, J. (2003). Pyogenic bacterial infections in humans with IRAK-4 deficiency. *Science 299*(5615), 2076-2079.

137. Poltorak, A., He, X., Smirnova, I., Liu, M. Y., Van Huffel, C., Du, X., Birdwell, D., Alejos, E., Silva, M., & Galanos, C. (1998). Defective LPS signaling in C3H/HeJ and C57BL/10ScCr mice: Mutations in Tlr4 gene. *Science, 282*(5396), 2085-2088.

138. Pugin, J., Schürer-Maly, C., Leturcq, D., Moriarty, A., Ulevitch, R. J., & Tobias, P. S. (1993). Lipopolysaccharide activation of human endothelial and epithelial cells is mediated by lipopolysaccharide-binding protein and soluble CD14. *Proceedings of the National Academy of Sciences, 90*(7), 2744.

139. Quesniaux, V. J., Nicolle, D. M., Torres, D., Kremer, L., Guérardel, Y., Nigou, J., Puzo, G., Erard, F., & Ryffel, B. (2004). Toll-like receptor 2 (TLR2)-dependent-positive and TLR2-independent-negative regulation of proinflammatory cytokines by mycobacterial lipomannans. *The Journal of Immunology, 172*(7), 4425-4434.

140. Raby, A., Le Bouder, E., Colmont, C., Davies, J., Richards, P., Coles, B., George, C.H., Jones, S.A., Brennan, P., Topley, N., & Labéta, M. O. (2009). Soluble TLR2 reduces inflammation without compromising bacterial clearance by disrupting TLR2 triggering. *The Journal of Immunology, 183*(1), 506-517.

141. Ranoa, D. R. E., Kelley, S. L., & Tapping, R. I. (2013). Human lipopolysaccharide-binding protein (LBP) and CD14 independently deliver triacylated lipoproteins to toll-like receptor 1 (TLR1) and TLR2 and enhance formation of the ternary signaling complex. *Journal of Biological Chemistry, 288*(14), 9729-9741.

142. Roach, J. C., Glusman, G., Rowen, L., Kaur, A., Purcell, M. K., Smith, K. D.,Hood, L.E., & Aderem, A. (2005). The evolution of vertebrate toll-like receptors. *Proceedings of the National Academy of Sciences, 102*(27), 9577-9582.

143. Rock, F. L., Hardiman, G., Timans, J. C., Kastelein, R. A., & Bazan, J. F. (1998). A family of human receptors structurally related to Drosophila Toll. *Proceedings of the National Academy of Sciences, 95*(2), 588-593.

144. Ruby, J., Rehani, K., & Martin, M. (2007). Treponema denticola activates mitogen-activated protein kinase signal pathways through toll-like receptor 2. *Infection and Immunity, 75*(12), 5763-5768.

145. Sandor, F., Latz, E., Re, F., Mandell, L., Repik, G., Golenbock, D. T., Espevik, T., Kurt-Jones, E.A., & Finberg, R. W. (2003). Importance of extra-and intracellular domains of TLR1 and TLR2 in NFκB signaling. *The Journal of Cell Biology, 162*(6), 1099-1110.

146. Sato, M., Sano, H., Iwaki, D., Kudo, K., Konishi, M., Takahashi, H., Takahashi, T., Imaizumi, H., Asai, Y., & Kuroki, Y. (2003). Direct binding of toll-like receptor 2 to zymosan, and zymosan-induced NF-κB activation and TNF-α secretion are down-regulated by lung collectin surfactant protein A. *The Journal of Immunology, 171*(1), 417-425.

147. Schimke, J., Mathison, J., Morgiewicz, J., & Ulevitch, R. J. (1998). Anti-CD14 mAb treatment provides therapeutic benefit after in vivo exposure to endotoxin. *Proceedings of the National Academy of Sciences, 95*(23), 13875-13880.

148. Schröder, N. W. J., Heine, H., Alexander, C., Manukyan, M., Eckert, J., Hamann, L., Göbel, U.B., & Schumann, R. R. (2004). Lipopolysaccharide binding protein binds to triacylated and diacylated lipopeptides and mediates innate immune responses. *The Journal of Immunology, 173*(4), 2683-2691.

149. Schröder, N. W. J., Morath, S., Alexander, C., Hamann, L., Hartung, T., Zähringer, U., Göbel, U.B., Weber, J.R., & Schumann, R. R. (2003). Lipoteichoic acid (LTA) of streptococcus pneumoniaeand staphylococcus aureus activates immune cells via toll-like receptor (TLR)-2, lipopolysaccharide-binding protein (LBP), and CD14, whereas TLR-4 and MD-2 are not involved. *Journal of Biological Chemistry, 278*(18), 15587-15594.

150. Schröder, N. W. J., Diterich, I., Zinke, A., Eckert, J., Draing, C., Baehr, V. V., Hassler, D., Priem, S., Hahn, K., Michelsen, K.S., Hartung, T., Burmester, G.R., Göbel, U.B., Hermann, C., & Schumann, R. R. (2005). Heterozygous Arg753Gln polymorphism of human TLR-2 impairs immune activation by borrelia burgdorferi and protects from late stage lyme disease. *The Journal of Immunology, 175*(4), 2534-2540.

151. Schröder, N. W. J., & Schumann, R. R. (2005). Non-LPS targets and actions of LPS binding protein (LBP). *Journal of Endotoxin Research, 11*(4), 237-242.

152. Schromm, A. B., Lien, E., Henneke, P., Chow, J. C., Yoshimura, A., Heine, H., Latz, E., Monks, B.G., Schwartz, D.A., Miyake, K., & Golenbock, D. T. (2001). Molecular genetic analysis of an endotoxin nonresponder mutant cell line: A point mutation in a conserved region of md-2 abolishes endotoxin-induced signaling. *The Journal of Experimental Medicine, 194*(1), 79-88.

153. Schumann, R., Leong, Flaggs, G., Gray, P., Wright, S., Mathison, J.,Tobias, P.S., & Ulevitch, R. (1990). Structure and function of lipopolysaccharide binding protein. *Science, 249*(4975), 1429-1431.

154. Schwandner, R., Dziarski, R., Wesche, H., Rothe, M., & Kirschning, C. J. (1999). Peptidoglycan- and lipoteichoic acid-induced cell activation is mediated by toll-like receptor 2. *Journal of Biological Chemistry, 274*(25), 17406-17409.

155. Sellati, T. J., Bouis, D. A., Caimano, M. J., Feulner, J. A., Ayers, C., Lien, E., & Radolf, J. D. (1999). Activation of human monocytic cells by borrelia burgdorferi and treponema pallidum is facilitated by CD14 and correlates with surface exposure of spirochetal lipoproteins. *The Journal of Immunology, 163*(4), 2049.

156. Sellati, T. J., Bouis, D. A., Kitchens, R. L., Darveau, R. P., Pugin, J., Ulevitch, R. J., Gangloff, S.C., Goyert, S.M., Norgard, M.V., & Radolf, J. D. (1998). Treponema pallidum and borrelia burgdorferi lipoproteins and synthetic lipopeptides activate monocytic cells via a CD14-dependent pathway distinct from that used by lipopolysaccharide. *The Journal of Immunology, 160*(11), 5455-5464.

157. Sen, R., & Baltimore, D. (1986). Inducibility of κ immunoglobulin enhancer-binding protein NF-κB by a posttranslational mechanism. *Cell, 47*(6), 921-928.

158. Setoguchi, M., Nasu, N., Yoshida, S., Higuchi, Y., Akizuki, S., & Yamamoto, S. (1989). Mouse and human CD14 (myeloid cell-specific leucine-rich glycoprotein) primary structure deduced from cDNA clones. *Biochimica Et Biophysica Acta (BBA)-Gene Structure and Expression, 1008*(2), 213-222.

159. Shimazu, R., Akashi, S., Ogata, H., Nagai, Y., Fukudome, K., Miyake, K., & Kimoto, M. (1999). MD-2, a molecule that confers lipopolysaccharide responsiveness on toll-like receptor 4. *The Journal of Experimental Medicine, 189*(11), 1777-1782.

160. Sims, J., March, C., Cosman, D., Widmer, M., MacDonald, H., McMahan, C., Grubin, C.E., Wignall, J.M., Jackson, J.L., & Call, S.M. (1988). cDNA expression cloning of the IL-1 receptor, a member of the immunoglobulin superfamily. *Science, 241*(4865), 585-589.

161. Spyvee, M. R., Zhang, H., Hawkins, L. D., & Chow, J. C. (2005). Toll-like receptor 2 antagonists. Part 1: Preliminary SAR investigation of novel synthetic phospholipids. *Bioorganic & Medicinal Chemistry Letters, 15*(24), 5494-5498.

162. Taguchi, T., Mitcham, J. L., Dower, S. K., Sims, J. E., & Testa, J. R. (1996). Chromosomal localization ofTIL,a gene encoding a protein related to theDrosophilaTransmembrane receptor toll, to human chromosome 4p14. *Genomics*, *32*(3), 486-488.

163. Takeda, K., & Akira, S. (2005). Toll-like receptors in innate immunity. *International Immunology*, *17*(1), 1-14.

164. Takeda, K., Kaisho, T., & Akira, S. (2003). Toll-like Receptors. *Annual Review of Immunology*, *21*(1), 335-376.

165. Takeuchi, O., Hoshino, K., Kawai, T., Sanjo, H., Takada, H., Ogawa, T., Takeda, K., & Akira, S. (1999). Differential roles of TLR2 and TLR4 in recognition of Gram-negative and Gram-positive bacterial cell wall components. *Immunity, 11*(4), 443-451.

166. Takeuchi, O., Kaufmann, A., Grote, K., Kawai, T., Hoshino, K., Morr, M., Mühlradt, P.F., & Akira, S. (2000). Cutting edge: Preferentially the R-stereoisomer of the mycoplasmal lipopeptide macrophage-activating lipopeptide-2 activates immune cells through a toll-like receptor 2-and MyD88-dependent signaling pathway. *The Journal of Immunology, 164*(2), 554.

167. Takeuchi, O., Kawai, T., Mühlradt, P. F., Morr, M., Radolf, J. D., Zychlinsky, A., Takeda, K., & Akira, S. (2001). Discrimination of bacterial lipoproteins by toll-like receptor 6. *International Immunology, 13*(7), 933-940.

168. Takeuchi, O., Sato, S., Horiuchi, T., Hoshino, K., Takeda, K., Dong, Z., Modlin, R.L. & Akira, S. (2002). Cutting edge: Role of toll-like receptor 1 in mediating immune response to microbial lipoproteins. *The Journal of Immunology, 169*(1), 10-14.

169. Takeuchi, O., Hoshino, K., & Akira, S. (2000). Cutting edge: TLR2-deficient and MyD88-deficient mice are highly susceptible to staphylococcus aureus infection. *The Journal of Immunology, 165*(10), 5392-5396.

170. Tanji, H., Ohto, U., Shibata, T., Miyake, K., & Shimizu, T. (2013). Structural reorganization of the toll-like receptor 8 dimer induced by agonistic ligands. *Science, 339*(6126), 1426-1429.

171. Tapping, R. I., & Tobias, P. S. (2003). Mycobacterial lipoarabinomannan mediates physical interactions between TLR1 and TLR2 to induce signaling. *Journal of Endotoxin Research, 9*(4), 264-268.

172. Teghanemt, A., Widstrom, R. L., Gioannini, T. L., & Weiss, J. P. (2008). Isolation of monomeric and dimeric secreted MD-2. *Journal of Biological Chemistry, 283*(32), 21881-21889.

173. Temperley, N., Berlin, S., Paton, I., Griffin, D., & Burt, D. (2008). Evolution of the chicken toll-like receptor gene family: A story of gene gain and gene loss. *BMC Genomics, 9*(1), 62.

174. Tobias, P. S., Soldau, K., & Ulevitch, R. J. (1986). Isolation of a lipopolysaccharide-binding acute phase reactant from rabbit serum. *The Journal of Experimental Medicine, 164*(3), 777-793.

175. Triantafilou, M., Gamper, F. G. J., Haston, R. M., Mouratis, M. A., Morath, S., Hartung, T., & Triantafilou, K. (2006). Membrane sorting of toll-like receptor (TLR)-2/6 and TLR2/1 heterodimers at the cell surface determines heterotypic associations with CD36 and intracellular targeting. *Journal of Biological Chemistry, 281*(41), 31002-31011.

176. Troutman, T. D., Hu, W., Fulenchek, S., Yamazaki, T., Kurosaki, T., Bazan, J. F., & Pasare, C. (2012). Role for B-cell adapter for PI3K (BCAP) as a signaling adapter linking toll-like receptors (TLRs) to serine/threonine kinases PI3K/akt. *Proceedings of the National Academy of Sciences, 109*(1), 273-278.

177. Ulevitch, R. J., & Tobias, P. S. (1999). Recognition of Gram-negative bacteria and endotoxin by the innate immune system. *Current Opinion in Immunology, 11*(1), 19-22.

178. Underhill, D. M., & Gantner, B. (2004). Integration of toll-like receptor and phagocytic signaling for tailored immunity. *Microbes and Infection, 6*(15), 1368-1373.

179. Underhill, D. M., Ozinsky, A., Hajjar, A. M., Stevens, A., Wilson, C. B., Bassetti, M., & Aderem, A. (1999). The toll-like receptor 2 is recruited to macrophage phagosomes and discriminates between pathogens. *Nature, 401*(6755), 811-815.

180. Vabulas, R. M., Ahmad-Nejad, P., da Costa, C., Miethke, T., Kirschning, C. J., Häcker, H., & Wagner, H. (2001). Endocytosed HSP60s use toll-like receptor 2 (TLR2) and TLR4 to activate the toll/interleukin-1 receptor signaling pathway in innate immune cells. *Journal of Biological Chemistry, 276*(33), 31332-31339.

181. van Bergenhenegouwen, J., Plantinga, T. S., Joosten, L. A. B., Netea, M. G., Folkerts, G., Kraneveld, A. D., Garssen, J., & Vos, A. P. (2013). TLR2 & co: A critical analysis of the complex interactions between TLR2 and coreceptors. *Journal of Leukocyte Biology, 94*(5), 885-902.

182. van Zoelen, M. A. D., Yang, H., Florquin, S., Meijers, J., Akira, S., Arnold, B., Nawroth, P.P., Bierhaus, A., Tracey, K.J., & Poll, T. (2009). Role of toll-like receptors 2 and 4, and the receptor for advanced glycation end products in high-mobility group box 1-induced inflammation in vivo. *Shock, 31*(3), 280-284.

183. Vasselon, T., Detmers, P. A., Charron, D., & Haziot, A. (2004). TLR2 recognizes a bacterial lipopeptide through direct binding. *The Journal of Immunology, 173*(12), 7401-7405.

184. Vignal, C., Guérardel, Y., Kremer, L., Masson, M., Legrand, D., Mazurier, J., & Elass, E. (2003). Lipomannans, but not lipoarabinomannans, purified from mycobacterium chelonae and mycobacterium kansasii induce TNF-α and IL-8 secretion by a CD14-toll-like receptor 2-dependent mechanism. *The Journal of Immunology, 171*(4), 2014-2023.

185. von Bernuth, H., Picard, C., Jin, Z., Pankla, R., Xiao, H., Ku, C., Chrabieh, M., Mustapha, I.B., Ghandil, P., Camcioglu, Y., Vasconcelos, J., Sirvent, N., Guedes, M., Vitor, A.B., Herrero-Mata, M.J., Arostegui, J.I., Rodrigo, C., Alsina, L., Ruiz-Ortiz, E., Juan, M., Fortuny, C., Yagüe, J., Anton, J., Pascal, M., Chang, H., Janniere, L., Rose, Y., Garty, B., Chapel, H., Issekutz, A., Marodi, L., Rodriguez-Gallego, C., Banchereau, J., Abel, L., Li, X., Chaussabel, D., Puel, A., & Casanova, J. (2008). Pyogenic bacterial infections in humans with MyD88 deficiency. *Science, 321*(5889), 691-696.

186. Wasserman, S. A. (1993). A conserved signal transduction pathway regulating the activity of the rel-like proteins dorsal and NF-kappa B. *Molecular Biology of the Cell, 4*(8), 767-771.

187. Weber, J. R., Freyer, D., Alexander, C., Schröder, N. W. J., Reiss, A., Küster, C., Pfeil, D., Tuomanen, E.I., & Schumann, R. R. (2003). Recognition of pneumococcal peptidoglycan: An expanded, pivotal role for LPS binding protein. *Immunity, 19*(2), 269-279.

188. Weis, J. J., Ma, Y., & Erdile, L. F. (1994). Biological activities of native and recombinant borrelia burgdorferi outer surface protein A: Dependence on lipid modification. *Infection and Immunity, 62*(10), 4632-4636.

189. Whitham, S., Dinesh-Kumar, S. P., Choi, D., Hehl, R., Corr, C., & Baker, B. (1994). The product of the tobacco mosaic virus resistance gene N: Similarity to toll and the interleukin-1 receptor. *Cell, 78*(6), 1101-1115.

190. Wilson, D. S., & Keefe, A. D. (2001). Random mutagenesis by PCR. *Current protocols in molecular biology.* John Wiley & Sons, Inc.

191. Wlasiuk, G., & Nachman, M. W. (2010). Adaptation and constraint at toll-like receptors in primates. *Molecular Biology and Evolution, 27*(9), 2172-2186.

192. Wooten, R. M., Ma, Y., Yoder, R. A., Brown, J. P., Weis, J. H., Zachary, J. F., Kirschning, C.J., & Weis, J. J. (2002). Toll-like receptor 2 is required for innate, but not acquired, host defense to borrelia burgdorferi. *The Journal of Immunology, 168*(1), 348-355.

193. Wooten, R. M., Morrison, T. B., Weis, J. H., Wright, S. D., Thieringer, R., & Weis, J. J. (1998). The role of CD14 in signaling mediated by outer membrane lipoproteins of borrelia burgdorferi. *The Journal of Immunology, 160*(11), 5485-5492.

194. Wright, S., Ramos, R., Tobias, P., Ulevitch, R., & Mathison, J. (1990). CD14, a receptor for complexes of lipopolysaccharide (LPS) and LPS binding protein. *Science, 249*(4975), 1431-1433.

195. Wurfel, M. M., Monks, B. G., Ingalls, R. R., Dedrick, R. L., Delude, R., Zhou, D., Lamping, N., Schumann, R.R., Thieringer, R., Fenton, M.J., Wright, S.D., & Golenbock, D. (1997). Targeted deletion of the lipopolysaccharide (LPS)-binding protein gene leads to profound suppression of LPS responses ex vivo, whereas in vivo responses remain intact. *The Journal of Experimental Medicine, 186*(12), 2051-2056.

196. Wyllie, D.H., Kiss-Toth, E., Visintin, A., Smith, S.C., Boussouf, S., Segal, D.M., Duff, G.W., & Dower, S.K. (2000). Evidence for an accessory protein function for toll-like receptor 1 in anti-bacterial responses. *The Journal of Immunology, 165*(12), 7125-7132.

197. Yamamoto, M., Sato, S., Hemmi, H., Hoshino, K., Kaisho, T., Sanjo, H., Takeuchi, O., Sugiyama, M., Okabe, M., Takeda, K., & Akira, S. (2003). Role of adaptor TRIF in the MyD88-independent toll-like receptor signaling pathway. *Science, 301*(5633), 640-643.

198. Yamamoto, M., Sato, S., Hemmi, H., Sanjo, H., Uematsu, S., Kaisho, T., Hoshino, K., Takeuchi, O., Kobayashi, M., Fujita, T., Takeda, K., & Akira, S. (2002). Essential role for TIRAP in activation of the signalling cascade shared by TLR2 and TLR4. *Nature, 420*(6913), 324-329.

199. Yamamoto, M., Sato, S., Hemmi, H., Uematsu, S., Hoshino, K., Kaisho, T., Takeuchi, O., Takeda, K., & Akira, S. (2003). TRAM is specifically involved in the toll-like receptor 4-mediated MyD88-independent signaling pathway. *Nature Immunology, 4*(11), 1144-1150.

200. Yang, D., Chen, Q., Su, S. B., Zhang, P., Kurosaka, K., Caspi, R. R., Michalek, S.M., Rosenberg, H.F., Zhang, N., & Oppenheim, J. J. (2008). Eosinophil-derived neurotoxin acts as an alarmin to activate the TLR2–MyD88 signal pathway in dendritic cells and enhances Th2 immune responses. *The Journal of Experimental Medicine, 205*(1), 79-90.

201. Yoon, S., Kurnasov, O., Natarajan, V., Hong, M., Gudkov, A. V., Osterman, A. L., & Wilson, I. A. (2012). Structural basis of TLR5-flagellin recognition and signaling. *Science, 335*(6070), 859-864.

202. Yoshimura, A., Lien, E., Ingalls, R. R., Tuomanen, E., Dziarski, R., & Golenbock, D. (1999). Cutting edge: Recognition of Gram-positive bacterial cell wall components by the innate immune system occurs via toll-like receptor 2. *The Journal of Immunology, 163*(1), 1-5.

203. Zarember, K. A., & Godowski, P. J. (2002). Tissue expression of human toll-like receptors and differential regulation of toll-like receptor mRNAs in leukocytes in response to microbes, their products, and cytokines. *The Journal of Immunology, 168*(2), 554-561.

204. Zhou, H., Gu, J., Lamont, S., & Gu, X. (2007). Evolutionary analysis for functional divergence of the toll-like receptor gene family and altered functional constraints. *Journal of Molecular Evolution, 65*(2), 119-123.

205. Zweigner, J., Gramm, H., Singer, O. C., Wegscheider, K., & Schumann, R. R. (2001). High concentrations of lipopolysaccharide-binding protein in serum of patients with severe sepsis or septic shock inhibit the lipopolysaccharide response in human monocytes. *Blood, 98*(13), 3800-3808.